

## INFORMATION TO USERS

This reproduction was made from a copy of a document sent to us for microfilming. While the most advanced technology has been used to photograph and reproduce this document, the quality of the reproduction is heavily dependent upon the quality of the material submitted.

The following explanation of techniques is provided to help clarify markings or notations which may appear on this reproduction.

1. The sign or "target" for pages apparently lacking from the document photographed is "Missing Page(s)". If it was possible to obtain the missing page(s) or section, they are spliced into the film along with adjacent pages. This may have necessitated cutting through an image and duplicating adjacent pages to assure complete continuity.
2. When an image on the film is obliterated with a round black mark, it is an indication of either blurred copy because of movement during exposure, duplicate copy, or copyrighted materials that should not have been filmed. For blurred pages, a good image of the page can be found in the adjacent frame. If copyrighted materials were deleted, a target note will appear listing the pages in the adjacent frame.
3. When a map, drawing or chart, etc., is part of the material being photographed, a definite method of "sectioning" the material has been followed. It is customary to begin filming at the upper left hand corner of a large sheet and to continue from left to right in equal sections with small overlaps. If necessary, sectioning is continued again—beginning below the first row and continuing on until complete.
4. For illustrations that cannot be satisfactorily reproduced by xerographic means, photographic prints can be purchased at additional cost and inserted into your xerographic copy. These prints are available upon request from the Dissertations Customer Services Department.
5. Some pages in any document may have indistinct print. In all cases the best available copy has been filmed.

**University  
Microfilms  
International**

300 N. Zeeb Road  
Ann Arbor, MI 48106

8312364

**Nieman, Jaime**

**CARBON DIOXIDE - LASER INDUCED IER AND CHEMISTRY OF  
CHROMYL CHLORIDE**

*City University of New York*

PH.D. 1983

**University  
Microfilms  
International** 300 N. Zeeb Road, Ann Arbor, MI 48106

PLEASE NOTE:

In all cases this material has been filmed in the best possible way from the available copy. Problems encountered with this document have been identified here with a check mark .

1. Glossy photographs or pages \_\_\_\_\_
2. Colored illustrations, paper or print \_\_\_\_\_
3. Photographs with dark background
4. Illustrations are poor copy \_\_\_\_\_
5. Pages with black marks, not original copy \_\_\_\_\_
6. Print shows through as there is text on both sides of page \_\_\_\_\_
7. Indistinct, broken or small print on several pages
8. Print exceeds margin requirements \_\_\_\_\_
9. Tightly bound copy with print lost in spine \_\_\_\_\_
10. Computer printout pages with indistinct print \_\_\_\_\_
11. Page(s) \_\_\_\_\_ lacking when material received, and not available from school or author.
12. Page(s) \_\_\_\_\_ seem to be missing in numbering only as text follows.
13. Two pages numbered \_\_\_\_\_. Text follows.
14. Curling and wrinkled pages \_\_\_\_\_
15. Other \_\_\_\_\_

University  
Microfilms  
International

CO<sub>2</sub>-Laser Induced IER and Chemistry of Chromyl Chloride

by

Jaime Nieman

A dissertation submitted to the Graduate Faculty in Chemistry in partial fulfillment of the requirements for the degree of Doctor of Philosophy, The City University of New York.

1983

This manuscript has been read and accepted for the Graduate Faculty in Chemistry in satisfaction of the dissertation requirement for the degree of Doctor of Philosophy.

Jan 28, 1983  
date

A. M. [Signature]  
Chairman of Examining Committee

28 January 1983  
date

David C. Lake  
Executive Officer

David A. Beveridge  
[Signature]  
Supervisory Committee

The City University of New York

## Abstract

### CO<sub>2</sub>-LASER INDUCED IER AND CHEMISTRY OF CHROMYL CHLORIDE

by

Jaime Neiman

Adviser: Professor A. M. Ronn

High order CO<sub>2</sub>-laser multiphoton excitation in the ground electronic state of collision-free CrO<sub>2</sub>Cl<sub>2</sub> has resulted in visible fluorescence.

The prompt fluorescence has been studied as a function of laser fluence, pulse duration, under collisional and collision-free conditions and was shown to arise from a spontaneous one-photon radiative decay of molecular eigenstates.

Intramolecular scrambling of vibronic levels corresponding to the ground state electronic manifold with a discrete level(s) belonging to the low lying excited electronic state is believed to be the origin of such eigenstates. A theoretical model based on this description is analyzed. It is shown that the long radiative lifetime of the observed CrO<sub>2</sub>Cl<sub>2</sub> emission is consistent with this interpretation. Molecular requirements for observation of this novel reverse internal conversion process in other molecular systems are suggested.

The fluorescent channel is shown to compete with a dissociative channel forming CrO<sub>2</sub>Cl + Cl; the radical further dissociates to the stable product CrO<sub>2</sub>. The threshold for fluorescence versus dissociation is discussed and a branching ratio, and a consequent chemical mechanism is suggested. The molecular and laser parameters involved in this competition are also discussed within the framework of the accepted model of infrared multiphoton excitation.

To the memories of my parents and Debbie.

## Acknowledgement

To Professor Vic Ronn, I will be forever grateful. His excellent scientific guidance was expected; his friendship and caring went well beyond the call of duty.

I was introduced to research, as an undergraduate, by Donald A. Gerber, M.D. I could not have had a better beginning.

The members of Vic's group always provided help, friendship, and lively conversation. I, thus, thank Barbara, Lenny, Myron, Ross, Shu, and Yediyah. Alan was, and still is, always there when I need him -- an invaluable friend. Shiann, the post-doc with infinite patience, deserves special mention. To learn from Visiting Professor José Riveros was a rare and valued opportunity. To Professor Richard Zare and his group at Stanford, thanks are due for their expert collaboration in some of this work.

The cooperation of the professional, technical, and administrative staff of the Chemistry Department, I must also acknowledge. In particular, Ottmar Safferling, our esteemed glassblower, and the machine shop crew, Saul and Marty, often performed two-day jobs in two hours. Herb Brodsky's response to unreasonable requests cannot go unmentioned.

Thanks are due to Mr. Fritz Goro for the beautiful color photographs that appear in this work. The week he spent in our laboratory enriched all of us.

Professor David Beveridge and Vojtech Fried, the members of my committee, provided many stimulating discussions. I am grateful for their kindness and their interest in my research.

To Belita, Abe, Isaac, and Lisa -- my family -- thanks for being you. Without their love and support, this thesis would not have been possible. I must thank Kathi for putting up with the difficult times.

For the expert typing of this manuscript, I thank Terry Rudd. For not throwing it at me, I will be forever grateful.

## TABLE OF CONTENTS

	<u>Page</u>
Introduction	1
References	4
Experimental	5
References	15
Theoretical Background	16
References	27
Results	29
References	80
Discussion	82
References	125

## LIST OF TABLES

	<u>Page</u>
Results Section	
Table 1. Published vibrational frequencies of $\text{CrO}_2\text{Cl}_2$ (ground state).	33
Discussion Section	
Table I. Comparison of density of vibrational states between $\text{CrO}_2\text{Cl}_2$ and $\text{SF}_6$	91

## LIST OF FIGURES

	<u>Page</u>
<b>Experimental Section</b>	
Figure 1. Schematic diagram of the CO <sub>2</sub> TEA laser	6
Figure 2. CO <sub>2</sub> laser pulses	7
Figure 3. Experimental apparatus	13
<b>Results Section</b>	
Figure 1. The infrared spectrum of CrO <sub>2</sub> Cl <sub>2</sub>	34
Figure 2. The opto-acoustic signal from CrO <sub>2</sub> Cl <sub>2</sub>	36
Figure 3. Photograph of the MPE-induced visible fluorescence in CrO <sub>2</sub> Cl <sub>2</sub>	37
Figure 4. Photograph of the plasma produced by CO <sub>2</sub> -LIDB in CrO <sub>2</sub> Cl <sub>2</sub>	39
Figure 5. Total luminescence amplitude versus CO <sub>2</sub> laser R-branch lines	41
Figure 6. Molecular fluorescence spectrum following low-power irradiation	43
Figure 7. SEM photograph of CrO <sub>2</sub> formed by CO <sub>2</sub> -laser multiphoton dissociation of CrO <sub>2</sub> Cl <sub>2</sub>	45
Figure 8. Infrared spectrum of CrO <sub>2</sub> Cl <sub>2</sub> as a function of laser pulses	46
Figure 9. Luminescence amplitude versus laser energy	48
Figure 10. Luminescence quenching by Cl <sub>2</sub>	51
Figure 11. Scope photographs of short and long laser pulses and their induced fluorescence signals	53
Figure 12. Wavelength resolved rise times	55
Figure 13. Effect of pressure and laser energy on the emission's rise time	57

LIST OF FIGURES (continued)

	<u>Page</u>
Results Section (continued)	
Figure 14. Effect of He on the fluorescence rise time	59
Figure 15. Stern-Volmer plot of 6328 Å fluorescence using a short laser pulse	65
Figure 16. Effect of He on the fluorescence signal	67
Figure 17. Effect of Ar on the luminescence decay time	70
Figure 18. Stern-Volmer plot of 1:200 mixture of CrO <sub>2</sub> Cl <sub>2</sub> in Ar	72
Figure 19. Fluorescence amplitude versus pressure	74
Figure 20. Luminescence signals emphasizing the collisional component	76

## INTRODUCTION

The growth of laser-induced chemistry in the last ten years has been remarkable. Countless number of reactions have now been achieved with the use of the laser. Perhaps the best evidence of the rapid development of this field is the countless number of review articles (1-5, for example). Whether this boom has resulted from the discovery of isotope separation via multiphoton pumping (6,7), the hope, as yet not realized, of bond-specific chemistry, the synthesis of new and novel compounds, or the projection of more efficiently produced industrial chemicals, the result is the same--namely, exponential growth.

What makes the laser unique? As its name implies (laser is an acronym for light amplification through stimulated emission of radiation), the laser is an amplifier of light. Very high powers (KW) and very high intensities ( $\text{GW}/\text{cm}^2$ ) can be achieved routinely with present-day lasers. In addition, the laser possesses two other characteristics, namely coherence and a high degree of directionality that makes it unique. The former allows one to design lasers with a high degree of monochromaticity. The linewidth of the laser radiation can be even smaller than those due to spontaneous emission from the molecules in the laser medium; thus, the laser is the most monochromatic source of radiation available. This property, coupled with the high degree of directionality and large output power, makes the laser ideal for studying photochemical and photophysical processes.

The overwhelming majority of the reactions have been performed with infrared lasers and, in particular, with the  $\text{CO}_2$  laser. The latter has become the standard tool of the field because of its high output power

(up to several kW, continuous wave), high intensities that are achievable ( $\text{GW}/\text{cm}^2$  in pulses of 100 nsec duration), high efficiency (conversion of about 20% of pumping power into radiant power), the laser wavelengths ( $9.6 \mu - 10.6 \mu$ ) which fall in the region where many molecules absorb, and its relatively moderate cost (typically \$10,000 for a home-built one). At this point, it is worthwhile to briefly mention what  $\text{CO}_2$ -laser induced chemistry entails. There are two basic mechanisms by which an infrared laser induces a chemical reaction. In one, dubbed laser-induced dielectric breakdown, the laser light does not have to be resonant with any absorption feature of the molecule. It is believed, as will be later discussed, that in this process it is the high fields generated by the laser that literally "rip the molecule apart," thereby allowing a reaction to occur.

The other mechanism, and the one which is the bulk of this work, is the on-resonance process named multiphoton absorption (MPA). In this case, the laser is tuned to an absorption feature of the molecule and, in the case of collisionless dissociation, it must absorb many infrared photons in order to reach the dissociation limit.

How does the molecule interact with the laser field in order to dissociate? Is the process coherent all the way up the vibrational ladder? Is the multiphoton-absorption process simultaneous or consecutive (albeit very fast)? Does the energy remain in the same vibrational mode or is it redistributed among all the modes of the molecule?

These are just some of the questions that chemists and physicists have tried to answer.

In this work, we have tried to address some of these. In addition, however, we have studied a new process (8,9), subsequently named Inverse Electronic Relaxation (IER)(10) which, to our knowledge, has

never been detected before. The first reports of infrared multiphoton dissociation stated that this process was accompanied by visible emission (11-17). The early experiments (11-13) used continuous wave (cw)  $\text{CO}_2$ -laser excitation and, therefore, were thought to produce luminescence by simple heating of the sample. This mechanism, however, cannot explain the visible luminescence observed from a pulsed  $\text{CO}_2$  laser at moderate power levels. Much of this molecular emission has been attributed to radical recombination or to chemical reaction (18-20). We, on the other hand, have studied the collisionless multiphoton dissociation of  $\text{CrO}_2\text{Cl}_2$  to yield  $\text{CrO}_2 + \text{Cl}_2$  and the collisionless production of electronically excited  $\text{CrO}_2\text{Cl}_2$ . This appears to be the first instance of vibrational-to-electronic energy transfer in a parent molecule effected via laser pumping. The rarity of this process seems to reflect the general rule that the ground state of a molecule correlates adiabatically with ground state products.  $\text{CrO}_2\text{Cl}_2$  may be the first example of a class of molecules in which the bound electronically excited state is located below the ground state dissociation limit.

In what is to follow, we shall first investigate the theoretical basis for laser induced multiphoton absorption and dissociation (MPD) processes. Armed with this background, we shall describe, interpret, and explain the experimental observations of these processes in  $\text{CrO}_2\text{Cl}_2$ .

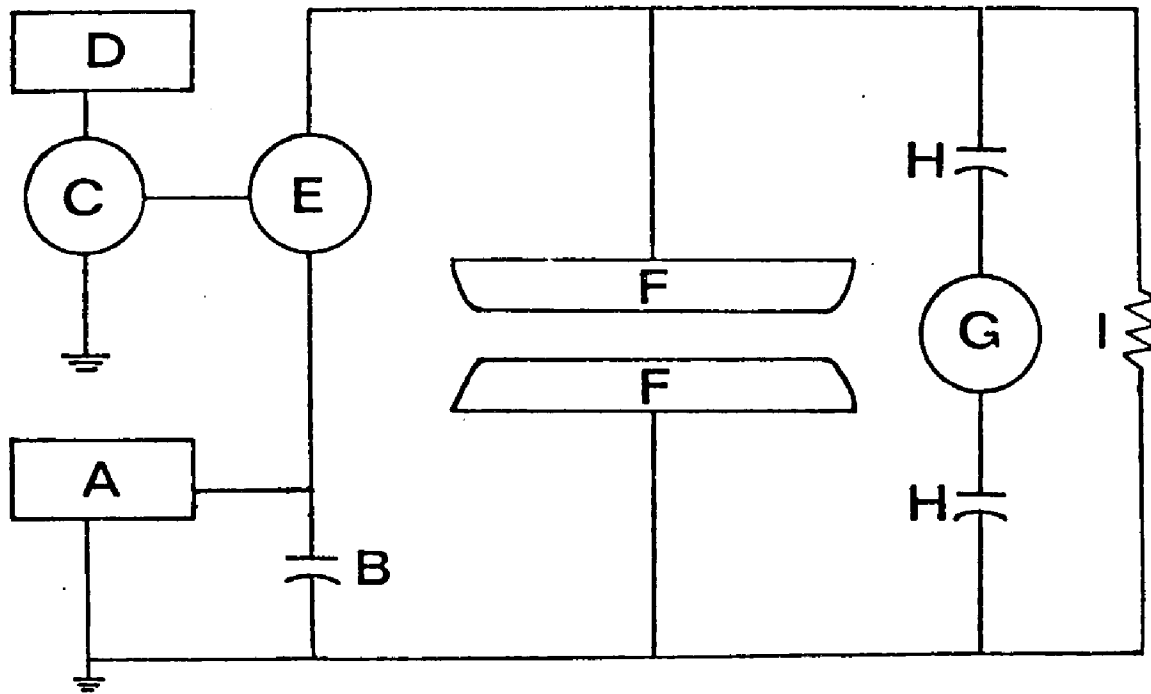
References

1. R. V. Ambartzumian and V. S. Letokhov, in Chemical and Biochemical Applications of Lasers, edited by C. B. Morre (Academic Press, New York, 1977) Vol. 3, Chapter 2.
2. V. S. Letokhov, Physics Today, May, 23 (1977).
3. C. D. Cantrell, S. M. Freund and J. L. Lyman, in Laser Handbook, edited by M. Stinch (North Holland, New York, 1978) Vol. 3.
4. N. Bloembergen and Eli Yablonovitch, Physics Today, May, 23 (1978).
5. A. M. Ronn, Scientific American, 240, #5, 114 (May, 1979).
6. R. V. Ambartzumian, V. S. Letokhov, E. A. Ryabov, N. V. Chekalin, JETP Lett. 20, 273 (1974).
7. J. L. Lyman, R. V. Jensen, J. Rink, C. P. Robinson, and S. D. Rockwood, Appl. Phys. Lett. 27, 87 (1975).
8. Z. Karny, A. Gupta, R. N. Zare, S. T. Lin, J. Nieman and A. M. Ronn, Chem. Phys. 37, 15 (1979).
9. J. Nieman and A. M. Ronn, Opt. Eng. 19, 39 (1980).
10. A. Nitzan and J. Jortner, Chem. Phys. Lett. 60, 1 (1978).
11. C. Borde, A. Henry and L. Henry, Compt. Rend. Acad. Sci. (Paris) B 262, 1389 (1966).
12. V. V. Losev, V. P. Papulovski, V. P. Tischinski, and C. A. Fedina, High Energy Chem. 8, 331 (1969).
13. N. V. Karlov, Yu. N. Petrov, A. M. Prokhorov and O. M. Stel'makh, JETP Letters 11, 135 (1970).
14. N. R. Isenor and M. C. Richardson, Appl. Phys. Lett. 18, 224 (1971).
15. V. S. Letokhov, E. A. Ryabov and O. A. Tumanov, Opt. Commun. 5, 168 (1972).
16. N. R. Isenor, V. Merchant, R. S. Hallsworth, and M. C. Richardson, Can. J. Phys. 51, 128 (1973).
17. R. V. Ambartzumian, N. V. Chekalin, V. S. Doljnikov, V. S. Letokhov and E. A. Ryabov, Chem. Phys. Lett. 25, 515 (1974).
18. R. V. Ambartzumian, N. V. Chekalin, V. S. Doljnikov, V. S. Letokhov and V. N. Kokhman, J. of Photochem. 6, 55 (1976).
19. R. V. Ambartzumian, Yu. A. Gorokhov, G. N. Markarov, A. A. Puretski, and N. P. Furzikov, Chem. Phys. Lett. 45, 231 (1977).
20. M. L. Lesiecki and W. A. Guillory, J. Chem. Phys. 66, 4317 (1977).

## EXPERIMENTAL

The experimental system was a conventional MPA one. A Rogowski type TEA (transversely excited atmospheric) CO<sub>2</sub> laser was used. This home-built (1) laser was grating-tuned and, therefore, lasing from most of the rotational lines of the 001-02°0 (9.6 μm) and 001-100 (10.6 μm) vibrational bands was available. Pulsing of this laser was accomplished with a trigger generator (model 050C, Tackisto Inc.) in conjunction with a pulse transformer (100:1 U.S. Scientific Instruments) and a pressurized spark gap (0-30 PSIG, 12-50KV, SG501, Tackisto Inc.) (See Figure 1). Typical line-selected energies of 0.1 J - 2.5 J per pulse could be achieved with this system. The laser operated on mixtures of CO<sub>2</sub>, He, and N<sub>2</sub>. In addition, triethylamine, carried in by the He gas, was used to assist preionizing and prevent arcing, thereby obtaining stable output energy.

In N<sub>2</sub>-rich mixtures, the laser pulse had a sharp rise of 200 nsec and ended with a 2 μsec tail. Using N<sub>2</sub>-lean mixtures (2), the tail could be eliminated and a 200 nsec FWHM (full width half maximum) pulse was available (see Figure 2). Ordinarily, the long multimode pulse produced an output beam of dimensions 1.5 cm by 1.0 cm, as measured by the burn pattern on heat sensitive paper, which was not completely uniform. Without N<sub>2</sub> and by inserting diaphragms in the laser cavity, single-mode output could be obtained but at a considerable loss of energy. This short pulse, single-mode beam was typically 0.5 cm by 0.5 cm, full, and without hot spots, but its energy was never more than 0.35 J. However, it should be pointed out, that the peak power or power intensity of this pulse is always much larger than that of the long pulse (N<sub>2</sub>-rich mixture) for a given total energy. Pulse shapes were determined using a HgTe:CdTe

Figure 1. Schematic diagram of the CO<sub>2</sub> TEA laser.

- A. High voltage dc power supply (50 KV, 70 mA)
- B. Discharge capacitor (50 KV, 0.05  $\mu$ F)
- C. Pulse transformer (100:1)
- D. Timing and trigger generator (0.1 to 100 pps)
- E. Pressurized spark gap (0-30 PSIG, 12-50 KV)
- F. Rogowski profile electrodes (aluminum)
- G. Spark plugs (Surface gap, L77V Champion)
- H. Trigger capacitors (30 KV, 500 pF each)
- I. Charging and discharging resistor (50 K $\Omega$ )

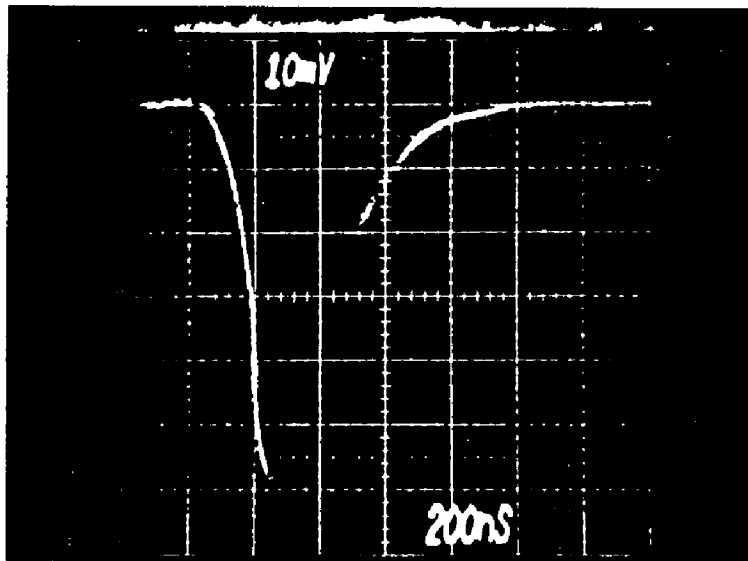
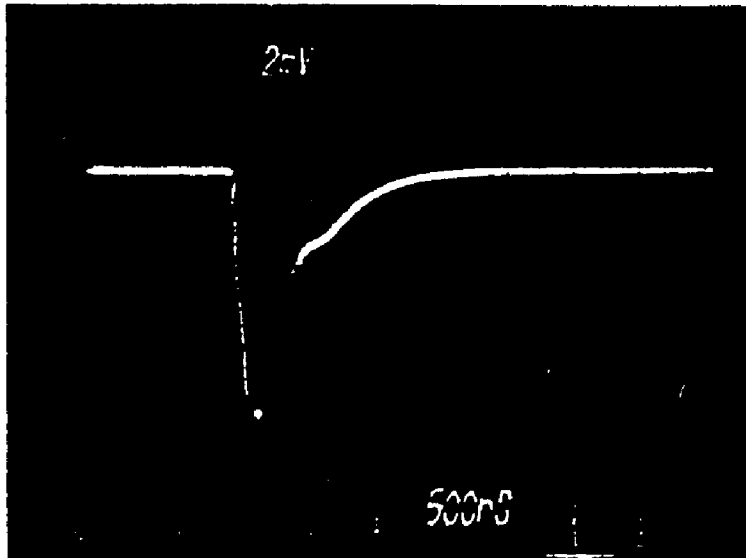


Figure 2. Scope photograph of typical long (top) and short CO<sub>2</sub>-laser pulses.

detector having a rise time of 5 nsec and also with a photodrag detector. Laser energy and fluence measurements were performed with either a Scientech 36-001 or a Coherent 201 power meter in conjunction with laser-pulse duration determinations.

As discussed in the Theoretical Section, both multiphoton absorption and dielectric breakdown require very large laser intensities. These are achieved by focusing the radiation into the reaction cells. Focusing was achieved by both AR (anti-reflection) coated Germanium of 10" focal length and ZnSe of 5" and 10" focal length lenses. In addition, soft focusing was achieved using collimating mirrors of Cu and Al having focal lengths of 20" and 40" respectively. The latter method of focusing, by producing a long collimated beam, is very useful for investigations that require knowledge of the total volume of sample that interacts with the laser at a given fluence (for example, number of photons absorbed per molecule). By placing a small cell in the path of the collimated beam, but well in front of the focal point, the beam cross-sectional area inside the cell can be safely regarded as constant. Thus, the volume of interaction can be obtained by assuming a cylindrical-shaped beam whose area and volume can be determined by burn patterns on thermal paper.

Determination of laser energy absorbed and, therefore, of the extinction coefficient were done with the above-mentioned power meters and also by optoacoustic techniques. When using the former method, the energy absorption measurements were corrected for window absorption by passing the beam through the cell with and without windows. In most experiments, NaCl windows were used; when far infrared analysis was required following laser excitation, ZnSe windows were used instead.

Cells of different lengths and diameters were used depending on the particular experiment involved. Factors determining the choice were the size of the beam, method of focusing, and whether collisions with the wall would inhibit the desired reaction (particularly for explosions). Typical cells had a pyrex body, of 1" or 2" i.d., and were, when appropriate, rectangular rather than cylindrical so that the phototube could be placed flush against them. Salt windows were invariably used. Infrared emission was detected using both metal (monel) or stainless steel cells with wide-viewing windows and the glass cells already mentioned. The former were used to insure that visible emission was not mistakingly attributed to infrared luminescence. In addition, silicon filters were placed in front of the infrared detectors to block visible luminescence.

All luminescence detection, whether infrared or visible, was performed perpendicular to the laser axis. Infrared emission was viewed through a silicon and, either, germanium or sapphire window combination in conjunction with band pass (Oriel) filters. Detection was achieved with an InSb (Spectronics) photovoltaic detector. The visible fluorescence was observed through either a  $\frac{1}{2}$ -meter Jarrel-Ash monochromator equipped with a 0.10 mm slits (spectral resolution  $\sim 10 \text{ \AA}$ ) or with laser filters (Corion) or band pass filters (Oriel). Photodetection was accomplished with three phototubes, an RCA C31034, a Hamamatsu R955, and an EMI 9816KB. All three phototubes had rise times of 5 nsec or less into  $50 \Omega$ . The detector's signal was preamplified when necessary and displayed on a Tektronix 7704 oscilloscope.

For a limited time, an Optical Multichannel Analyzer (OMA) on loan from Princeton Applied Research was available in our laboratory. This system consists of a 1205A console, 1250D SIT intensified photomultiplier detector, and 1208 polychromator, which is a specially modified Jarrel

Ash 0.25 meter double monochromator. The OMA is a modular electro-optical signal processing system. Optical signals are detected on the target of an image tube which is divided into 500 detection channels. Data may be enhanced by integration over several laser pulses followed by background subtraction of interfering signals. Each of the 500 OMA channels was approximately  $6 \text{ \AA}$  wide as determined by calibration with the 4350, 5461, and 5770  $\text{\AA}$  atomic Hg lines. This system allowed complete scanning of the emission spectrum between 3093  $\text{\AA}$  - 7164  $\text{\AA}$  in 2 laser pulses. The OMA was used to obtain the luminescence spectrum of dielectric breakdown experiments and of explosive chain reactions. Unfortunately, despite numerous attempts, fluorescence signals due to MPA could not be detected by the OMA. It appears that, at least for the model that was used, the signal was both too weak and too fast for the instrument.

The  $\text{CrO}_2\text{Cl}_2$  used was of 99.5% purity, obtained from Research Organic/Inorganic Chemicals Corp. and underwent freeze-thaw cleanout before each experiment. This red liquid was always kept in either a dark bottle or, when attached to the vacuum system, in a glass container which was wrapped with aluminum foil in order to prevent photodecomposition. Similarly, care was taken when running an experiment to minimize the exposure of the vapor to fluorescent light in order to insure that the reaction was due to infrared laser action and not to room lights.

The other gases used were obtained from Matheson and were of research grade with stated purities as follows:  $\text{H}_2$  (99.9%), He (99.5%), and Ar (99.995%). These were used without further purification.

A glass vacuum system was used to handle all gases. Besides the mechanical pump, it was equipped with a two-stage oil diffusion pump. This system, with the cell attached, could be evacuated to  $10^{-6}$  torr. Pressure readings were obtained with either a capacitance manometer

(Baratron, MKS) or an ionization gauge (Veeco RG75N) attached directly to the cell. Typically, the leak rate of the entire gas handling vacuum system was less than 10 mtorr/hour. In addition to the static cells mentioned above, a flow cell was constructed for very low pressure (below 10 mtorr) experiments. A long (65 cm) cell with inlet and outlet ports at the two opposite ends allowed a smooth even flow throughout the cell. The flow rate was calculated to be 2.7 l/sec. This system, besides insuring continuously replenished fresh sample and diminishing collisions with the cell walls during the laser pulse, also insured a constant low pressure of  $\text{CrO}_2\text{Cl}_2$ . This is difficult to obtain in a static cell since  $\text{CrO}_2\text{Cl}_2$  is adsorbed to glass and to vacuum grease, thereby making it difficult to obtain accurate low pressure measurements in static systems. Another advantage of the long cell is that, for low-pressure, weak fluorescence-signal measurements, the focal point--at which fluorescence was observed--can be maintained sufficiently far away from the windows so as to avoid any "window fluorescence." The large laser intensities used in MPD experiments can sometimes exceed the threshold for window damage. This effect can manifest itself in the form of extraneous emission, due to ions, atoms, or ion-electron recombination. In addition, impurities deposited on the windows can lower the intensity threshold of this emission. The gas sample used in multi-photon experiments can promote this window fluorescence by this or other mechanisms, such as heterogeneous reaction at the window surface. A flowing sample, low laser power at the windows, together with a physically distant focal point insure that the observed molecular emission is free of this unwanted experimental artifact. In addition, cells were often wrapped with black tape, leaving only a small uncovered viewing area for the phototube, to prevent detection of any stray light. Analysis of

reactants and products of the laser induced reactions were performed with both a Beckman Model IR-18A and Model IR-10A infrared spectrophotometers. Mass spectral analysis was also utilized via an existing Varian CH-7 spectrometer.

Particle morphology of the  $\text{CrO}_2$  and  $\text{Cr}_2\text{O}_3$  formed in the reactions was determined by Scanning Electron Microscopy (SEM) at the International Nickel Corporation (INCO). The formation of the microparticles could be detected by their diffraction of a visible He-Ne laser beam passed through the cell. This method was also used to insure the freshness of the  $\text{CrO}_2\text{Cl}_2$  gas before reaction.

At this point, prior to the Results Section but having described all the separate details of the experimental methods, it is instructive to discuss a typical fluorescence experiment. The schematic of the apparatus is shown in Figure 3. It is seen that the laser radiation is directed towards the focusing lens which achieves the high power intensity in the cell necessary to produce multiphoton absorption in  $\text{CrO}_2\text{Cl}_2$ , followed promptly by molecular luminescence and/or photochemical reaction. The photodetecting devices are perpendicular to the cell as already mentioned and their output, amplified if necessary, is displayed on the oscilloscope. The signal can be photographed or traced by an X-Y recorder for analysis. Triggering of the scope was accomplished with the pulse generator or, as we unfortunately found out, with the electronic noise from the laser itself.

The last point, that of noise, needs further discussion. It was found that, when the experiment was carried out physically near the laser, interfering electronic noise of amplitude up to 50 mV was detected. In addition, the photodetectors could observe scattered light from the laser discharge which could be as large as the desired

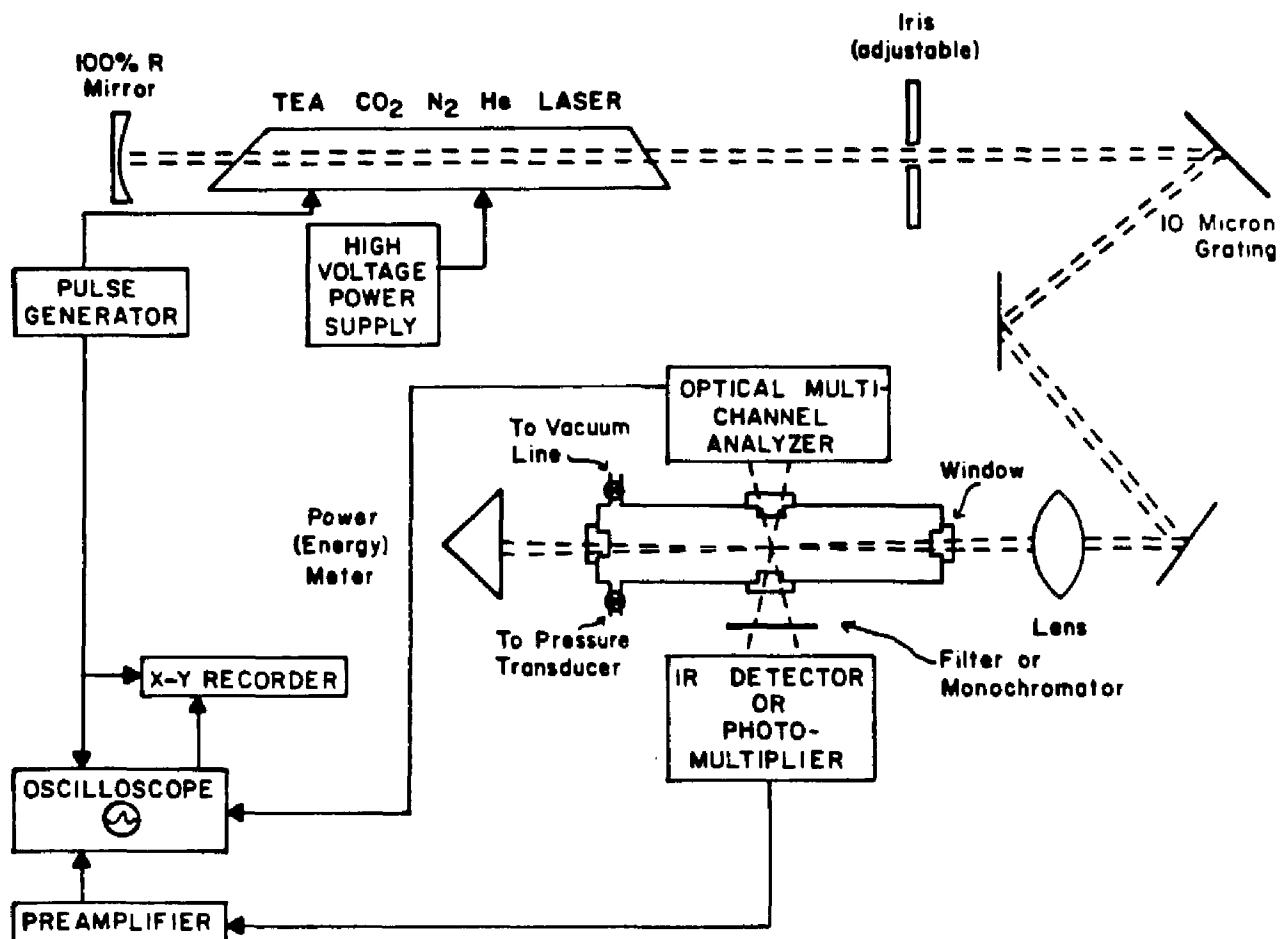


Figure 3. Experimental apparatus for laser-induced fluorescence studies.

signal. To eliminate this problem, the laser radiation was directed with mirrors through a hole in the concrete wall into an adjacent room, a distance of 10-12 meters. The laser power lost by this procedure did not exceed 25%, but a great reduction in both electronic and optical noise was achieved. The scattered light from the laser discharge was avoided, yet scattered room light was still present. To prevent all types of stray light from reaching the phototube, a copper box was constructed and all detection equipment--the cell, monochromator, and phototube--was placed inside the box. Only the BNC cable connected to the scope extended out of this enclosure. The laser radiation was directed into the cell through a small aperture drilled ( $d = 2$  cm) in the box. The focusing lens was placed in front of this hole and outside the box. This allowed for easier handling and, at the same time, it also prevented most visible light from reaching the phototube.

The very low pressure experiments that were carried out with short laser pulses produced very low intensity signals. Because, as already mentioned, with  $N_2$ -free mixtures, the loss of laser energy is great, it was preferable to perform these experiments as close to the laser as possible utilizing the minimum number of auxiliary optics so as to minimize any further energy losses. The above-mentioned copper box proved very useful in this regard. In addition, a ground wire soldered to the box, attached to the ground of the scope, and then to a grounded water drain pipe eliminated, considerably, the electrical noise. With these precautions and with the phototube inside a metal housing to achieve magnetic and electrostatic shielding, good, relatively noiseless signals could be detected even from weakly fluorescing samples.

References

1. S. T. Lin, Ph.D. Dissertation, City University of New York, (1978).
2. P. R. Pearson and H. M. Lambertson, IEEE J. Quant. Electron. QE-8, 145 (1972).

## THEORETICAL BACKGROUND

Although, as already mentioned, infrared laser chemistry has become a bona-fide field of study of physical chemistry pursued by many, the details of the interaction of infrared-laser radiation with molecules are not completely understood. Nevertheless, as experimental activity has multiplied, so has our understanding of the processes involved. Laser induced chemistry can be said to have begun in 1966 with the pioneering work of L. Henry, et al (1), who irradiated ammonia with a continuous wave (cw) laser and obtained both dissociation and visible luminescence from bands of the  $\text{NH}_2$  radical. Subsequently, the first report of infrared multiphoton dissociation by Isenor and Richardson (2) appeared in the literature. Activity continued in this field, culminating in 1974-5 with the almost simultaneous publication by Russian (3) and American (4) groups of isotope separation induced by pulsed  $\text{CO}_2$ -lasers.

Since that discovery using  $\text{SF}_6$ , the H atom of laser chemistry, similar experiments have been done on this (5,6) and other molecules (7) with the same unequivocal result--laser induced dissociation can separate isotopes. The significance of this development, not just from a technical but also from a scientific viewpoint, cannot be overemphasized.

In the case of  $\text{SF}_6$ , for example, when the  $\text{CO}_2$  laser is tuned to the P(20)10.6  $\mu$  line, the exciting radiation coincides with the  $\nu_3$  absorption of  $^{32}\text{SF}_6$ , but not with any infrared band of the  $^{34}\text{SF}_6$  molecule. Essentially, complete reaction, using relatively low pressures of the  $^{32}\text{SF}_6$  species was achieved, whereas most of the  $^{34}\text{SF}_6$  remained unreacted. Similarly, when the exciting radiation was tuned to the  $^{34}\text{SF}_6$   $\nu_3$  absorption feature (at  $925\text{ cm}^{-1}$ ), it was this isotope, rather than the  $^{32}\text{S}$ , that underwent reaction. Therefore, the results are clear

proof of the selectivity of the laser excitation.

However, if one considers that a  $\text{CO}_2$  laser photon ( $\sim 1000 \text{ cm}^{-1}$ ) contains approximately 2.9 kcal/mole and that, in order to break the S-F bond, 93 kcal/mole of energy is needed, the conclusion is reached that each  $\text{SF}_6$  molecule, in the absence of dielectric breakdown, must absorb at least 32 photons in order to dissociate. As it is well known, the vibrations of molecules are anharmonic rather than harmonic. This fact results in a reduction in the energy difference between successive levels of a vibrational mode as the quantum number,  $v$ , increases. Therefore, we must explain theoretically the interaction of this anharmonic oscillator with the monochromatic laser radiation. As we shall subsequently see, for medium (at least 4 atoms) and large polyatomics, the resonance requirement must be maintained for at least the first 4 or 5 levels of the vibrational ladder. This maintenance of coherence has been explained by either one or a combination of a few factors. One of these is the dynamic Stark effect. In the intense fields provided by pulsed- $\text{CO}_2$  laser radiation, line absorption broadening is induced via splitting of molecular vibrational-rotational sublevels. This broadening, a result of the dynamical Stark shift, can partially offset the anharmonicity of the vibrational levels. For a diatomic molecule (rigid rotor approximation), the magnitude of the splitting is given by the equation (8)

$$\Delta v = \left(\frac{B_e}{2}\right)\left(\frac{\mu E}{h\nu}\right)^2, \quad \text{cm}^{-1} \quad (1)$$

where  $B_e$  is the rotational constant in  $\text{cm}^{-1}$ ,  $\mu$  is the mean value of the transition dipole moment matrix element between vibrational transitions in  $\text{esu}\cdot\text{cm}$ ,  $E$  is the electric field strength in  $\text{statvolts}/\text{cm}^2$ ,  $h$  is

Planck's constant, and  $\nu$  is the laser frequency in  $\text{sec}^{-1}$ . In order to calculate this effect for  $\text{CrO}_2\text{Cl}_2$ , one must obtain the transition dipole matrix element,  $\mu$ . This was done using the equation (9)

$$|\mu|^2 = \frac{3hc(B_0)(1000)}{8\pi^3 N \nu}, \quad \text{esu}^2 \cdot \text{cm}^2 \quad (2)$$

where  $c$  is the speed of light,  $\nu$  is the absorption frequency in  $\text{sec}^{-1}$ , and  $B_0$  is the integrated band intensity in units of  $\text{cm}^{-1} \text{sec}^{-1} \text{liters mole}^{-1}$ . The latter was obtained for  $\text{CrO}_2\text{Cl}_2$  by graphical integration of the absorption band of  $\text{CrO}_2\text{Cl}_2$  at about  $1000 \text{ cm}^{-1}$  at a saturating pressure. This band is due to two transitions (see Table I),  $\nu_1$  at  $995 \text{ cm}^{-1}$  and  $\nu_6$  at  $1000 \text{ cm}^{-1}$ . No attempt was made to resolve these two transitions, since being practically degenerate and both coincident with the exciting laser frequency, it would be impossible to separate their respective effects on the MPA process. Thus, the dipole moment matrix element obtained from this procedure is a rough estimate of the strength of the combined transitions. Using this prescription, a value of 0.40 Debye or  $4.0 \times 10^{-19} \text{ esu} \cdot \text{cm}$  was obtained for  $|\bar{\mu}|$ . Inserting this value into equation (1) and using a value (10) of  $0.1073 \text{ cm}^{-1}$ , that of the largest rotational constant (A) in  $\text{CrO}_2\text{Cl}_2$ , for  $B_e$ , we obtain a value of  $0.0040 \text{ cm}^{-1}$  for the Stark splitting in the presence of a typical laser field of  $10^6 \text{ V/cm}^2$  ( $3.3 \times 10^3 \text{ statvolts/cm}^2$ ).

Although the anharmonicity of the  $\nu_1 + \nu_6$  absorption features are not known, since their respective overtones have not been observed, we estimate the anharmonic shift to be of the order of  $5\text{-}10 \text{ cm}^{-1}$  for the first overtone transitions. This estimate is consistent with the shift observed for the combination band  $\nu_1 + \nu_6$  (11,12) in  $\text{CrO}_2\text{Cl}_2$ . Not-

withstanding the approximations used, the important fact is that, for  $\text{CrO}_2\text{Cl}_2$ , the dynamic Stark shift ( $.004 \text{ cm}^{-1}$ ) plays a negligible role in overcoming the red shift as the molecule is driven up the vibrational ladder.

Another effect which may partially maintain coherent absorption of the laser radiation is the phenomenon known as power broadening (8). This phenomenon, which is commonly observed in NMR and microwave experiments, is not normally important in other branches of spectroscopy. In infrared-laser pumping, however, because of the high electric fields present, power broadening, or a.c. Stark effect as it is sometimes called, must be taken into account. Basically, this perturbation arises because a transition between oscillator levels occurs in a time which is short compared to the time in which the laser field gets out of phase with the oscillator. A normal Boltzmann distribution between the levels cannot be obtained; the result is a decreased extinction coefficient and a broadening of the absorption line. This effect is characterized by the Rabi frequency,  $\bar{\nu}_R$ , whose average value is given by

$$\bar{\nu}_R = \frac{\mu E_0}{hc}, \quad \text{cm}^{-1} \quad (3)$$

where the terms have already been defined. Again, using a typical field of  $3.3 \times 10^3 \text{ statvolts/cm}^2$ , and  $\mu = 4.0 \times 10^{-19} \text{ esu}\cdot\text{cm}$ , we obtain a value of  $\bar{\nu}_R = 6.7 \text{ cm}^{-1}$  for the  $\text{CrO}_2\text{Cl}_2$  transition coincident with the  $\text{CO}_2$  laser radiation. As was done above for the Stark effect, we must compare the broadening, namely  $\bar{\nu}_R$ , with the detuning  $(\bar{\nu} - \bar{\nu}_0)$ , where  $\bar{\nu}$  is the frequency and  $\bar{\nu}_0$  is the oscillator frequency. It is clear that, although this is a much more significant effect than the Stark shift,

power broadening can, at most, compensate for the detuning of the first few up-the-ladder transitions in  $\text{CrO}_2\text{Cl}_2$ . When one realizes that it takes approximately 25 i.r. photons to dissociate this molecule, it becomes evident that other factors must also be responsible for multiphoton absorption. This discrepancy is not particular to  $\text{CrO}_2\text{Cl}_2$ . Thus, for the much-studied  $\text{SF}_6$  molecule, a similar Rabi frequency calculation yields  $\bar{\nu}_R = 5 \text{ cm}^{-1}$  and a Stark effect shift which is negligible ( $< 0.03 \text{ cm}^{-1}$ ). Assuming an anharmonicity constant of about  $10 \text{ cm}^{-1}$  (13,14) for the  $\nu_3$  mode of this molecule, it is again evident that these field-induced effects can only be partly responsible for the maintenance of resonance in MPD experiments.

A concept that explains absorption of the first three infrared photons is the "triple vibrational-rotational resonance" or "PQR transitions" model proposed by Ambartzumian, et al (15). Basically, it attributes maintenance of coherence in the vibrational manifold to rotational shifts in the absorbing sequence. If the laser is tuned to the P-branch of the vibrational band, then the first absorption can be represented by ( $\nu=0, J \rightarrow \nu=1, J-1$ ). The second step will be ( $\nu=1, J-1 \rightarrow \nu=2, J-1$ ), a Q-branch transition, and finally the R-branch transition ( $\nu=2, J-1 \rightarrow \nu=3, J$ ) will excite the second overtone. Thus, it is rotational compensation of anharmonicity that, according to this model guarantees the resonance condition for the first three steps of the vibrational ladder, even at modest power densities. Although we shall discuss the evidence in support of the "PQR" concept shortly, it should be mentioned that calculations on  $\text{SF}_6$  (15) seem to indicate that this mechanism can indeed compensate for the vibrational anharmonicity in this molecule.

There are other factors which can, to different degrees in different molecules, compensate for vibrational detuning of the molecular transition frequency from that of the incident laser. Thus, effects such as anharmonic splitting of vibrational overtone levels of a degenerate mode (16), Fermi resonance between overtones or combination bands and fundamentals, and hindered internal rotations (17) about a particular molecular bond, which provides for strong vibrational-vibrational and vibrational-rotational coupling, can also compensate for anharmonicity. However, in general, the current belief is that power broadening and PQR resonant excitation are the major factors responsible for the absorption of the first few photons in on-resonance laser induced chemistry.

As has been stated before, infrared collisionless multiphoton dissociation typically requires the absorption of 20 or more photons. The mechanisms which have been discussed above can account for, perhaps, the first three to five transitions. Once this energy range is reached, maintenance of resonance between the molecular vibrational levels and the laser radiation must be achieved by other means. For polyatomic molecules with several vibrational degrees of freedom, the density of vibrational states grows rapidly with increasing energy. It was postulated by Bloembergen and colleagues (18,19) that, in this region, dubbed the quasicontinuum, the resonance condition is maintained because of the large number of states available. Thus, the molecule can gain enough energy until the third region, the dissociative continuum, is reached. Perhaps, the best way to view the quasicontinuum is to isolate the discrete levels that interact strongly with the laser radiation (the  $\nu_1$  and  $\nu_6$  levels in  $\text{CrO}_2\text{Cl}_2$ ) and to view the other modes as the

reservoir. The excited modes are coupled to the reservoir via anharmonic terms of the potential energy function. These terms, of course, also increase as the density of states increases. Basically, the quasicontinuum begins when the width caused by this vibrational relaxation or damping is considerably larger than the anharmonic defect. For  $\text{SF}_6$ , for example, this condition is believed to occur when the density of states is about  $10^4/\text{cm}^{-1}$  or when the molecule has absorbed 3-5  $\text{CO}_2$  i.r. photons (18,19). Since  $\text{CrO}_2\text{Cl}_2$  is a smaller molecule with fewer infrared-active modes, it can be safely assumed that the onset of the quasicontinuum occurs at an even higher energy. The theoretical description of MPA and MPD based on the three regions--the first characterized by discrete levels with little intrastate mixing, the quasicontinuum exhibiting strong coupling between the excited mode and background states, and the dissociative continuum--is well established experimentally. A brief review of the evidence will now be given.

The most salient feature of i.r. laser multiphoton excitation is that it is isotope selective. If the infrared isotope shift is large enough, the laser can be tuned to coincide with the absorption feature of only one of the molecular isotopic species. Therefore, only this isotope reacts as long as the pressures are low enough to prevent collisional energy transfer. Multiphoton isotope separation has been observed in many systems including  $\text{SF}_6$  (3,4),  $\text{SF}_5\text{Cl}$  (20), and  $\text{OsO}_4$  (21). This fact supports the existence of at least one region, the first, where absorption is selective and where the resonance condition must be maintained.

An elegant experiment performed by Ambartzumian, et al (22) corroborated the mechanism of multiphoton absorption. These Russian

workers dissociated  $\text{SF}_6$  using two lasers. Low power radiation from the first laser excited the  $^{32}\text{SF}_6$  molecules to about the second overtone of the  $\nu_3$  vibrational mode. A second  $\text{CO}_2$  pulse, completely detuned from any  $\text{SF}_6$  absorption band, was capable of dissociating the  $^{32}\text{SF}_6$  molecules using considerably smaller laser-field intensities than those required for single-frequency fragmentation. Thus, this experiment, which has been repeated on other molecules, supports the notion of a quasicontinuum in which resonance between the laser radiation and a molecular absorption feature is not required. Additionally, they showed that optimal isotopic separation and yields were obtained when the first laser was detuned  $10\text{ cm}^{-1}$ , to the red, from the resonance line. This, they concluded, corroborated the PQR mechanism previously described.

Lastly, it should be mentioned that the probability of dissociation has been found to be strongly dependent on energy density or fluence ( $\text{joules/cm}^2$ ) and only slightly dependent on power intensity or peak power of the laser pulse (19,23,24). This means that sequential absorption of photons and not non-linear effects is playing an important role in MPD. Furthermore, since as we saw, the Rabi frequency is proportional to the electric field and, therefore, to the square root of the power intensity, power broadening must be playing only a minor role (i.e., only in the first region) in determining the extent of dissociation as long as a minimum power threshold is exceeded. Again these results, obtained by varying the pulse width, point to the validity of the currently accepted mechanism of MPD and, particularly, of the importance of the quasicontinuum.

Many theoretical treatments of MPD and, particularly, of the quasicontinuum have been published (for example, see 15,25,26, and 34).

Although most of these agree on the basic descriptions discussed in the preceding pages, some questions still remain. Perhaps the most pressing question is that of the distribution of energy among the normal modes of the laser excited molecule. It is a fact that in most if not all the MPD experiments done to date, it is the weakest bond that is broken regardless of the mode that is excited. This implies that some energy redistribution must occur since vibrational energy must be fed into, say, the S-Cl bond of SF<sub>5</sub>Cl in order to break it, although it was the S-F mode that was resonant with the exciting laser field (20). Moreover, from the velocity distribution of dissociation fragments that were measured under molecular beam conditions, Lee and co-workers (27,28) have concluded that the absorbed laser radiation is randomly distributed when the molecule has sufficient energy to dissociate. Recently, two different groups of workers (19,29,27,28) have shown that the collisionless dissociation of SF<sub>6</sub> by CO<sub>2</sub>-laser radiation can be treated using the RRKM theory of unimolecular reactions. This picture of MPA followed by dissociation has led to rate-equation descriptions of the process. Ignoring the discrete-level absorption process, the time evolution of the population in level  $m$ ,  $N_m$ , at an energy of  $mh\nu$  may be described (25,28) by

$$\frac{dN_m}{dt} = \frac{I(t)}{h\nu} \left[ \sigma_{m-1} N_{m-1} + \frac{g_m}{g_{m+1}} \sigma_m N_{m+1} - \left( \frac{g_{m-1}}{g_m} \sigma_{m-1} + \sigma_m \right) N_m \right] - k_m N_m \quad (4)$$

where  $I(t)$  is the laser intensity,  $g_m$  is the density of vibrational states of level  $m$ ,  $\sigma_m$  is the absorption cross section from level  $m$  to level  $(m + 1)$  and  $k_m$  is the dissociation rate constant from level  $m$  which may be calculated using the statistical RRKM model for unimolecular

reactions. We may rearrange this equation to yield

$$dN_m = [\sigma_{m-1}N_{m-1} + \frac{g_m}{g_{m+1}}\sigma_m N_{m+1} - (\frac{g_{m-1}}{g_m}\sigma_{m-1} + \sigma_m)N_m] \frac{I(t)}{h\nu} dt - k_m N_m dt \quad (5)$$

Expression (5) shows explicitly that all the radiative terms are multiplied by a factor,  $I(t)dt$ . Thus, the absorption process and, since the dissociation rate is relatively small (and identically zero below the dissociative continuum), the temporal evolution of the population is directly proportional to intensity  $\times$  time = energy fluence (joules/cm<sup>2</sup>). That such kinetic treatments have been successfully used in interpreting the gross features of multiphoton absorption followed by dissociation of several polyatomic molecules (25,28) emphasizes the importance of the quasicontinuum in laser-induced chemistry. It should be evident, however, that it is the discrete levels that render the process isotope-selective and, therefore, their effect on the overall excitation process may be small but not insignificant. Furthermore, any hope of attaining bond-selective laser chemistry rests on maintaining coherence all the way up the vibrational ladder.

Although successful in describing the gross features of the process, master equations, such as (4), rely on prompt ( $\sim 10^{-12}$  seconds) (30) vibrational energy redistribution in the quasicontinuum. There is evidence (31,32), however, that at least in some molecules IVR may be considerably slower. Moreover, in a recent multiphoton experiment by Hall and Kaldor (33), the branching ratio of two distinct dissociation channels of cyclopropane, isomerization, and fragmentation appears to depend on the frequency of the exciting laser radiation. These results, and others (34), may indicate that only partial energy randomization is operative in the time domain of interest.

i.e., IVR is fast within certain groups of states but slow among the different groups. This evidence has spawned new theoretical approaches. Schek and Jortner (35), for example, have proposed a theory based on the random coupling model, which rests on the concept that radiative coupling terms in the quasicontinuum exhibit a large variation in both sign and amplitude and, therefore, the IVR concept is omitted in this treatment.

It should be emphasized that, whether the absorbed energy is completely or partially randomized and whether it is coupling among the high lying vibrational states of the molecule or IVR that is the correct description of the process, the results are the same; the weakest dissociation channel is overwhelmingly followed. However, and particularly with respect to the work described in this thesis, treatment of the process by RRKM theory does not explain the collisionless production of electronically excited fragments and/or parent molecules by MPA followed by dissociation. Thus, allowance must be made in these treatments for the possibility of populating excited electronic states via these processes.

References

1. C. Borde, A. Henry and L. Henry, *Compt. Rend. Academ. Sci. (Paris) B*, 262, 1389 (1966).
2. N. R. Isenor and M. C. Richardson, *Appl. Phys. Lett.* 18, 225 (1971).
3. R. V. Ambartzumian, V. S. Letokhov, E. A. Ryabov, and N. V. Chekalin, *JETP Lett.* 20, 273 (1974).
4. J. L. Lyman, R. V. Jensen, J. Rink, C. P. Robinson, S. D. Rockwood, *Appl. Phys. Lett.* 27, 87 (1975).
5. J. L. Lyman, S. D. Rockwood and S. M. Freund, *J. Chem. Phys.* 67, 4545 (1977).
6. M. E. Gower and K. W. Billman, *Opt. Comm.* 20, 123 (1977).
7. J. L. Lyman, G. P. Quigley and O. P. Judd, in Multiple-Photon Excitation and Dissociation of Polyatomic Molecules, edited by C. Cantrell (Springer-Verlag, Heidelberg, West Germany, 1980).
8. J. P. Aldridge, J. H. Birely, C. D. Cantrell and D. C. Cartwright, in Physics of Quantum Electronics, edited by S. F. Jacobs, M. Sargent III, N. O. Scully and C. T. Walken, (Addison-Wesley, Reading, Mass., 1977).
9. M. D. Harmony, Introduction to Molecular Energies & Spectra, Holt, Rinehart & Winston, Inc., New York (1972).
10. J. A. Blazy and D. H. Levy, *J. Chem. Phys.* 69, 2901 (1978).
11. W. E. Hobbs, *J. Chem. Phys.* 28, 1220 (1958).
12. F. A. Miller, G. L. Carlson & W. B. White, *Spectrochim. Acta* 9, 709 (1959).
13. R. S. McDowell, J. P. Aldridge, and R. F. Holland, *J. Phys. Chem.* 80, 1203 (1976).
14. H. Kildal, *J. Chem. Phys.* 67, 1287 (1977).
15. R. V. Ambartzumian and V. S. Letokhov, *Acc. Chem. Res.* 10, 61 (1977).
16. C. D. Cantrell and H. W. Galdbraith, *Optics Commun.*, 21, 374 (1977).
17. C. D. Cantrell, S. M. Freund and J. L. Lyman in Laser Handbook edited by M. Stinch, (North Holland, New York, 1978) Vol. 3.
18. N. Bloembergen, *Opt. Commun.*, 15, 416 (1975).
19. J. G. Black, E. Yablonovitch, N. Bloembergen and S. Mukamel, *Phys. Rev. Lett.* 38, 1131 (1977).

20. K. M. Leary, J. L. Lyman, L. B. Asprey and S. M. Freund, *J. Chem. Phys.* 68, 1671 (1978).
21. R. V. Ambartzumian, Yu. A. Gorokhov, G. N. Makarov, A. A. Puretskii, and N. P. Furzikov, *Chem. Phys. Lett.* 45, 231 (1977).
22. R. V. Ambartzumian, Yu. A. Gorokhov, V. S. Letokhov, G. N. Makarov, A. A. Puretskii, and N. P. Furzikov, *Pis'ma Zh. Eksp Teor. Fig.* 23, 217 (1976).
23. J. L. Lyman and S. D. Rockwood, *J. Appl. Phys.* 47, 595 (1976).
24. J. L. Lyman, W. C. Danen, A. C. Nilsson and A. V. Nowak, *J. Chem. Phys.* 71, 1206 (1979).
25. N. Bloembergen and E. Yablonovitch, *Phys. Today*, 31, 23 (1978).
26. S. Mukamel and J. Jortner, *Chem. Phys. Lett.* 40, 150 (1976).
27. M. J. Coggiola, P. A. Schulz, Y. T. Lee and Y. R. Shen, *Phys. Rev. Lett.* 38, 17 (1977).
28. Aa. S. Subdø, P. A. Schulz, E. R. Grant, Y. R. Shen and Y. T. Lee, *J. Chem. Phys.* 70, 912 (1979).
29. J. G. Black, P. Kolodner, M. J. Shultz, E. Yablonovitch, and N. Bloembergen, *Phys. Rev. A* 19, 704 (1979).
30. H. S. Kwok and Eli Yablonovitch, *Phys. Rev. Lett* 41, 745 (1978).
31. R. Naaman, D. M. Lubman, and R. N. Zare, *J. Chem. Phys.* 71, 4192 (1979).
32. K. V. Reddy, M. J. Berry, *Chem. Phys. Lett.* 66, 223 (1979).
33. R. Hall and A. Kaldor, *J. Chem. Phys.* 70, 4027 (1979).
34. R. G. Bray and M. J. Berry, *J. Chem. Phys.* 71, 4909 (1979).
35. I. Schek and J. Jortner, *J. Chem. Phys.* 70, 3016 (1979).

## RESULTS

The observation of ultraviolet and visible luminescence in infrared-laser induced multiphoton dissociation (MPD) experiments is well documented (1-10). In many of these studies, the pressures were too high, given the width of the laser pulse, for the excitation to be truly collisionless. Recently, however, the observation of MPD in molecular beams (11,12) and the detection of ultraviolet and visible fluorescence at very low pressures (13) give credence to the collisionless production of electronically excited species via infrared multiphoton absorption (MPA) followed by dissociation.

The emission in the above-mentioned reports was thought to be due to one or more of the following processes. Firstly, at relatively high fluences, optical dielectric breakdown can be induced with an infrared laser, and this process, in turn, produces electronic luminescence that can be ascribed to high energy species such as ions and radicals. Secondly, the emission has been ascribed to radical recombination or to subsequent chemical reaction of the fragments. Thirdly, recombination of charged species can result in luminescence. Fourthly, the formation of electronically excited products can yield ultraviolet as well as visible emission.

One unifying feature of all these processes is that the luminescence is thought to originate from daughter species (fragments, products, etc.) rather than from the parent molecule. This is merely a confirmation of the general rule that the ground state of a molecule correlates adiabatically with ground state products. Thus, electronic emission is mostly observed when either the pressure is high and/or the laser power is sufficient to induce dielectric breakdown.

This study--the MPA and MPD of  $\text{CrO}_2\text{Cl}_2$  is, to our knowledge, the first to report (14,15) the production of electronically excited parent molecules via infrared-laser pumping. The  $\text{CrO}_2\text{Cl}_2$  emission was detected, as will be shown below, in the collisionless regime and, therefore, must be ascribed directly to the laser excitation.

Before embarking on a detailed description of the experiments and the results, it is worthwhile to briefly discuss the features that made  $\text{CrO}_2\text{Cl}_2$  a prime candidate for  $\text{CO}_2$ -laser induced collisionless V-E transfer, a phenomenon that has been dubbed "inverse electronic relaxation" (16). The key feature that  $\text{CrO}_2\text{Cl}_2$  possesses, aside from the obvious need for a coincident absorption with the  $\text{CO}_2$ -laser radiation, is at least one excited electronic state whose energy is below that of the dissociation limit. The energy required to rupture the  $\text{CrO}_2\text{Cl}-\text{Cl}$  bond (the weakest one) is estimated to be 83 kcal/mole from mass spectrometric studies (17) and 68 kcal/mole from the appearance potential of photodecomposition products (18). In either case, the dissociation limit exceeds the origin of the first excited state by 19-34 kcal/mole. Actually, as we will see, there are at least two additional excited electronic states which are almost degenerate with the lowest one. Thus, on energy considerations alone, population of electronically excited states via infrared-laser excitation is a highly probable channel in this molecule.

$\text{CrO}_2\text{Cl}_2$  was investigated spectroscopically as early as 1933 (19); vibrational gas phase assignments were relatively easy since the molecule is nearly tetrahedral and yet retains the  $\text{C}_{2v}$  symmetry (20). The vibrational bands are listed in Table I (20-23) and shown in Figure 1 under low resolution. The strong absorption near  $10 \mu$  is due to both the  $\nu_1(\text{A}_1)$  symmetric Cr-O stretch at  $995 \text{ cm}^{-1}$  and the  $\nu_6(\text{B}_1)$  asymmetric

Cr-O stretch at  $1000\text{ cm}^{-1}$ . The existence of this strong absorption, the high vapor pressure of the system and the early spectroscopic observation of resolvable vibrational (and rotational) structure in the electronic spectrum, both in absorption and emission, combine to make  $\text{CrO}_2\text{Cl}_2$  a unique candidate for MPA experiments.

In recent years, both the dynamic and conventional electronic spectroscopic investigations of  $\text{CrO}_2\text{Cl}_2$  in gas and solid phases have been extensive. Dunn and co-workers (24,25) have measured both the absorption and emission spectra of the solid as single crystal at 1.7 K and in Argon matrices at 4 K. Their observations culminated in three observed band systems in the region  $3800\text{ \AA} - 6000\text{ \AA}$ : a weak system whose origin was at  $5891\text{ \AA}$ , a stronger one at  $5796\text{ \AA}$ , and a structureless system beginning at  $4400\text{ \AA}$ . The  $5891$  and  $5796$  systems were assigned as transitions to the lowest triplet and singlet respectively. The  $5796\text{ \AA}$  singlet was further identified as that giving rise to the early gas phase absorption study by Kronig (19).

More recent studies by McDonald (26) concentrated on both the dynamics and spectroscopy in the gas phase. He found that the fluorescence quantum yield drops to near zero at wavelengths shorter than  $5650\text{ \AA}$ . He attributes this fact to either photodissociation at longer wavelengths than that ( $4200\text{ \AA}$ ) reported by Halonbrenner (17) and/or to radiationless processes. McDonald's work also shows that only the vibrationally cold level in the excited state is free of radiationless decay. More recently, Blazy and Levy (27), using a free jet expansion system, have shown that fluorescence is negligible blue of  $5550\text{ \AA}$ . Assuming that, in their vibrationally cold relatively collisionless jet, these workers can observe emission from higher members of the vibrational progressions of the excited state, these results are in good agreement

with McDonald's work.

Molecular orbital calculations (28,29,30) assign the highest occupied molecular orbitals as  $B_1$ ,  $B_2$ , and  $A_2$  in symmetry ( $C_{2v}$ ), all lying very close in energy. The first virtual orbital is thus  $A_1^*$  which is strongly Cr-Cl anti-bonding and weakly Cr-O bonding. Thus, the three expected excited electronic states are  $A_2$ ,  $B_1$ , and  $B_2$ . The origins of the first excited systems are near  $17,200 \text{ cm}^{-1}$  and the energy discrepancy between these near-lying states is thus around  $200\text{-}300 \text{ cm}^{-1}$ . An additionally interesting semi-classical calculation (31) shows that the density of ground state vibrational levels near the  $17,200 \text{ cm}^{-1}$  origin is approximately  $3 \times 10^6$  per  $\text{cm}^{-1}$ .

A study by Halonbrenner, et al (18) using flash photolysis indicated that  $\text{CrO}_2\text{Cl}_2$  photodissociates to yield  $\text{CrO}_2$  and  $\text{Cl}_2$  via formation of the transient  $\text{CrO}_2\text{Cl}$ . Furthermore, these workers tentatively assigned the electronic spectra of  $\text{CrO}_2\text{Cl}$  and  $\text{CrO}_2$ . Based on these results, three wavelengths, namely  $6300 \text{ \AA}$ ,  $5300 \text{ \AA}$ , and  $4000 \text{ \AA}$ , which are sufficiently far apart to be identified as originating from  $\text{CrO}_2\text{Cl}_2$ ,  $\text{CrO}_2$ , and  $\text{CrO}_2\text{Cl}$ , respectively, were chosen for detailed analysis.

Armed with this brief introduction, we will now describe the results of our work on  $\text{CrO}_2\text{Cl}_2$ , which we believe is only the first of a family of molecules which will exhibit IER upon infrared-laser excitation.

The  $\text{CrO}_2\text{Cl}_2$  infrared frequencies are shown in Table I and the absorption spectrum, under low resolution, is shown in Figure 1. As already mentioned, there are two absorptions,  $\nu_1$  and  $\nu_6$  in the  $10 \mu$  region that coincide with the  $\text{CO}_2$ -laser emission. These correspond to the Cr-O symmetric stretch at  $995 \text{ cm}^{-1}$  and to the asymmetric Cr-O stretch

TABLE 1. Published vibrational frequencies of  $\text{CrO}_2\text{Cl}_2$  (ground state).<sup>a</sup>

Symmetry ( $C_{2v}$ )	Mode	$\nu$ ( $\text{cm}^{-1}$ )	Description
$A_1(z)$	$\nu_1$	995 <sup>b</sup>	Cr-O stretch
	$\nu_2$	475 <sup>b</sup>	Cr-Cl stretch
	$\nu_3$	356 <sup>b</sup>	$\text{CrO}_2$ bend
	$\nu_4$	140 <sup>c</sup>	$\text{CrCl}_2$ bend
$A_2$	$\nu_5$	224 <sup>c</sup>	$\text{O}_2\text{-Cl}_2$ torsion
$B_1(x)$	$\nu_6$	1000 <sup>b</sup>	Cr-O stretch
	$\nu_7$	215 <sup>c</sup>	$\text{CrO}_2$ rock
$B_2(y)$	$\nu_8$	500 <sup>b</sup>	Cr-Cl stretch
	$\nu_9$	257 <sup>c</sup>	$\text{CrCl}_2$ rock

<sup>a</sup>As taken from Ref. 21<sup>b</sup>Vapor values 20<sup>c</sup>Liquid values 22, 23

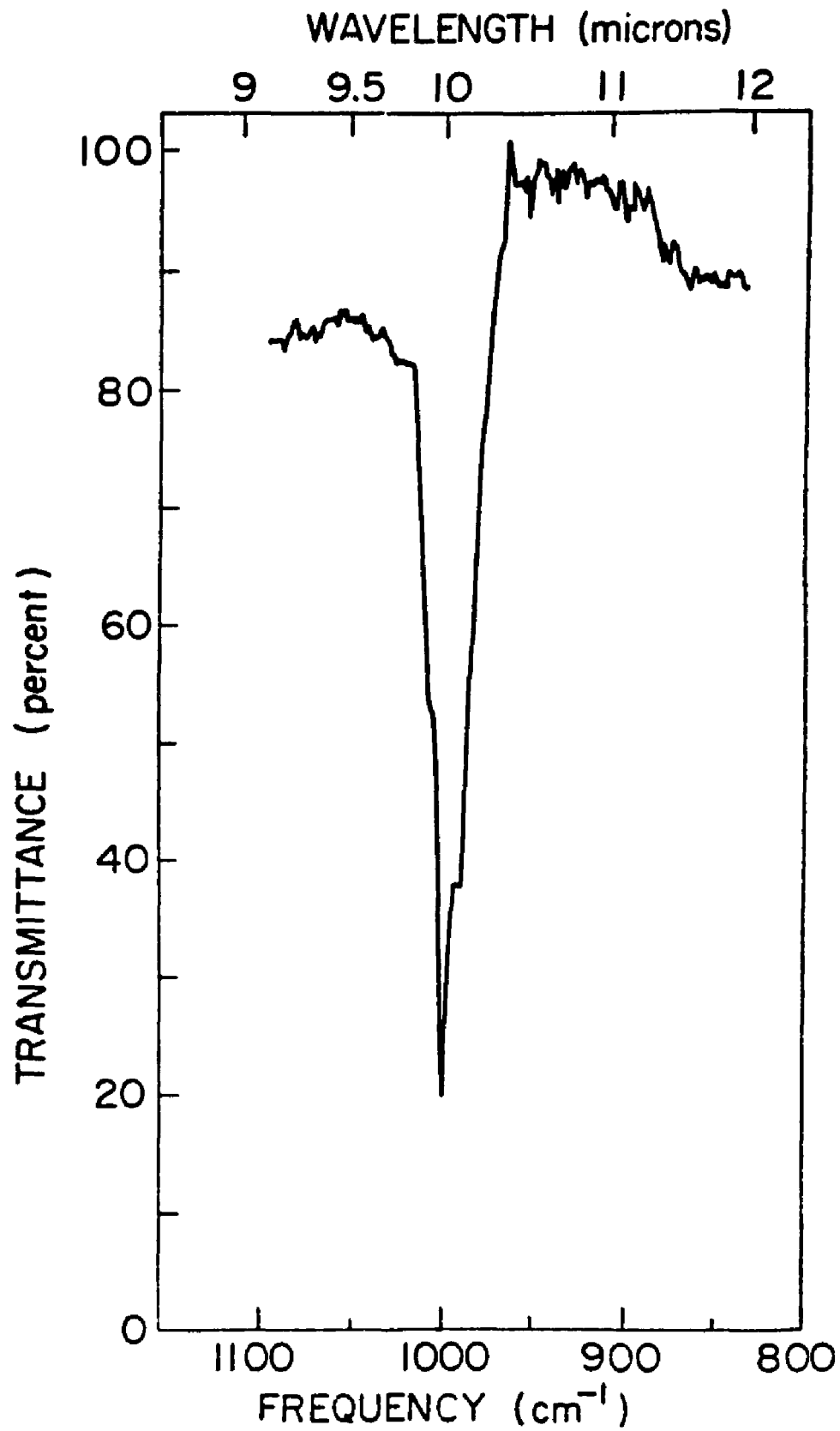


Figure 1. The infrared spectrum of  $\text{CrO}_2\text{Cl}_2$  (5 torr).

at  $1000\text{ cm}^{-1}$  respectively. Absorption measurements, with unfocused geometry utilizing both conventional power-meter and opto-acoustic techniques, revealed  $\text{CrO}_2\text{Cl}_2$  absorption of radiation from the R-branch transitions of the  $10.6\ \mu$  band of the  $\text{CO}_2$  laser. No significant absorption could be detected using P-branch  $10.6\ \mu$  transitions or those from the  $9.6\ \mu$  band. Figure 2 displays the absorption spectrum obtained using opto-acoustic measuring techniques. Conventional absorption experiments, measured at three laser fluences, yielded absorption coefficients of  $0.074\text{ cm}^{-1}$  and  $0.0035\text{ cm}^{-1}$  for the R(30) and R(20) lines respectively. Thus, both techniques yielded similar results. Upon focusing the laser radiation from the  $10.6\ \mu$  R-branch transitions into a cell containing  $\text{CrO}_2\text{Cl}_2$ , an orange emission can be detected across the cell. A picture of the fluorescence is shown in Figure 3. No fluorescence is observed when  $\text{CrO}_2\text{Cl}_2$  is irradiated with P-branch transitions of the  $10.6\ \mu$  band nor with transitions of the  $9.6\ \mu$  band. At times, emission was observed using the P-branch transitions. However, this luminescence was not consistently observed and invariably freeze-thaw cleanout of the  $\text{CrO}_2\text{Cl}_2$  sample would eliminate it. Therefore, P-branch induced luminescence is probably due to impurities in the gas. Only under severe conditions--relatively high pressure, energies above 2.0 J, and very tight (5.0 in lens) focusing--could  $10.6\ \mu$  P-branch laser radiation consistently induce fluorescence in a clean  $\text{CrO}_2\text{Cl}_2$  sample. In this regard, it is important to reiterate and perhaps amplify on the care that must be taken when performing MPD experiments. Not only can emission result from sample impurities, but also, at the high laser intensities (megawatts and gigawatts) used in these studies, from window fluorescence. Either by exceeding the

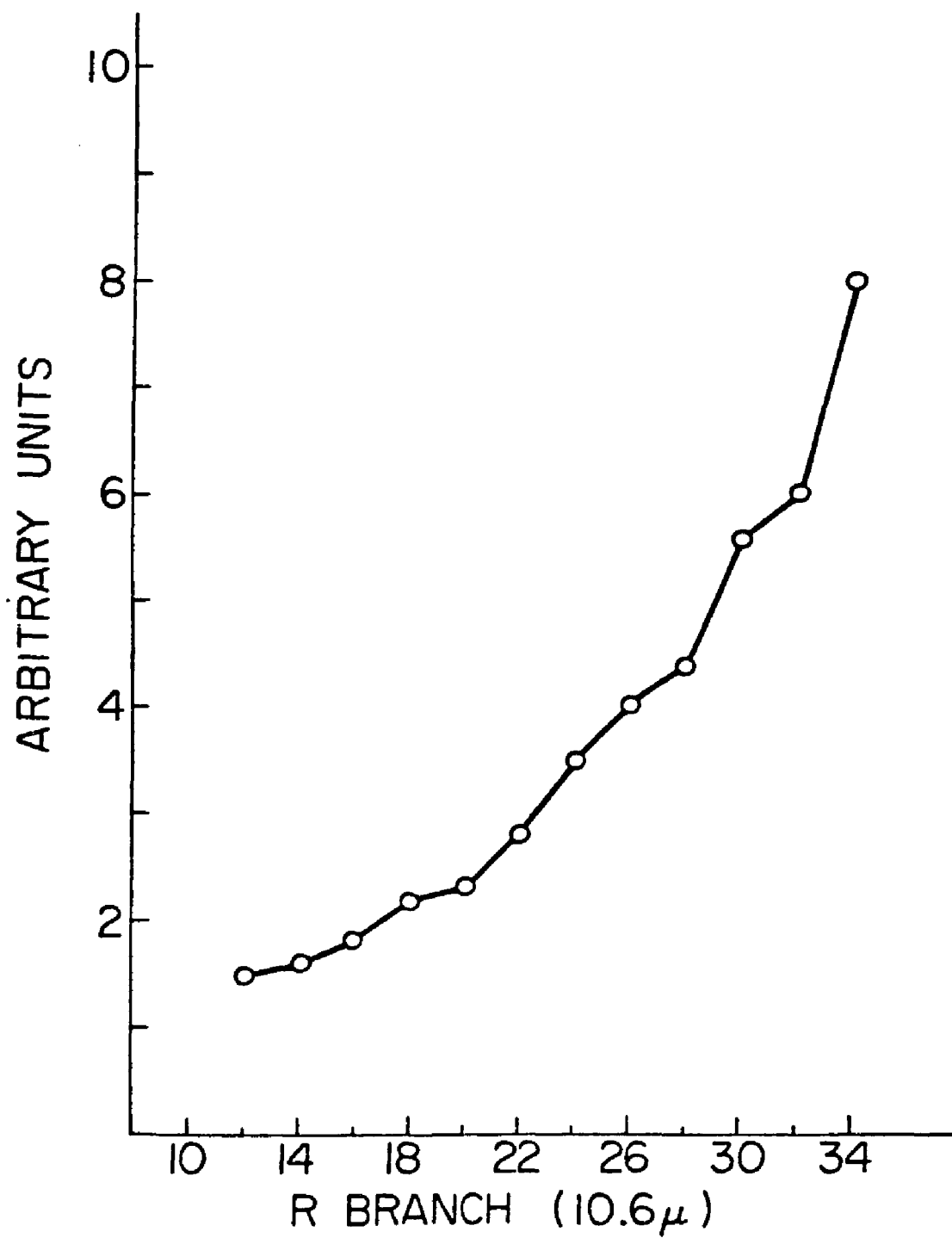


Figure 2. The opto-acoustic signal from  $\text{CrO}_2\text{Cl}_2$  (unfocused geometry).

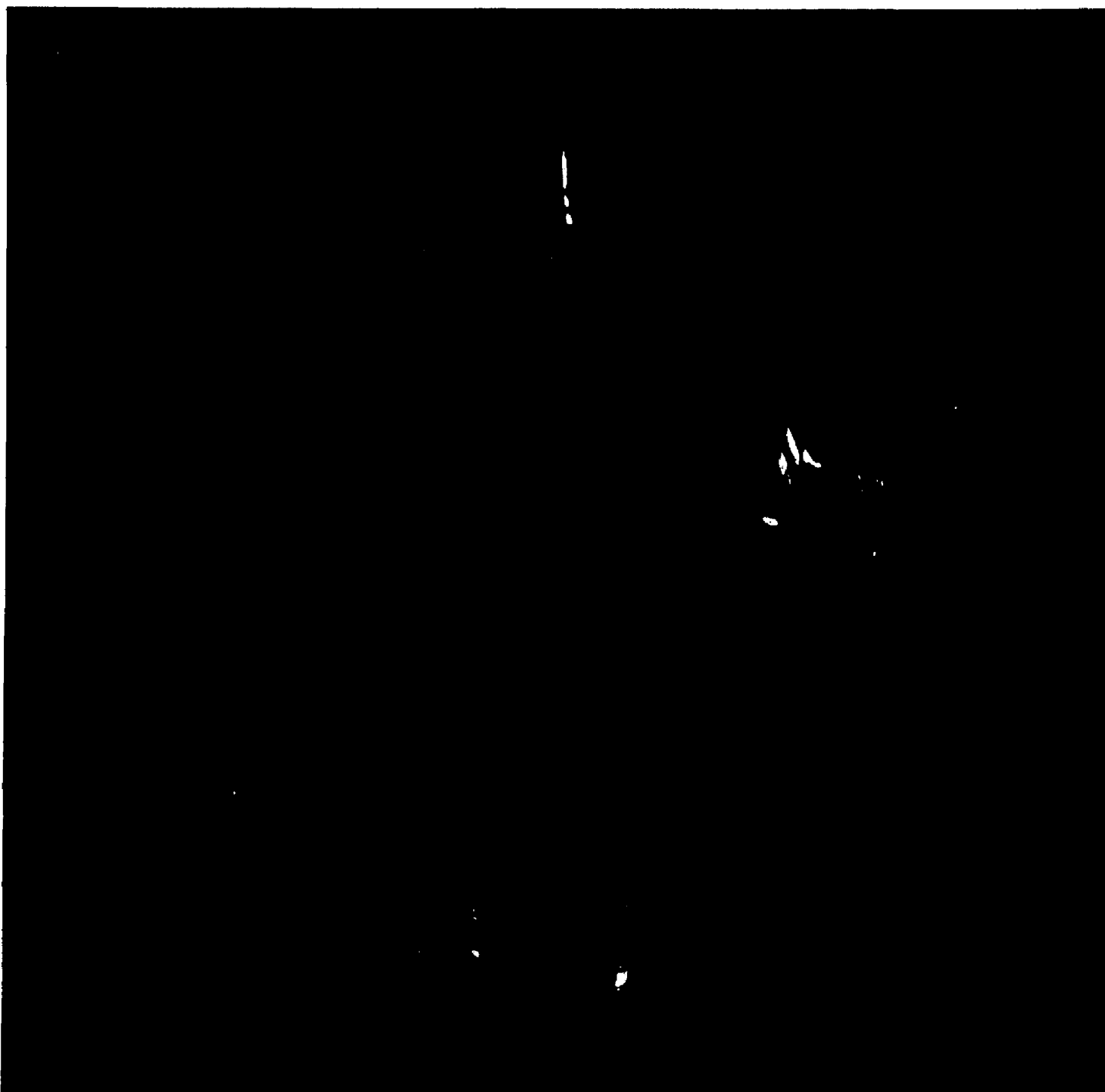


Figure 3. Photograph of the MPE-induced visible fluorescence in  $\text{CrO}_2\text{Cl}_2$  (2 torr).

threshold-laser intensity for window damage or by using dirty ones, so-called window fluorescence can be observed even in completely evacuated cells. The extraneous emission is usually of much shorter duration, confined to the window area at moderate laser intensities, and can be easily eliminated by using clean windows and by proper focusing of the laser radiation. In all the experiments reported in this work, care was taken to insure that no window fluorescence was present.

Another problem which can also be encountered and may perhaps explain some unexplainable results found in the literature is emission caused by laser induced dielectric breakdown (LIDB). Again, because of the high intensities used in these experiments, plasma formation can be induced by gases by laser excitation. Preliminary results of this interesting phenomenon in  $\text{CrO}_2\text{Cl}_2$  have been published (14), but it is sufficient to say that  $\text{CrO}_2\text{Cl}_2$  can be easily "broken down" at relatively low pressures (a few torrs). The light emitted from this process, which originates from high energy species such as ions and excited radicals, is usually observed in the focal region only, not throughout the cell, and is confined to the focal cone of the lens used. The breakdown emission is identified by the white light (plasma) in the center which encompasses most of the emission cross section surrounded by a colored (orange-red in the case of  $\text{CrO}_2\text{Cl}_2$ ) emission characteristic of the gas undergoing excitation. A photograph of this process, in  $\text{CrO}_2\text{Cl}_2$ , is shown in Figure 4. It is, thus, relatively easy to distinguish between the LIDB induced emission and the fluorescence observed in the MPE of  $\text{CrO}_2\text{Cl}_2$ . Again, care was taken to insure that, except when desired, the observed emission was only due to multiphoton excitation.

In Figure 5, the total luminescence signal vs. exciting laser

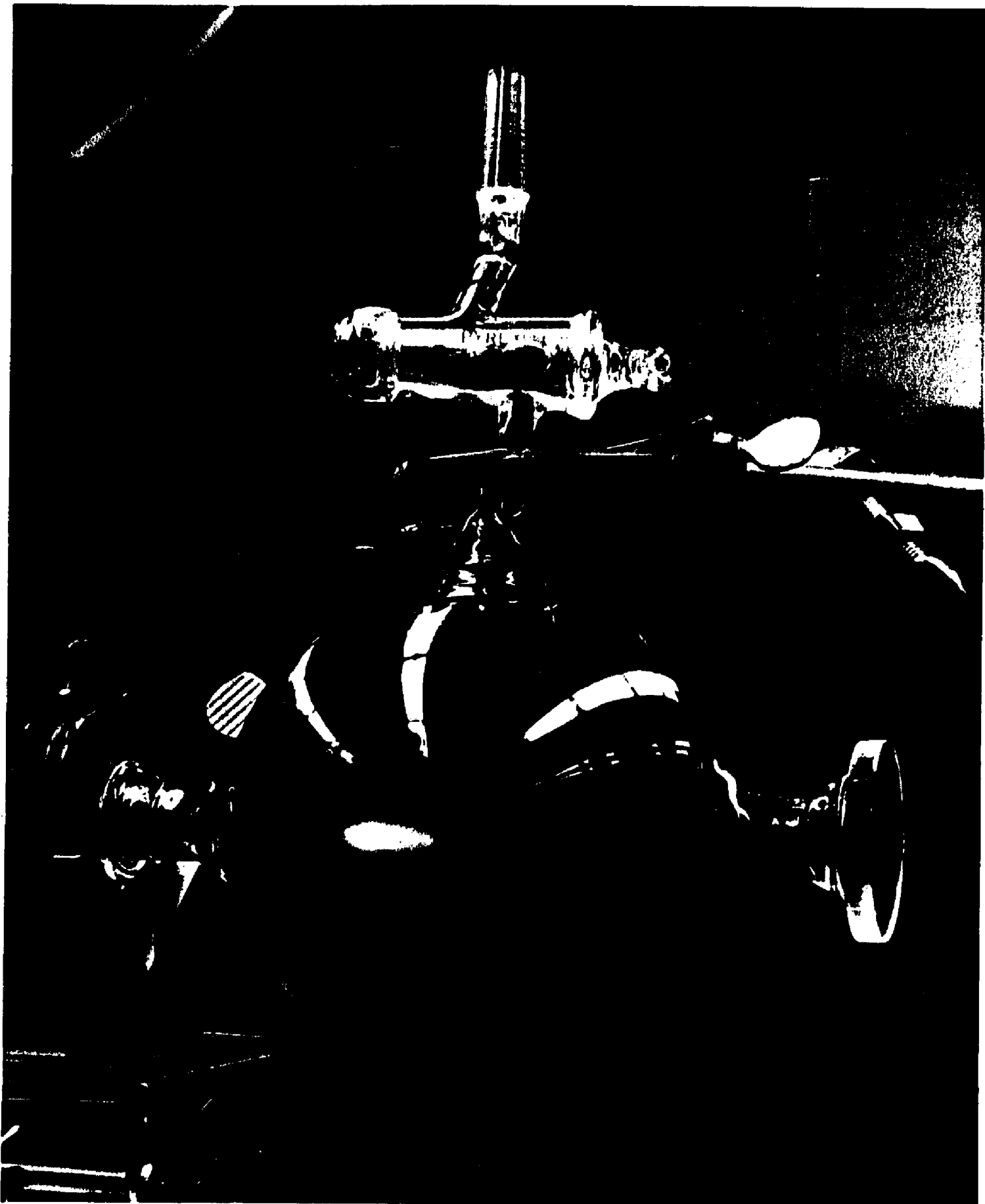


Figure 4. Photograph of the plasma produced by  $\text{CO}_2$ -LIDB in  $\text{CrO}_2\text{Cl}_2$  (5 torr).

frequency is shown. It is evident from this spectrum that the fluorescence-amplitude dependence on different laser lines within the R-branch of the  $10.6 \mu$  band is very small. The different behaviors of the infrared absorption and visible emission spectra, Figures 3 and 5 respectively, is striking. This is not surprising, however, since the opto-acoustic results with unfocused geometry measure the absorption coefficient one or at most a few photons per molecule, whereas, in the fluorescence experiments, the  $\text{CrO}_2\text{Cl}_2$  molecule must absorb a minimum of about 18 infrared photons in order to reach the excited electronic state and then emit a visible photon. This behavior is consistent with the presence of a low-lying quasicontinuum which is relatively easily reached at moderate laser fluences and in which, because of the high density of states, essentially all frequencies can be absorbed. The much smaller dependence of the visible emission on excitation frequency supports the proposition that, at sufficient laser power intensities to overcome the anharmonic bottleneck in the first few vibrational levels, multiphoton excitation can proceed efficiently in the quasicontinuum. Moreover, it is interesting to point out that the fluorescence intensity reaches its maximum value with excitation from the R(26)  $10.6 \mu$  ( $979.7 \text{ cm}^{-1}$ )  $\text{CO}_2$ -laser transition. Excitation from the higher members of this R-branch transition, as seen in Figure 5, is no more efficient in effecting  $\text{CrO}_2\text{Cl}_2$  fluorescence than that from the R(26) laser line. This shift in the spectrum may be interpreted as a shift in the absorption spectrum due to anharmonicity as the molecule climbs the vibrational ladder. This same behavior has been observed in the absorption spectrum of thermally heated molecules (32,33). It is noteworthy, however, that, comparing Figures 2 and 5, the shift, which of course is limited by the frequencies accessible with our  $\text{CO}_2$  laser, is from  $984.4 \text{ cm}^{-1}$

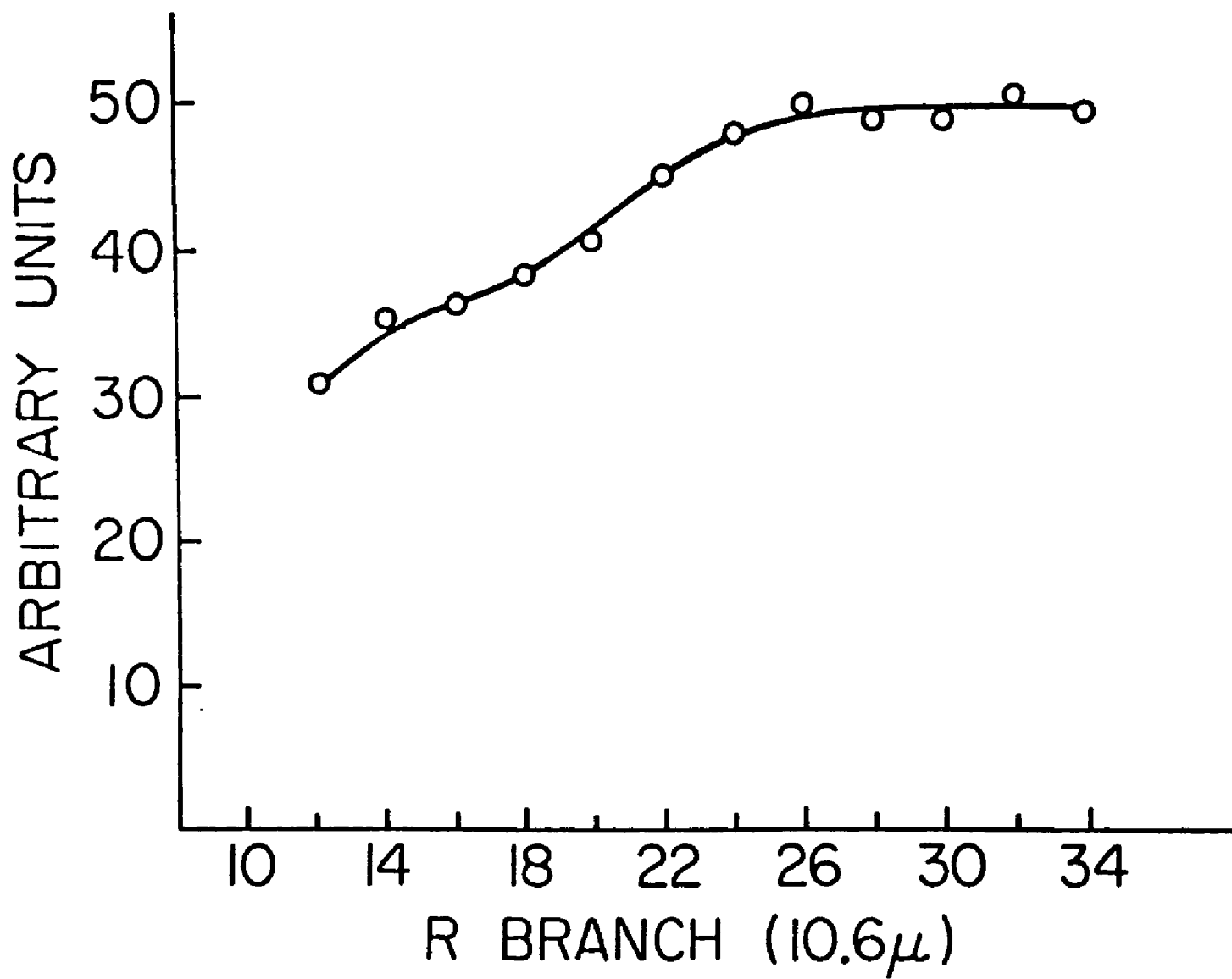


Figure 5. Plot of the total luminescence amplitude versus CO<sub>2</sub> laser R-branch lines (10.6 μ).

[R(34)] to  $979.7 \text{ cm}^{-1}$  [R(26)] or  $5.3 \text{ cm}^{-1}$ . This value, undoubtedly, is not a true measure of the anharmonic shift but a "compromise" value between exact resonance within the first few transitions and effects such as power broadening and rotational compensation which tend to overcome mismatches between the laser excitation and the molecular transitions. It is, however, important not to overemphasize these "discrete levels" effects. The striking behavior in Figure 6 is the small dependence of luminescence intensity with excitation wavelength-- a fact which is characteristic of the quasicontinuum.

Figure 6 presents the visible emission observed when the output of the  $\text{CO}_2$  laser (0.2 J) is focused in a cell containing  $\text{CrO}_2\text{Cl}_2$  at a pressure of  $5.0 \times 10^{-4}$  torr. When the laser output is unfocused, no emission is observed. By comparing Figure 6 to previously published spectra (25,26,27), the fluorescence is identified as originating from electronically excited  $\text{CrO}_2\text{Cl}_2$ . The nature of the electronic transition responsible for the emission is not clear. As already mentioned, there are at least three singlet-singlet transitions in this energy region. In addition, the possibility of triplet-singlet transitions cannot be ruled out since such a spin forbidden transition may be responsible for the emission observed in matrix-isolated  $\text{CrO}_2\text{Cl}_2$  (25,34). Although phosphorescence from the triplet state has not been observed in gas-phase studies of  $\text{CrO}_2\text{Cl}_2$  (26,27), it cannot be a priori dismissed in our infrared multiphoton experiments. This point will be discussed in the next section. Upon tighter focusing (i.e., higher fluence) of the laser radiation and/or at higher  $\text{CrO}_2\text{Cl}_2$  pressures, the visible spectrum observed broadens to the blue up to and beyond  $3400 \text{ \AA}$ . In addition, under these conditions, solid particles appear in the cell. These were detected by

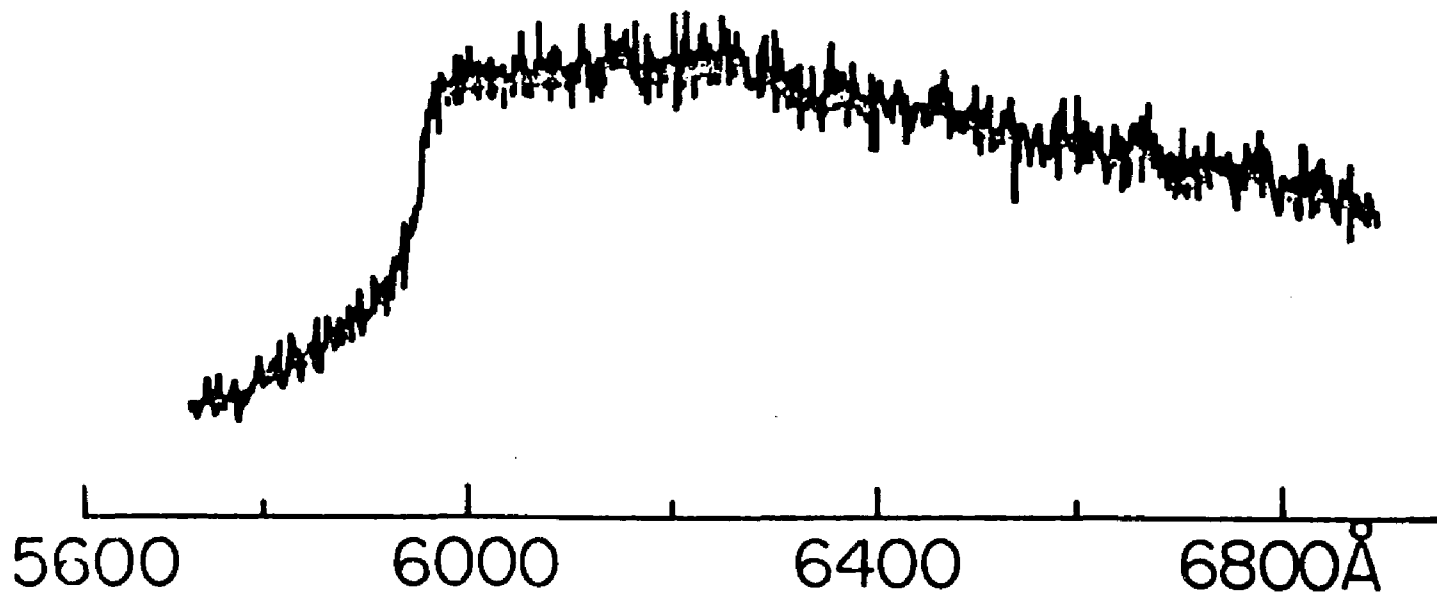


Figure 6. Molecular fluorescence spectrum following low-power irradiation of  $\text{CrO}_2\text{Cl}_2$  by a  $\text{CO}_2$  laser.

light scattering from a He-Ne laser. Infrared spectroscopy (18), x-ray analysis (35), and chemical methods characterized the solid as  $\text{CrO}_2$ . In Figure 7, a photograph obtained using scanning electron microscopy (SEM) shows the unusually small size ( $< 1 \mu$ ) of these  $\text{CrO}_2$  particles. The only other detectable product, gaseous  $\text{Cl}_2$ , was identified by mass spectrometry. Figure 8, which shows the diminution of the  $\text{CrO}_2\text{Cl}_2$  infrared signal as a function of laser pulses, corroborates these findings. The reduction in amplitude of this band is accompanied by the build-up of brown particles in the cell.

Thus, it is apparent that, under more vigorous conditions, a dissociative channel in  $\text{CrO}_2\text{Cl}_2$  is achieved by infrared-multiphoton pumping. As mentioned in the introduction, based on Halonbrenner's (18) photodissociation studies of  $\text{CrO}_2\text{Cl}_2$ , three wavelengths were chosen for the study, namely,  $6300 \text{ \AA}$ ,  $5300 \text{ \AA}$ , and  $4000 \text{ \AA}$ , as representative of the three species,  $\text{CrO}_2\text{Cl}_2$ ,  $\text{CrO}_2$ , and  $\text{CrO}_2\text{Cl}$  respectively.

The luminescence behavior at each of the three wavelengths as a function of laser energy is shown in Figure 9. The signals were obtained using 0.040 torr  $\text{CrO}_2\text{Cl}_2$  with the  $\text{N}_2$ -rich laser mixture using a focusing geometry (10 inch lens) and with a monochromator-phototube assembly placed at the focal point and perpendicular to the laser optical axis. It is important to note that the energy measurements are those obtained in front of the entrance window. Of course, because of the focusing geometry, the fluence (energy/area) can be relatively high (thus, a  $0.1 \text{ J/cm}^2$ , 1  $\mu\text{sec}$  laser pulse focused to a spot of approximately  $1 \text{ mm}^2$  yields a fluence of  $10 \text{ J/cm}^2$ ). This fluence, however, is equivalent to an average power density of  $10 \text{ megawatts/cm}^2$ --enough to effect multiphoton absorption in most polyatomic molecules. The data is reported in energy units, however, since this is the quantity that was measured directly. The y-axis of this graph displays the peak amplitude obtained

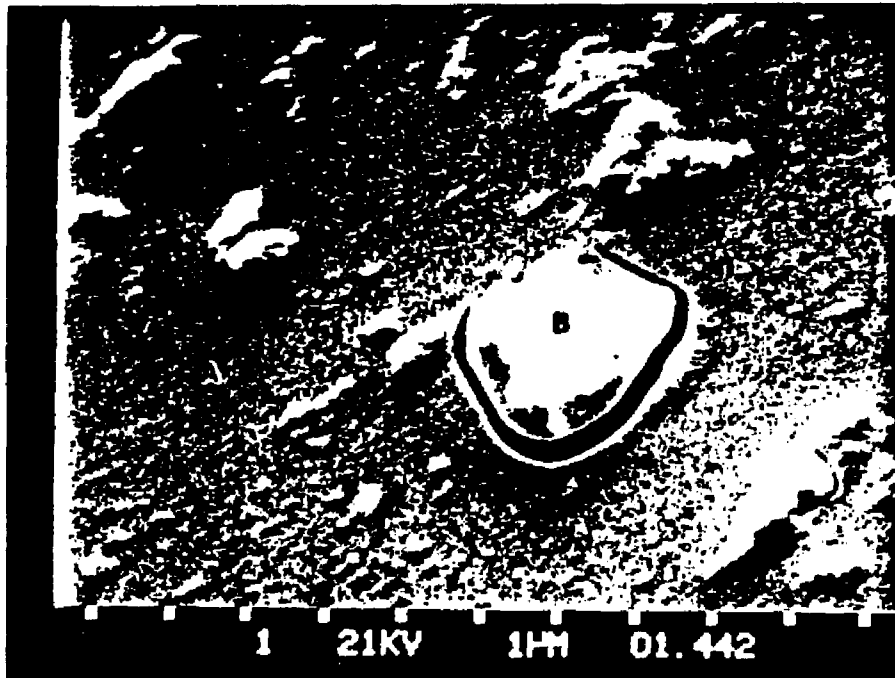


Figure 7. Scanning Electron Microscopy (SEM) photograph of  $\text{CrO}_2$  formed by  $\text{CO}_2$ -laser multi-photon dissociation of  $\text{CrO}_2\text{Cl}_2$ .

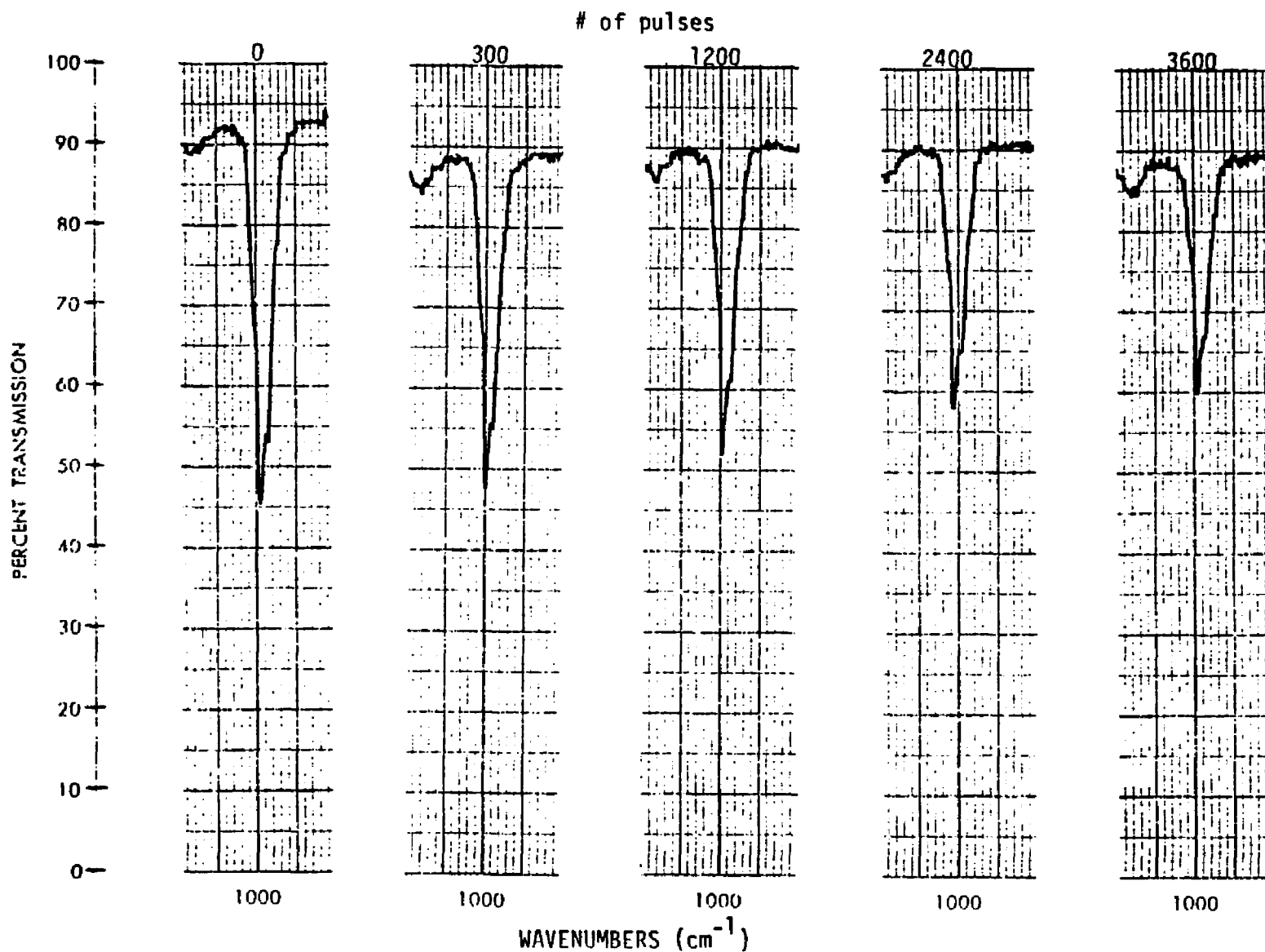


Figure 8. Infrared spectrum of  $\text{CrO}_2\text{Cl}_2$  (2 torr) as a function of laser pulses. The dissociation of  $\text{CrO}_2\text{Cl}_2$  with pulses of  $10 \text{ J/cm}^2$  was monitored using the  $\nu_1$  and  $\nu_6$  vibrational transitions.

from the oscilloscope signals. These have been corrected for phototube response according to the manufacturer's (RCA) specifications and normalized to the 4000 Å signal.

The 6300 Å signal, as can be seen from the graph, varies linearly in the range 0.2-0.7 J. It is also evident that, although the 6300 Å emission has the smallest energy threshold, the other two signals have much steeper slopes. This, of course, means that at moderate and high fluences the 5300 Å and 4000 Å emissions are more intense than the 6300 Å fluorescence. The behavior of the emission ascribed to  $\text{CrO}_2\text{Cl}$  and  $\text{CrO}_2$  species is consistent with that of photofragments and photoproducts that either luminesce or, at higher pressures, are deactivated via collisions. Thus, under irradiation with sufficient fluence and at relatively low pressures, the fragments emit very strongly. The  $\text{CrO}_2\text{Cl}_2$  excited molecules, on the other hand, have one additional channel, photodissociation, by which their fluorescence is quenched. This is evidenced by the much higher fluorescence quantum yield observed for the daughters' luminescence as compared to the parent's fluorescence. As can be seen in Figure 9, both the 4000 Å and the 5300 Å signals eventually saturate. As a matter of fact, the  $\text{CrO}_2\text{Cl}$  signal seems to decrease in intensity for this pressure at about 0.75 J. The 6300 Å signal on the other hand does not exhibit this behavior. This behavior was mimicked, albeit at higher fluence, using 0.60 torr  $\text{CrO}_2\text{Cl}_2$  and laser energies up to 1.2 J. Under these conditions, the photofragments' emission plateaued (5300 Å) or turned over (4000 Å) at about a laser energy of 1 J. The saturation of the emission with increasing fluence is believed to stem from the finite number of molecules that can interact at the focal region with the laser radiation. This interaction volume is smaller for photofragment-production since

Figure 9. Plot of the luminescence amplitude versus laser energy for the three wavelength regions: 6300 Å (squares), 5300 Å (triangles) and 4000 Å (circles).  $\text{CrO}_2\text{Cl}_2$  pressure was 0.040 torr.

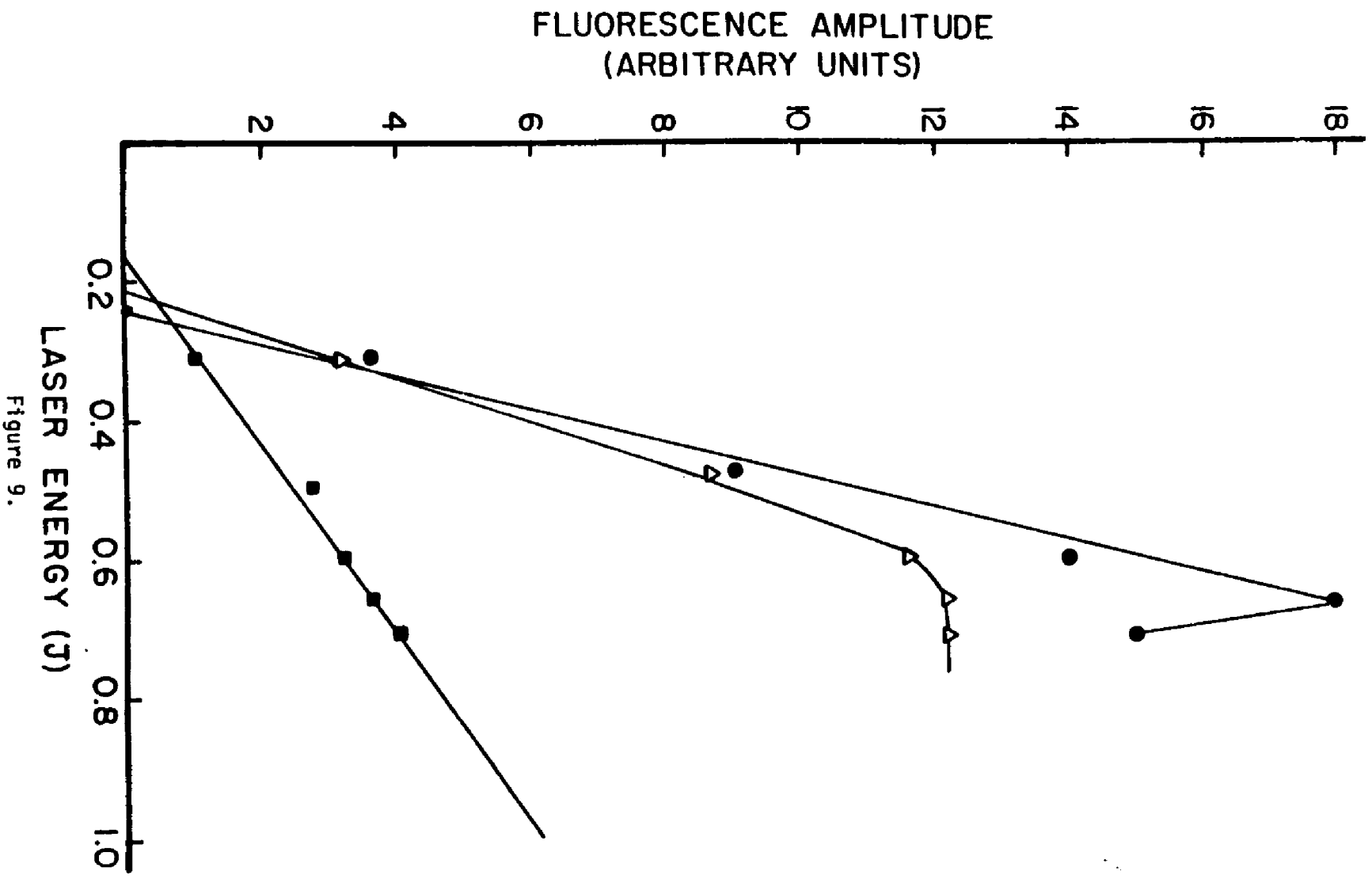


Figure 9.

absorption of some 25 infrared photons per molecule and, therefore, very high power densities are required. The parent emission at  $6300 \text{ \AA}$  can be achieved by absorption of 1 laser photons. Thus, as expected, this signal is considerably more difficult to saturate. These saturation effects have been observed in other MPD experiments (see reference 33, for example).

The reason for the decrease in fluorescence amplitude of the  $4000 \text{ \AA}$  signal, as shown in Figure 9, at relatively high energies is not immediately obvious. Although the output energy of the laser limited our ability to extend the data to very high energies, the results at different pressures seem to indicate that this is a real phenomenon. A possible explanation for this behavior is that, at these high energies, some of the  $\text{CrO}_2\text{Cl}_2$  molecules are actually dissociating in one step to  $\text{CrO}_2$ . This pathway, requiring the simultaneous (or very rapid  $< 50 \text{ nsec}$ ) fission of two chlorine-chromium bonds, would explain the high energies required and also the decrease in  $\text{CrO}_2\text{Cl}$  formation and, therefore, luminescence. It would be interesting to see if this decrease in the signal ascribed to the radical would continue at very high fluences.

Other experiments that were performed to prove the difference between the  $6300 \text{ \AA}$  signal and the others consisted of multiphoton excitation of  $\text{CrO}_2\text{Cl}_2$  in the presence of  $\text{Cl}_2$ . The rationale behind these was that, if the  $5300 \text{ \AA}$  and  $4000 \text{ \AA}$  signals were due to excited  $\text{CrO}_2$  and  $\text{CrO}_2\text{Cl}$ , respectively,  $\text{Cl}_2$  should quench the radical's and the product's emissions more efficiently than the parent's. Indeed, it was found that, with mixtures of  $\text{CrO}_2\text{Cl}_2$  to  $\text{Cl}_2$  in the ratios of 1:3 through 1:11, the  $5300 \text{ \AA}$  and  $4000 \text{ \AA}$  amplitudes were typically quenched three and two times, respectively, as efficiently as the  $6300 \text{ \AA}$  signal. A typical set of experiments using 1 torr of  $\text{CrO}_2\text{Cl}_2$  and 11 torr of  $\text{Cl}_2$  is displayed in Fig. 10. This

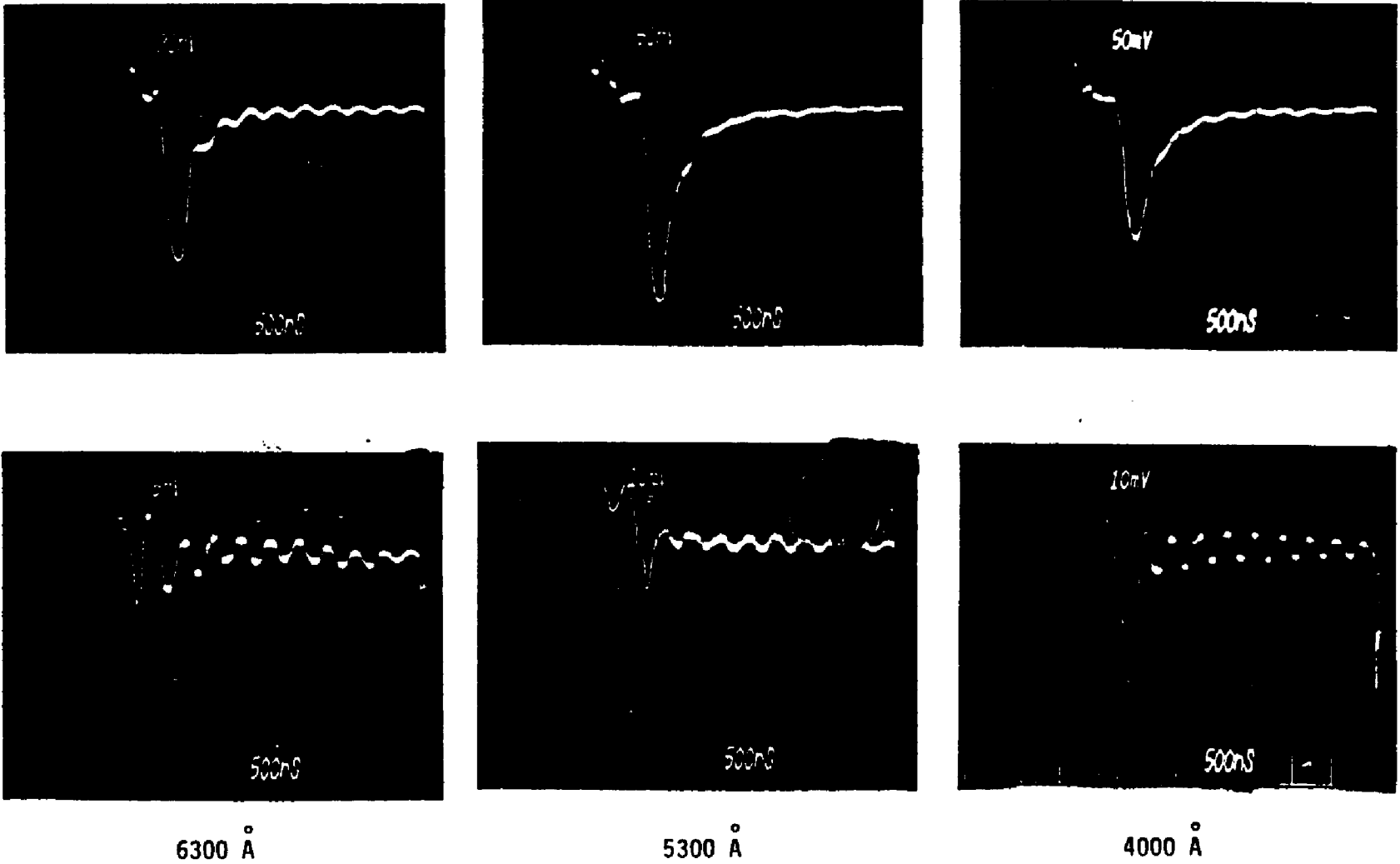


Figure 10. Scope photographs of the emission in neat  $\text{CrO}_2\text{Cl}_2$  (1 torr), top row, and in a 1:10 mixture of  $\text{CrO}_2\text{Cl}_2:\text{Cl}_2$  (bottom row) resulting from multiphoton excitation with a  $\text{CO}_2$  laser. Reading from left to right: 6300 Å, 5300 Å, and 4000 Å,

behavior is clearly consistent with inhibition of product formation by  $\text{Cl}_2$ . It, furthermore, is another indication that the  $6300 \text{ \AA}$  emission is distinct in origin from the other two.

The time-pressure behavior of the fluorescence signal was also studied. Before discussing these experiments, it is worthwhile to point out that "collisionless conditions" is a term which is used differently by different researchers. On the one hand, there are the "purists" who believe that anything less than a molecular beam constitutes a collisional experiment. At the other extreme, there are those who are satisfied by using "low" pressures. This term, of course, without any accompanying evidence is certainly not enough to insure that collisions do not play a role. Although not under molecular beam conditions, we will see that the excitation and subsequent dissociation of  $\text{CrO}_2\text{Cl}_2$  can be carried out under appropriately controlled pressure regimes and laser pulse durations to truly achieve collisionless conditions.

In Figure 11, the behavior of the  $\text{CrO}_2\text{Cl}_2$  emission at  $6300 \text{ \AA}$  using both long and short laser pulses is displayed. For comparison, typical laser pulses with and without  $\text{N}_2$  in the mixture are also shown. It is quite evident that, although the signal's rise time (time required to reach 90% of maximum) is the same in both cases, the lifetimes are not. Moreover, upon close examination, a second rise time or shoulder can be observed in the decay of the signal obtained using the long pulse. The shape of this signal closely resembles that of the long laser pulse. Furthermore, when the tail of the laser pulse was eliminated by using  $\text{N}_2$ -free laser-gas mixtures, only the rapid rise component of the fluorescence was present. This two-component long pulse behavior of

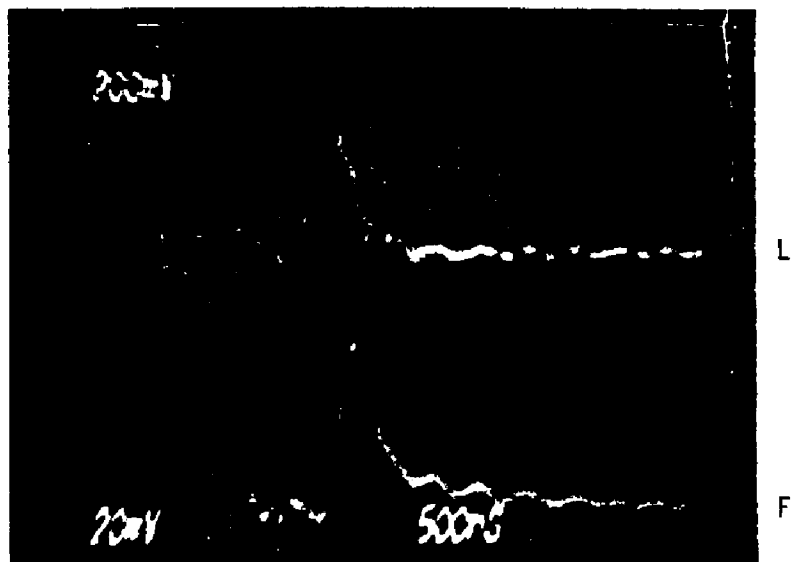
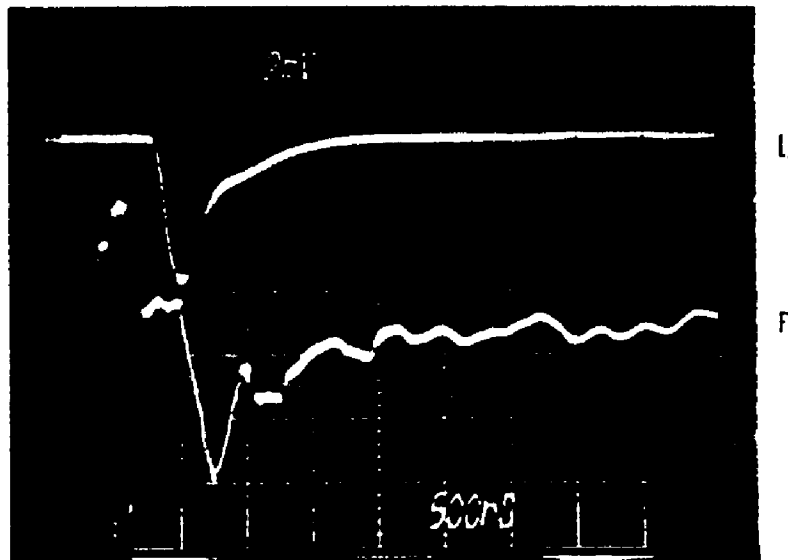


Figure 11. Scope photographs of the laser pulse, R(26)  $10.6 \mu$ , L, and of fluorescence at  $6300 \text{ \AA}$ , F, using long (top) and short (inverted) laser pulses.

the luminescence was observed at different pressures (mtorrs to torrs) and different energies (up to 2 J). As Figure 11 shows, the second component comes considerably later than the initial spike--and reaches maximum intensity at about 1  $\mu$ sec. Since, as we shall see, there are at least 10  $\text{CrO}_2\text{Cl}_2$ - $\text{CrO}_2\text{Cl}_2$  collisions in one  $\mu$ sec at a pressure of 10 mtorr, this second component cannot be considered to be collisionless except at extremely low pressures ( $\ll$  1 mtorr). Moreover, this delayed emission will interfere with fluorescence lifetime studies as a function of pressure. What these facts indicate is the need to account for pulse length as well as pressure in interpreting MPD experiments. In the present work, therefore, the  $\text{N}_2$ -free short pulse was used to study the time development of the luminescence signal. Before describing the time resolved studies, it is interesting to briefly discuss the origin of the second rise time. Although the pressure conditions under which it was observed were never truly collisionless, the fact remains that the second component can be clearly observed at pressures as low as 10 mtorr. This seems to indicate that there is enough energy in the tail of the laser pulse to cause the absorption of most if not all of the 18 to 25 photons required for observation of emission or dissociation of  $\text{CrO}_2\text{Cl}_2$  respectively. This observation again shows that, if the power intensity requirements to overcome the "up the ladder" anharmonicity effect for the first few levels are met, MPD can proceed efficiently at relatively low laser energies--as low as those available in the tail of the pulse. Similar results have been observed in other molecules (13,35).

Having established the importance of pressure and laser pulse length in time development studies, we are ready to discuss the results. In Figure 12, the rise time of the luminescence signal, using the short pulse

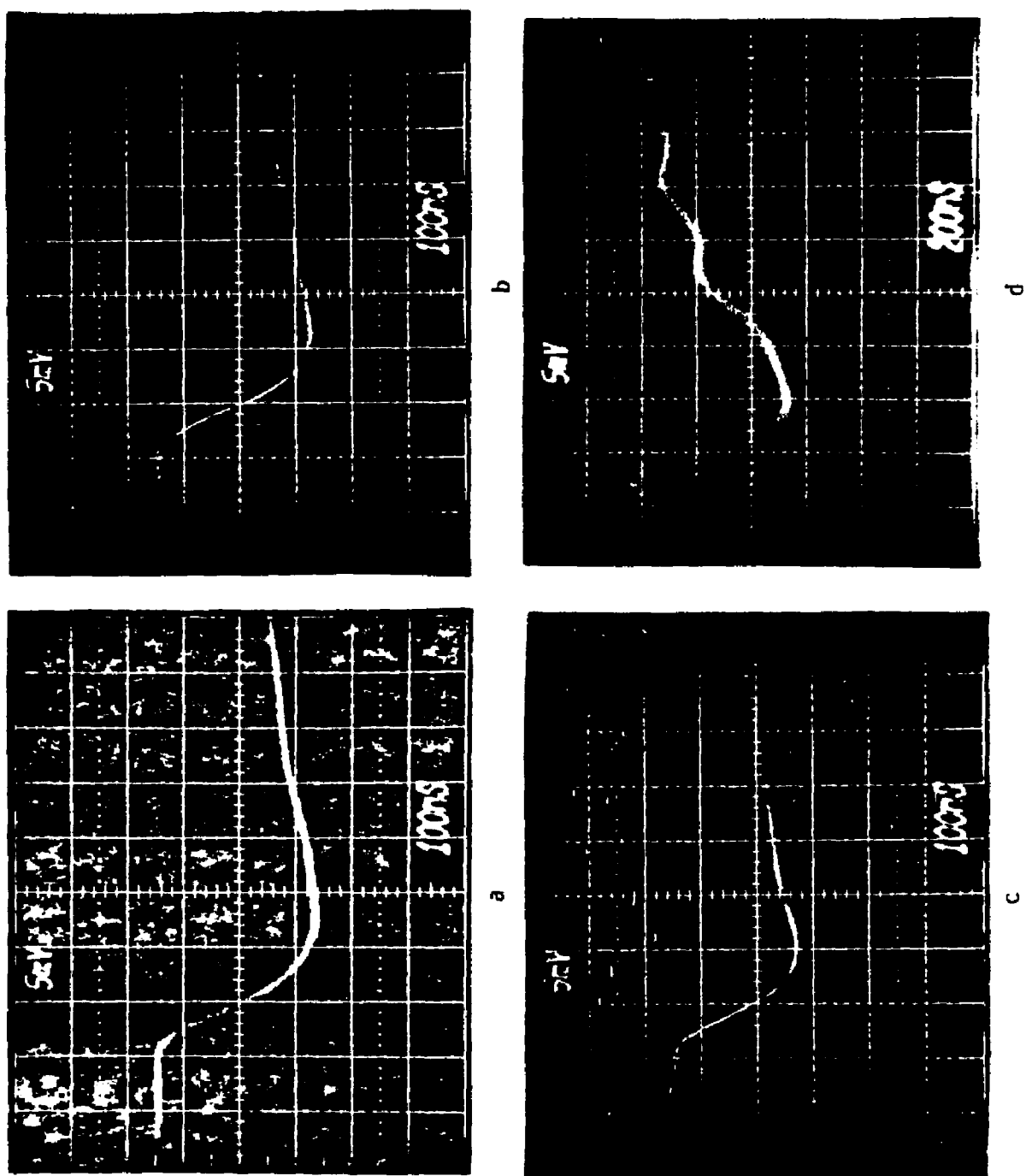


Figure 12. Scope traces emphasizing the rise times of the emission signals in  $\text{CrO}_2\text{Cl}_2$  (50 mtorr) at the three wavelengths 6300 Å (a), 5300 Å (b), and 4000 Å (c) using a long laser pulse. Also, the signal detected through a 6328 Å (d) laser filter using the short laser pulse is shown.

is displayed for the three wavelengths chosen for detailed study. The first thing to notice is that the three rise times are indistinguishable. Moreover, the onset of all three signals is approximately the same--50 to 100 nsec--after the start of the laser pulse. These facts, although disappointing in view of our hypothesis that the three emissions are due to different species, are not unexpected given our 50 nsec experimental uncertainty. The dissociation of a parent molecule and the subsequent absorption of infrared photons by the photofragments are processes that occur in picoseconds or at most nanoseconds (11,12). Therefore, given our detection uncertainty and a laser pulse of 200 nsec FWHM, these extremely fast steps are instantaneous. Thus, any rise time differences that might exist among the three signals are beyond our detection.

The emission rise time is essentially equal to that of the laser pulse ( $\sim 200$  nsecs) and it is independent of pressure even as low as  $10^{-4}$  torr. At this pressure, from kinetic theory, we can calculate that there are approximately  $10^{-1}$  collisions/ $\mu$ sec. Since the rise time of the luminescence occurs well within the pulse envelope (200 nsecs FWHM), Figure 11, the collisionless nature of the process is established.

At low pressure and low fluences, a second component to the rise time can be observed. Figure 13 clearly displays this behavior. This slower buildup of the signal is not observed when either the fluence and/or the pressure is increased, as evidenced by signals b and d and by Figure 12. This would seem to indicate that it is a collisional induced component. As the pressure is raised and the collision frequency increases and/or as the fluence is increased and the number of states reached by the laser pumping increases, this part of the signal gets faster until it ultimately coincides with the collisionless rise time.

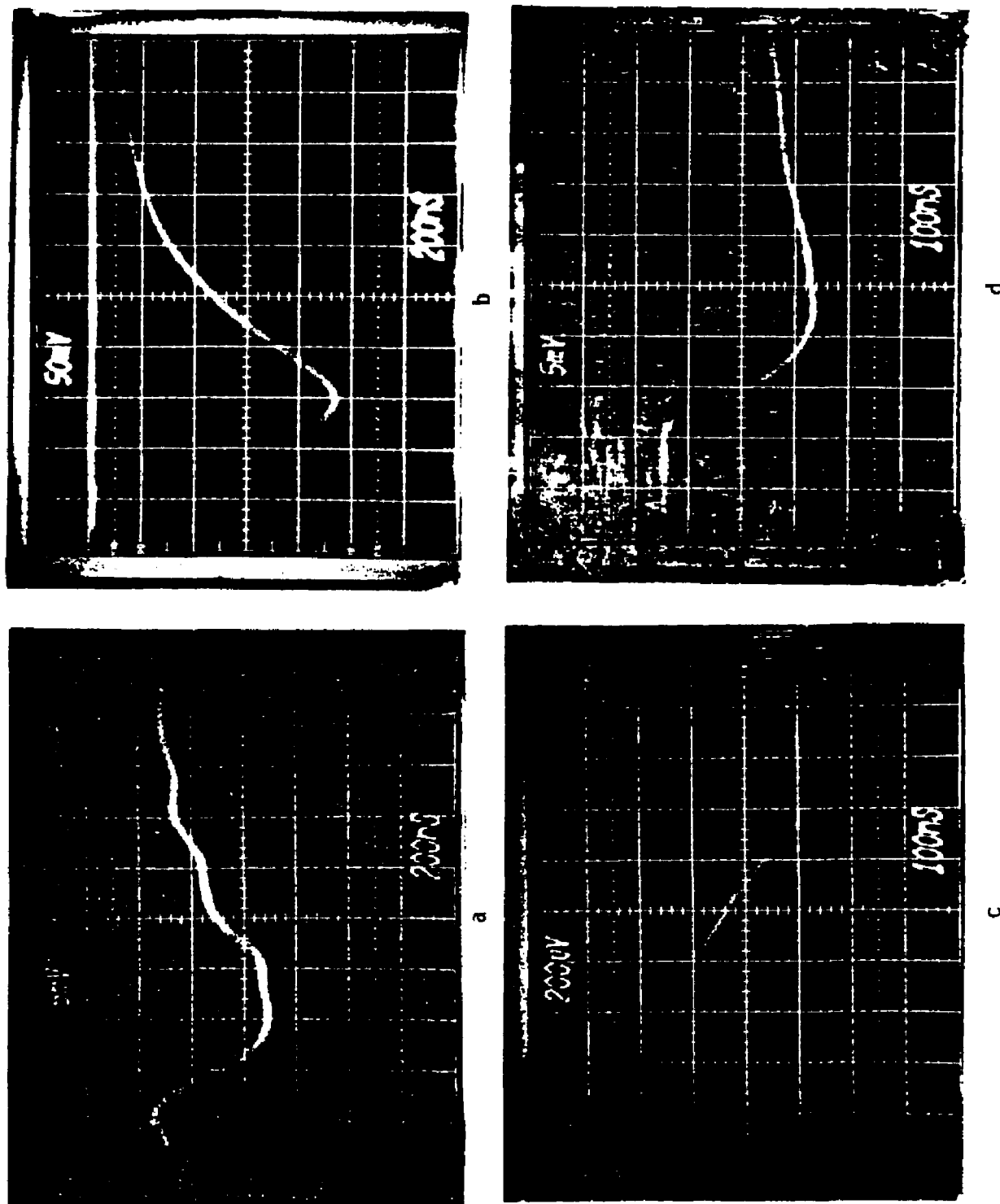


Figure 13. Scope photographs of the 6328 Å signal using the short laser pulse (0.15 J) but different  $\text{CrO}_2\text{Cl}_2$  pressures:  
 a) 50 mtorr      b) 2 torr.  
 Also, bottom row, shows the 6300 Å emission produced in 50 mtorr of  $\text{CrO}_2\text{Cl}_2$  by long laser pulses of energies 0.20 J (c) and 0.70 J (d).

i.e., the signal is pulse limited. However, caution must be exercised with this interpretation as will be shown below.

Experiments were done with pre-mixed mixtures of  $\text{CrO}_2\text{Cl}_2$  and He in the ratio 1:240. These were done using both static and flow systems. In addition to rotational equilibration, this system allowed us to reach very low  $\text{CrO}_2\text{Cl}_2$  pressures in a bath of rare gas. Moreover,  $\text{CrO}_2\text{Cl}_2$ - $\text{CrO}_2\text{Cl}_2$  collisions are virtually non-existent even at times as long as  $\mu\text{s}$ . Figure 14 shows a typical fluorescence ( $6300 \text{ \AA}$ ) signal at a total mixture pressure of 24.1 torr (0.1 torr of  $\text{CrO}_2\text{Cl}_2$ ). The rise time clearly consists of only one component, the collisionless (in the  $\text{CrO}_2\text{Cl}_2$ - $\text{CrO}_2\text{Cl}_2$  sense) one. For comparison, the emission signal of a 0.1 torr sample of neat  $\text{CrO}_2\text{Cl}_2$  is also displayed. Although it would appear that this proves the collisional nature of the second component, the fact that the total amplitude does not decrease and, in fact, increases in the presence of rare gas does not support this interpretation. An alternative explanation is that the rotational bottleneck due to mismatches resulting from anharmonicity in the pumped vibrational mode is not homogeneously overcome at low pressures of neat  $\text{CrO}_2\text{Cl}_2$  and low laser intensities. Thus, some molecules are in states within the rotational manifold from which excitation is either very unfavorable or impossible at a given laser intensity.

However, in the presence of He, this barrier is easily overcome by  $\text{CrO}_2\text{Cl}_2$ -rare gas collisions. These increase the fraction of the population that can be sufficiently excited by the laser to effect emission. This enhanced infrared laser absorption by molecules in rare gas baths has been documented before in other molecules (36,37). What these facts imply is that the slow rise component is due to molecules

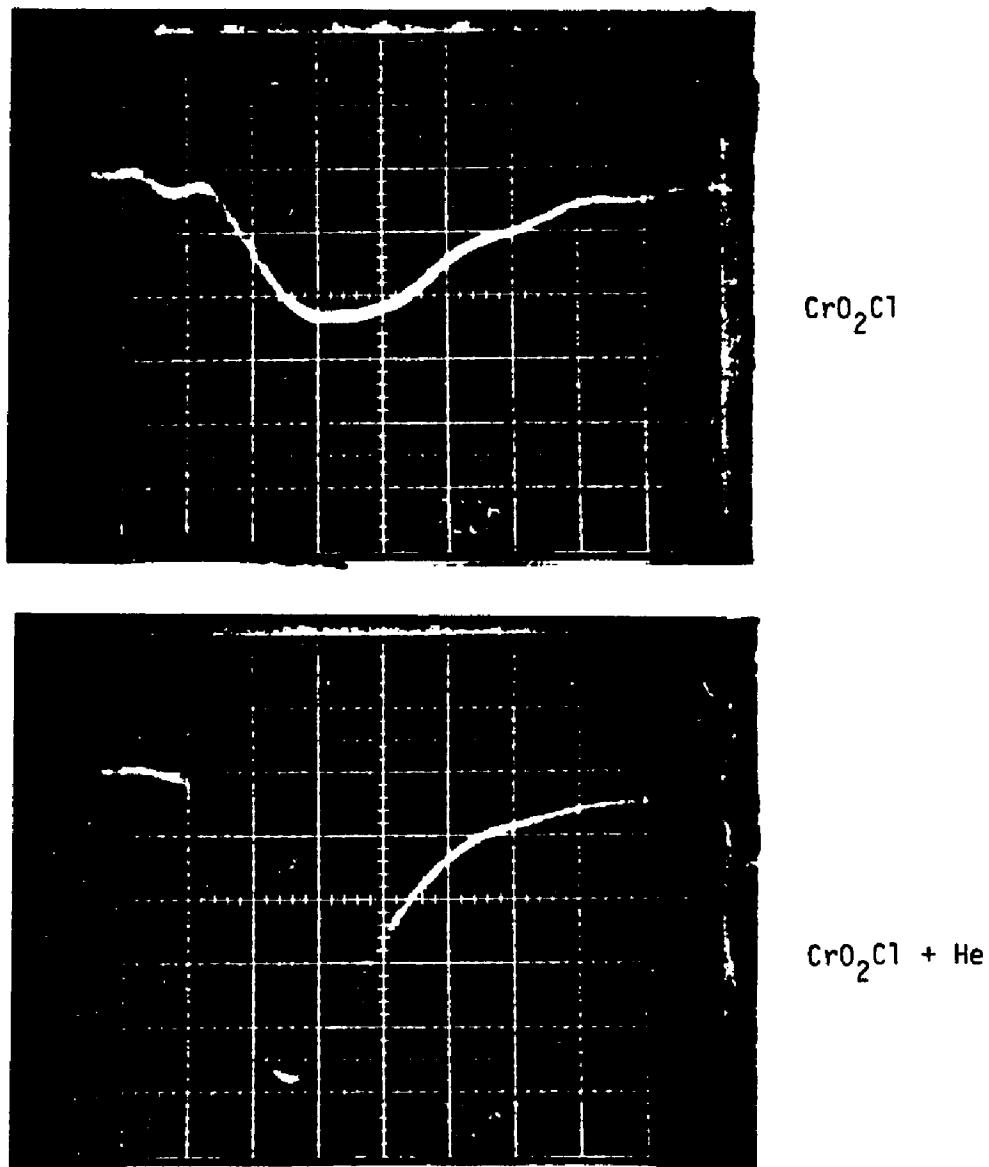


Figure 14. Fluorescence signal at 6300 Å induced by a short laser pulse in neat CrO<sub>2</sub>Cl<sub>2</sub> (0.10 torr), top, and a mixture He of 0.10 torr CrO<sub>2</sub>Cl<sub>2</sub> and 240 torr.

that are "bottlenecked" by mismatches in the discrete vibrational levels until the laser intensity is sufficiently high so that the Rabi frequency is large enough to bring these molecules into the quasicontinuum. It is important to point out that this explanation is also consistent with the absence of a slow rise time component with higher  $\text{CrO}_2\text{Cl}_2$  pressures since  $\text{CrO}_2\text{Cl}_2$ - $\text{CrO}_2\text{Cl}_2$  collisions should be extremely efficient in making up small rotational energy gaps. Thus, we must conclude that the slow rise component is due to the distribution of rotational states within the ground vibrational level. Collisional compensation, whether by  $\text{CrO}_2\text{Cl}_2$  or rare gas molecules, of this rotational bottleneck is not only reflected by the pulse limited rise time at low pressures, but also by the larger fraction of molecules that emit, i.e., increased fluorescence amplitude. Parenthetically, the rare gas experiments clearly demonstrate the collisionless nature of the excitation and dissociation of  $\text{CrO}_2\text{Cl}_2$ , since the large He: $\text{CrO}_2\text{Cl}_2$  ratios and low total pressures used insured the absence of  $\text{CrO}_2\text{Cl}_2$ - $\text{CrO}_2\text{Cl}_2$  collisions during the laser pulse.

The existence of a rotational bottleneck in the MPE and MPD of  $\text{CrO}_2\text{Cl}_2$  is also consistent with the observation that, for a given fluence, the truncated pulse yielded both a higher luminescence quantum yield and also a smaller (or no) slow rise time component than the normal pulse did. As previously stated, the Rabi frequency and, thus, the power broadening induced by the laser field is proportional to the peak intensity rather than to the laser fluence. Therefore, compensation for mismatches in the "up-pumping" process, whether due to anharmonic effects and/or the ensemble's distribution of rotational energies within a vibrational level, is more easily realized with a short rather than a

long pulse for a given laser fluence.

Studies of the fluorescence lifetime as a function of pressure were also performed. Lifetimes were recorded from the oscilloscope traces and, for a given pressure, were obtained by measuring the signal's width (in say,  $\mu\text{secs}$ ) at 0.667 times the peak amplitude. This is essentially equivalent as will be shown below, to measuring the decay time of the signal from its peak value and, in addition, accounting for the slope of the rise time. The terms, lifetime and decay time, are often used interchangeably when the build-up of the signal, as is true in the present case, is instantaneous compared to its decay.

The lifetime measuring procedure is based on the following observations. The amplitude decay of the luminescence signal can be expressed by an exponential:

$$A = A_0 e^{-kt}$$

where  $A$  is the signal's amplitude at time,  $t$ ;  $A_0$  is the maximum amplitude; and  $k$  is the rate constant for the quenching process. Since this equation as written is independent of pressure or, more appropriately, is valid for the signal at a particular pressure,

$$k = (\tau)^{-1}$$

where  $\tau$  is the decay time of the excited state and, therefore, we have

$$A = A_0 e^{-t/\tau}$$

Since we are interested in finding the decay time, we let  $t = \tau$  in the last equation with the result that:

$$A = \frac{A_0}{e} \quad \text{for } t = \tau$$

This equation states that the lifetime of the state is that time for which the signal has decayed to  $1/e$  (or 0.368) of its maximum value. Thus, in practice, the lifetimes were obtained by noting the time at which the signal had lost 2/3 of its peak value.

Using this procedure, the fluorescence lifetime as a function of  $\text{CrO}_2\text{Cl}_2$  pressure was investigated under short laser pulse irradiation. The results of this study for the 6300 Å signal are plotted in Figure 15. This Stern-Volmer plot obeys the relationship

$$\frac{1}{\tau} = \frac{1}{\tau_0} + \frac{P}{\tau_q}$$

where  $\tau$  is the lifetime,  $\tau_0$  is the collisionless (monomolecular) or purely radiative lifetime,  $\tau_q^{-1}$  is the collisional quenching rate constant, and  $P$  is the  $\text{CrO}_2\text{Cl}_2$  pressure. Thus, if  $\tau^{-1}$  is plotted against  $\text{CrO}_2\text{Cl}_2$  pressure, as in Figure 15, the slope of the resulting straight line is the collisional quenching rate constant,  $\tau_q^{-1}$ , and the y-intercept is the inverse monomolecular lifetime,  $\tau_0^{-1}$ .

Each point plotted in Figure 15 is the average of at least five separate experiments and, to insure sample purity and pressure readings accuracy, at least one (more for the lower pressure points) experiment was performed with the  $\text{CrO}_2\text{Cl}_2$  constantly flowing through the cell. No significant differences in the lifetimes were observed between the

static and the flow experiments. The quenching rate constant obtained from the slope of the line in Figure 15 yields a value of  $1.0 \times 10^7 \text{ sec}^{-1} \text{ torr}^{-1}$ . This collisional value is in excellent agreement with that obtained by McDonald ( $1.8 \times 10^7 \text{ sec}^{-1} \text{ torr}^{-1}$ ) (26) using dye laser excitation of  $\text{CrO}_2\text{Cl}_2$ . The result obtained for the bimolecular quenching rate of the electronic fluorescence can be put in perspective with the aid of the collisional frequency expression for a hard sphere model,

$$Z = \frac{\pi \sigma^2}{\sqrt{2}} n^2 \bar{v}$$

where  $Z$  is the number of collisions per unit time and unit pressure,  $\sigma^2$  is the collisional cross section,  $n$  is the number of molecules per cubic centimeter, and  $\bar{v}$  is the average molecular velocity. To obtain a collisional frequency of  $10^7$  collisions/sec·torr using this equation requires a cross section of almost  $100 \text{ \AA}^2$ . This large value of  $\sigma^2$  emphasizes the efficiency of the fluorescence quenching process in  $\text{CrO}_2\text{Cl}_2$ --undoubtedly greater than gas kinetic. It should be pointed out, and more will be said in the discussion, that such effective quenching of fluorescence is usually associated with electronically excited states that are strongly coupled to other states (ground or triplet states).

The fluorescence quenching rate constants of the  $4000 \text{ \AA}$  and  $5300 \text{ \AA}$  signals were  $1.0 \pm 1 \times 10^7$  and  $9 \pm 1 \times 10^6 \text{ sec}^{-1} \text{ torr}^{-1}$  respectively. These values are similar to that obtained for the parent emission--a fact not totally unexpected since it is the  $\text{CrO}_2\text{Cl}_2$  bath of molecules that is deactivating the excited specie, be it parent, radical, or product. Additionally, as will be further discussed in the next section, the fre-

quency of the O-Cr-O symmetric stretch remains at about  $1000\text{ cm}^{-1}$  in  $\text{CrO}_2$  and can be safely postulated to have a similar value in  $\text{CrO}_2\text{Cl}$ . Near-resonant energy transfer from daughter species to the cold  $\text{CrO}_2\text{Cl}_2$  bath can contribute to the efficiency of the quenching process.

The collision-free lifetime of the  $6300\text{ \AA}$  signal as obtained from Figure 15 by extrapolating to zero pressure was  $3.85 \pm 0.5\ \mu\text{sec}$ . The  $5300\text{ \AA}$  and  $4000\text{ \AA}$  signals exhibited monomolecular lifetimes of  $4.5 \pm 0.5\ \mu\text{sec}$  and  $2.6 \pm 1.0\ \mu\text{sec}$ , respectively. However, work performed at lower pressures than those in the figure, down to  $10^{-4}$  torr, indicate that a different quenching rate predominates for all three species. The data is difficult to analyze because of the small signal/noise ratio. The most satisfactory approach, given our experiment, to improve the signal was by increasing the laser energy. However, with a short pulse, we were still limited to at best 0.25-0.30 Joules. At any rate, it seems clear that collisionless lifetimes in excess of 15  $\mu\text{secs}$  were repeatedly obtained and, moreover, there was a definite increase of decay time with a decrease in pressure. It appears that the large fluorescence quenching cross-section exhibited by  $\text{CrO}_2\text{Cl}_2$  coupled with our 200 nsec FWHM laser pulse demands even lower pressures (and, thus, better detection equipment) than those available to this researcher. The possibility that these long lifetimes are diffusion controlled was examined. However, at these low pressures ( $10^{-4}$  torr), the time of flight of a molecule from the detector's view--the time required for a molecule to leave the phototube's field of view--was calculated to be about 60  $\mu\text{secs}$ . Thus, even the lifetimes of 15-20  $\mu\text{secs}$  observed in our experiments can be safely attributed to molecular processes rather than experimental artifacts.

The single-photon fluorescence experiments of McDonald (26) yielded a

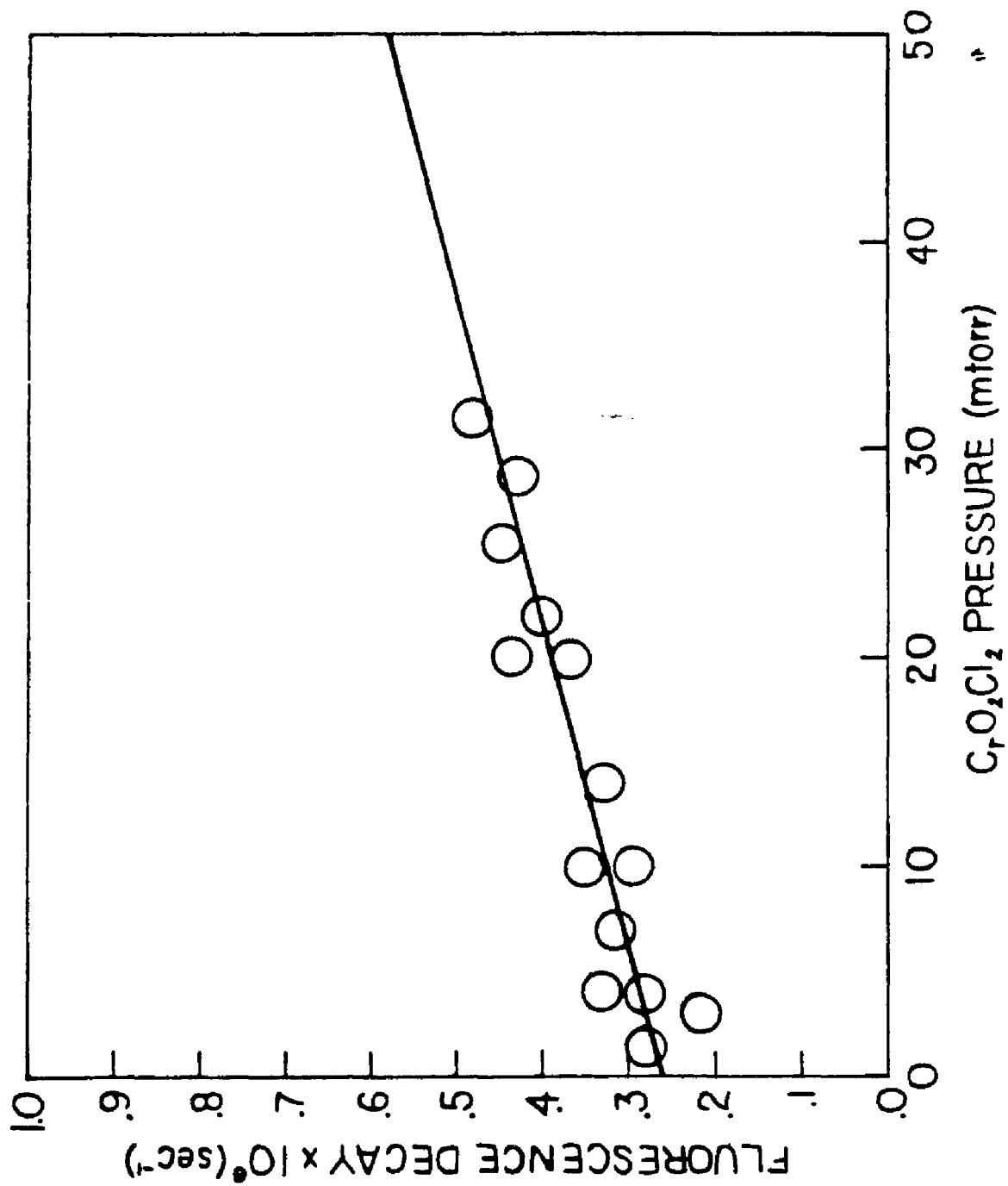
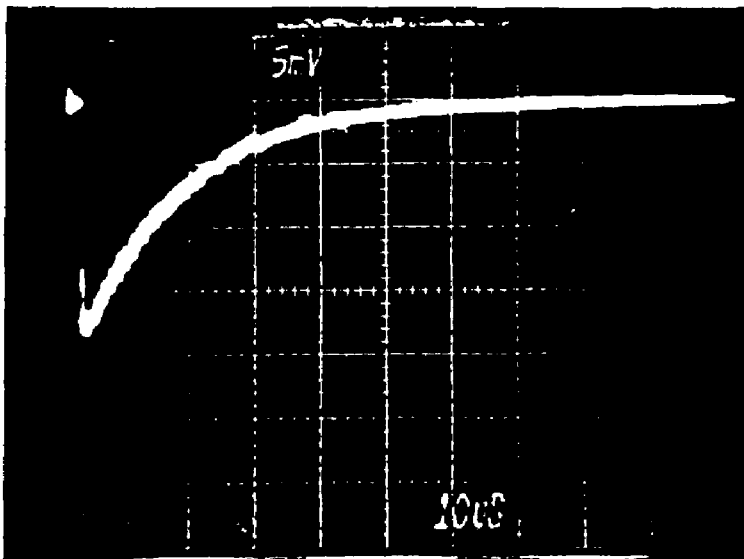
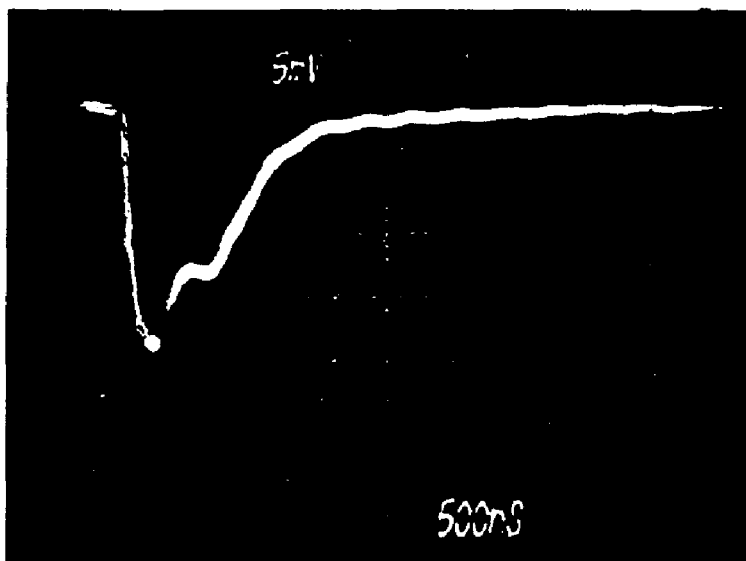
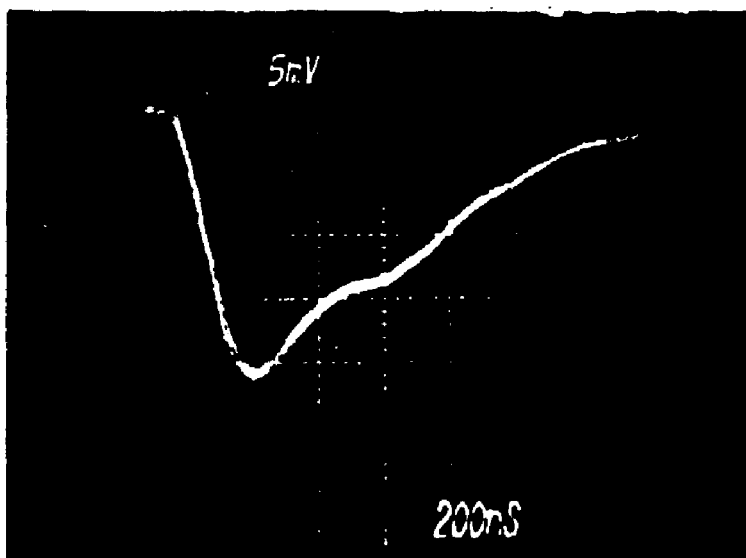


Figure 15. Stern-Volmer plot of 6328 Å fluorescence using a short laser pulse.

monomolecular lifetime of 1.34  $\mu$ secs for the vibrationally cold, electronically excited state. Moreover, this value is in agreement with that obtained from oscillator strength calculations (26). These results seem puzzling at first glance. However, in anticipation of the discussion, it should be stated that similar lifetimes should be expected only if MPA prepared the molecules in the same states as conventional fluorescence experiments do. It is, therefore, entirely possible, and as we shall see likely, that this is indeed not the case.

The problem of weak signals at low pressures was circumvented, although not solved, by the following experiment. Fluorescence from MPE of  $\text{CrO}_2\text{Cl}_2$  ( $10^{-4}$  torr) was monitored through an Oriel 63LP (long pass) filter, which transmits radiation of wavelengths equal to or greater than 6300  $\text{\AA}$ . Figure 16 shows an oscilloscope trace of this signal, which has a lifetime of 18.5  $\mu$ secs. Thus, at the expense of resolution, we were able to clearly show the long emission lifetimes at low  $\text{CrO}_2\text{Cl}_2$  pressures. In addition, Figure 16 displays the effect of added He on the decay time of this signal. It is evident that He collisions shorten the lifetime considerably without affecting or at most slightly increasing the emission's peak amplitude. Both the 55 torr and 140 torr He signals exhibit a two component decay. The fast decay is followed by a longer-lived tail whose lifetime is approximately 1.2 and 1.1  $\mu$ secs for the 55 and 140 torr He signals respectively. Thus, addition of He to very low ( $10^{-4}$  torr)  $\text{CrO}_2\text{Cl}_2$  pressures considerably reduces the fluorescence lifetime. This is an intriguing fact, since ordinarily inert gases do not effectively quench electronic fluorescence. Inert gases have no internal degrees of freedom and,

Figure 16. Oscilloscope trace of signals through a 63 L P filter using a short laser pulse induced in  $10^{-4}$  t  $\text{CrO}_2\text{Cl}_2$  (a),  $10^{-4}$  t  $\text{CrO}_2\text{Cl}_2$  + 55 t He (b), and  $10^{-4}$  t  $\text{CrO}_2\text{Cl}_2$  + 140 t He (c).

a)  $\text{CrO}_2\text{Cl}_2$ b)  $\text{CrO}_2\text{Cl}_2 + \text{He}$ c)  $\text{CrO}_2\text{Cl}_2 + \text{He}$

therefore, the quenching would require electronic to translational or, at least, vibrational (within the excited electronic state) to translational energy transfer. These are inefficient processes that are very slow (typically many  $\mu$ secs) because they require many collisions. It should be mentioned that only in cases such as methylglyoxal (38) where the excited radiative state is strongly coupled to a non-(ground state) or weakly (triplet, for example) emitting state, have rare gases been found to effectively quench electronic emission.

The effect of added rare gas on the MPE-induced  $\text{CrO}_2\text{Cl}_2$  emission was investigated in another experiment. A mixture of  $\text{CrO}_2\text{Cl}_2$  and Ar, in the ratio 1:200 respectively, was prepared and allowed to sit for several hours in order to insure proper mixing. Then, samples of this mixture, at different pressures, were laser pumped and the resulting luminescence was detected as in previous experiments through a 6328 Å laser filter. This procedure allowed attainment of very low  $\text{CrO}_2\text{Cl}_2$  partial pressures, while higher and more accurate total pressure measurements were being performed. The study ranged from 4.70 torr to 20.0 mtorr total pressure or from 2400 to 0.100 mtorr  $\text{CrO}_2\text{Cl}_2$  pressure.

In Figure 17, two oscilloscope traces, taken at 1.70 and 0.0201 torr total pressure, 8.50 and 0.100 mtorr of  $\text{CrO}_2\text{Cl}_2$  respectively, are displayed. The higher pressure trace exhibits two distinct decay times--a short exponential decay followed by a long tail. The 0.0201 torr signal, however, consists of a single luminescence lifetime. The double decay behavior persisted for pressures as low as 0.500 torr (2.50 mtorr  $\text{CrO}_2\text{Cl}_2$ ). The long tail might be ascribed to diffusion-controlled luminescence quenching, since the decay rate decreases with increasing pressure. The diffusion rate is proportional to  $1/P$  and,

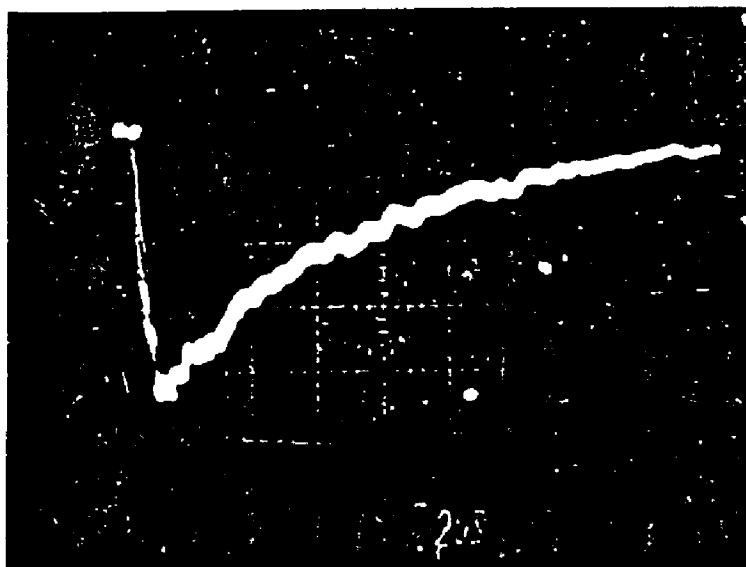
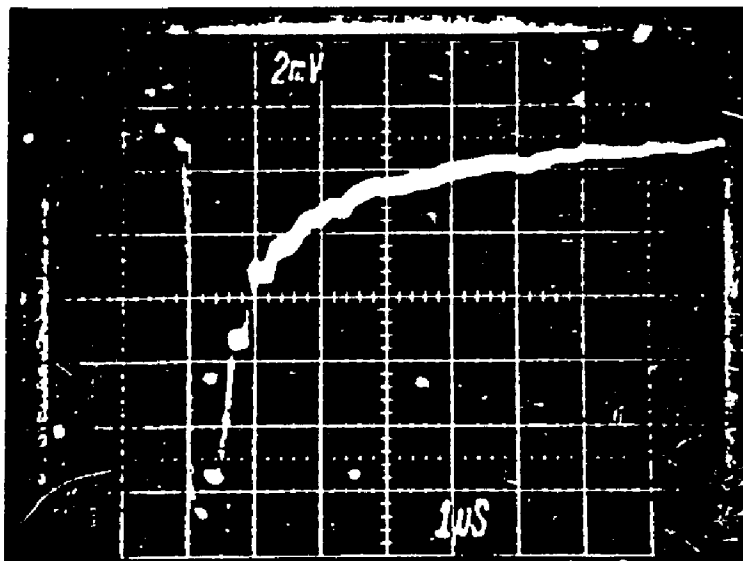


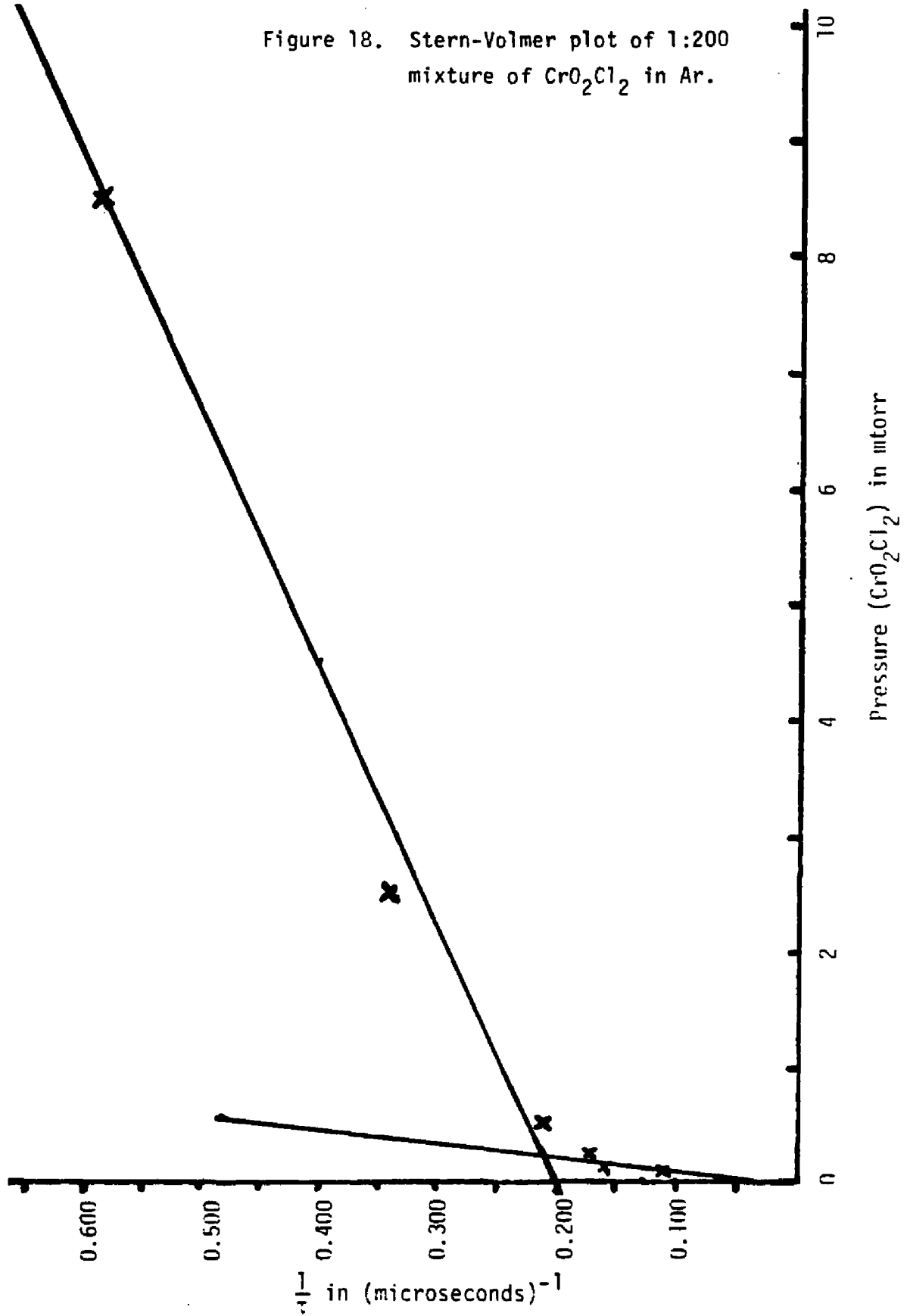
Figure 17. Emission observed through a  $6328 \text{ \AA}$  filter at 1.70 t (top) and 0.0201 t total pressure of a mixture of  $\text{CrO}_2\text{Cl}_2:\text{Ar}$  (1:200) induced by a short laser pulse.

therefore, the lifetime of such a process is proportional to P. The presence of the long-lived tail at a total mixture pressure of 1.70 torr, but its absence, when the pressure is lowered below 0.500 torr (Figure 17), is consistent with this behavior. At low pressures, diffusional effects disappear and only a single exponential is observed.

The results of the luminescence lifetime (short one) obtained in this experiment are plotted in Figure 18 as a function of  $\text{CrO}_2\text{Cl}_2$  pressure. It should be parenthetically mentioned that lifetimes were obtained from plots of  $\ln A$  vs.  $t$ , where  $A$  is the amplitude and  $t$  is the time, and using  $\ln A = \ln A_0 - kt$ , the slope of the resulting straight line yielded the rate constant  $k$  and, therefore, the lifetime  $\tau = 1/k$ . The use of this procedure rather than that of the simpler  $1/\lambda$  method previously described was necessary in order to insure that only the short exponential lifetimes were being analyzed.

It is clear, from Figure 18, that a single straight line (Stern-Volmer behavior) is not consistent with the data. A straight line can be drawn for the higher pressures down to about 0.500 mtorr of  $\text{CrO}_2\text{Cl}_2$ . The slope of this line yields a bimolecular quenching rate constant of  $4.55 \times 10^7 \text{ sec}^{-1} \text{ torr}^{-1}$  which is indeed very similar to that of the Stern-Volmer plot of neat  $\text{CrO}_2\text{Cl}_2$  ( $1.0 \times 10^7 \text{ sec}^{-1} \text{ torr}^{-1}$ ). This would imply that this slope is dominated by  $\text{CrO}_2\text{Cl}_2$  bimolecular collisions and the added Ar had a small effect. At lower pressures, a different less efficient rate prevails. As we shall see, this behavior may be explained by considering dephasing (long range) collisions as being efficient in deactivating excited molecules. This is consistent with rare gas quenching of the luminescence and with the decreased efficiency of added gas pressure ( $\text{CrO}_2\text{Cl}_2$  or Ar) in deactivating excited molecules. This experiment also points to the long single-molecule lifetimes that can be expected. Extrapolation of the low

Figure 18. Stern-Volmer plot of 1:200 mixture of  $\text{CrO}_2\text{Cl}_2$  in Ar.



pressure curve, although by no means an accurate procedure, yields an intercept of about  $0.0200 \mu\text{sec}^{-1}$  or a collisionless lifetime of about 50.0  $\mu\text{secs}$ . Given the presence of Ar in the experiment, this value is probably an upper limit.

Thus, summarizing, a mixture of  $\text{CrO}_2\text{Cl}_2$  in a large excess of Ar can be multiphotonically excited to yield visible fluorescence. The excitation is, undoubtedly, collisionless since it can be observed at pressures as low as  $1.0 \times 10^{-4}$  torr  $\text{CrO}_2\text{Cl}_2$ . The quenching by the cold bath displays at least two different rates; the higher pressure one being very similar to that obtained for neat  $\text{CrO}_2\text{Cl}_2$ . An upper limit for the monomolecular lifetime is 50  $\mu\text{secs}$ --again considerably longer than McDonald's 1.34  $\mu\text{secs}$ . All these results, as explained in the Discussion, are consistent with the nature of the mixed (ground and electronically excited) molecular states in which the molecule is prepared by multiphoton excitation followed by inverse electronic relaxation.

The behavior of the luminescence intensity, monitored at  $6328 \text{ \AA}$ , with pressure is shown in Figure 19 using the 200 nsec-FWHM laser pulse containing 0.200 J of energy. The peak amplitude dependence on  $\text{CrO}_2\text{Cl}_2$  pressure is linear for low to moderate pressures. This portion of the curve supports the claim of collisionless production of the fluorescence by the laser radiation. At about 1.00 torr, the dependence ceases to be linear as the slope continually decreases until a plateau is reached at about 3.00 torr. Thus, the fluorescence signal saturates at moderately high  $\text{CrO}_2\text{Cl}_2$  pressures. Beyond 4.00 torr, the  $6328 \text{ \AA}$  emission actually began to decrease in intensity. This collisional quenching of the fluorescence amplitude is not surprising since we can calculate that

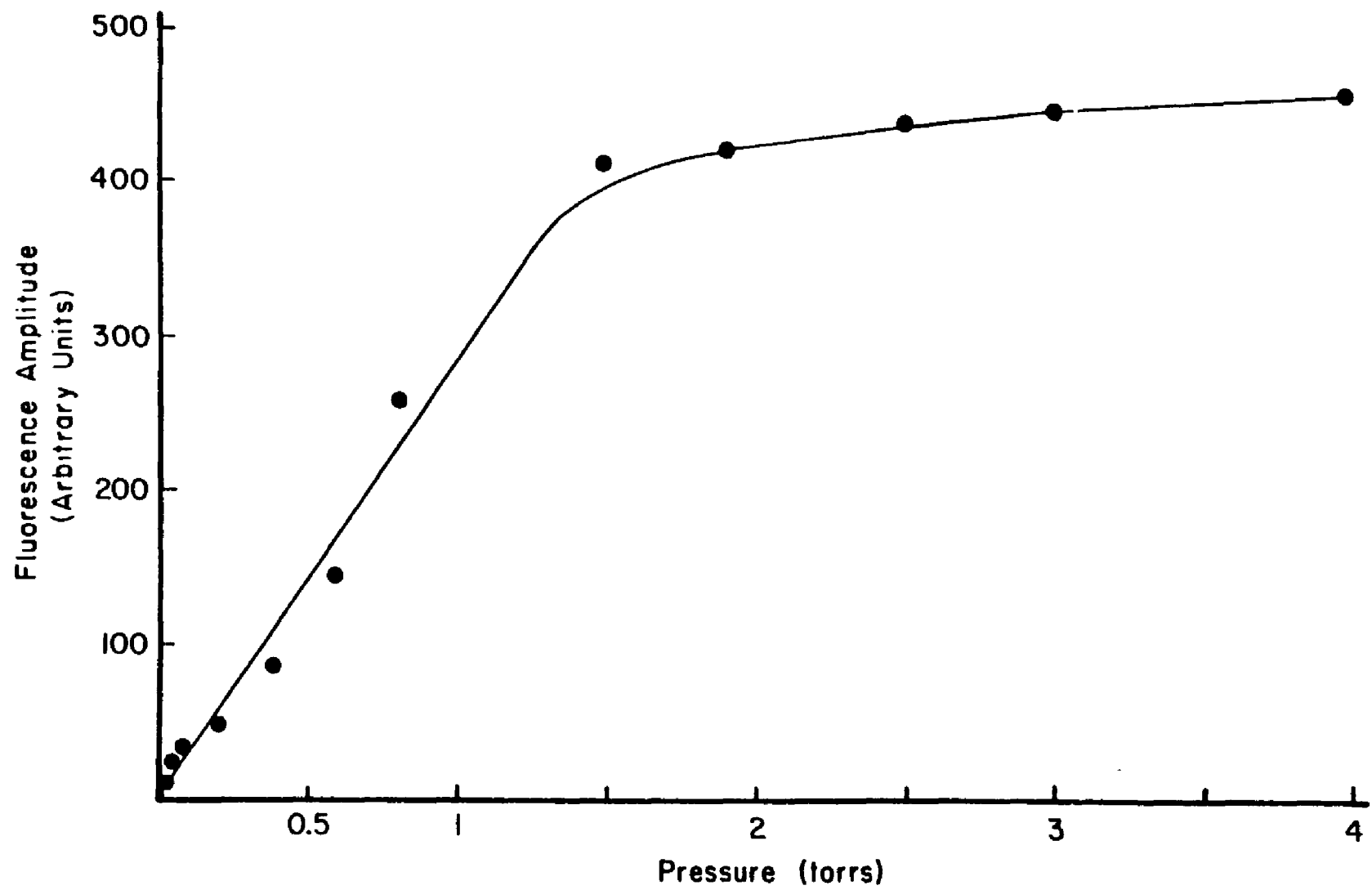


Figure 19. Plot of fluorescence amplitude, 6300 Å, versus pressure.

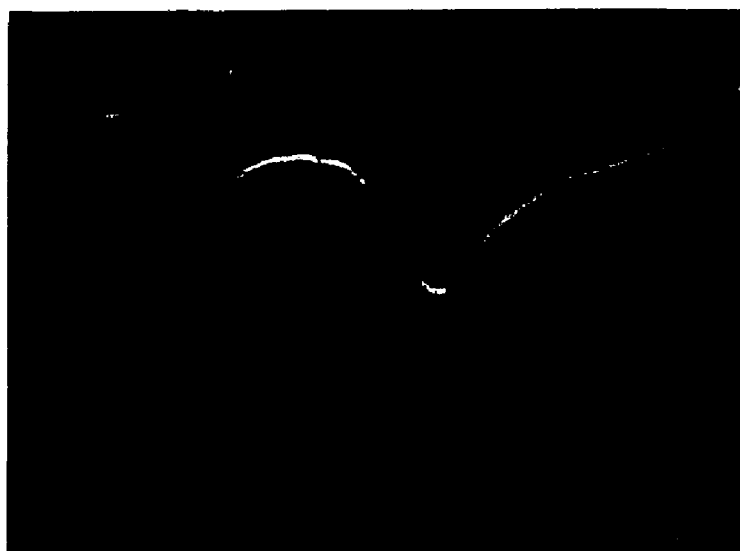
a vibrationally hot  $\text{CrO}_2\text{Cl}_2$  molecule can suffer about 800 collisions by the cold  $\text{CrO}_2\text{Cl}_2$  bath (4 torr) during the time that the laser pulse is on.

Though the principal theme of this work is the collisionless production of luminescence and, more specifically of parent fluorescence, via multiphoton absorption, collisions whenever important have not been ignored. As a matter of fact, much work was often invested in insuring collisionless conditions. However, the fact that, even at low to moderate pressures, a collisional component of the luminescence was present is surprising. Figure 20 depicts the two components of the luminescence signal at the three wavelengths, 6328 Å, 5308 Å, and 4000 Å respectively reading clockwise from left to right. The  $\text{CrO}_2\text{Cl}_2$  pressure was 6.0 mtorr. As is evident from the oscilloscope pictures, emphasis was placed on the delayed component and, therefore, the initial luminescence pulse is not completely observable in two of the pictures.

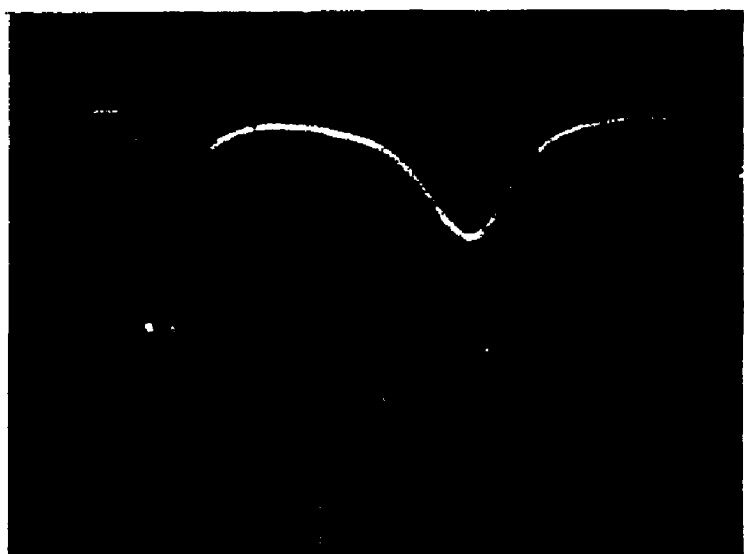
The collisional nature of the second signal is clearly established since it begins at least 1.8 to 2.0 μsecs after the beginning of the laser pulse; i.e., it begins to develop at least 1.2 μsecs after the laser pulse is off. Additionally, the rise times are considerably longer than those obtained under collisionless conditions and which followed the laser pulse rise (200 nsecs).

This collisional signal increases in amplitude with laser pulse energy, with  $\text{CrO}_2\text{Cl}_2$  pressure, and its onset can be accelerated with increased  $\text{CrO}_2\text{Cl}_2$  pressure. Rare gases, added to  $\text{CrO}_2\text{Cl}_2$ , eliminated this signal by preventing  $\text{CrO}_2\text{Cl}_2$  collisions. These facts, in contrast to previously described collisionless experiments, are as expected for

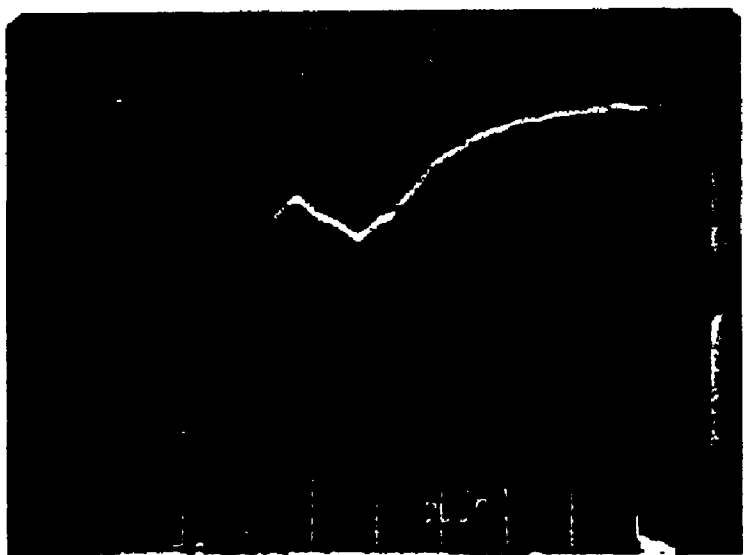
Figure 20. Luminescence signals, emphasizing the collisional component,  
at 6328 Å, 5308 Å, and 4000 Å.



6328 Å



5308 Å



4000 Å

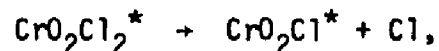
collisionally-induced luminescence.

A careful analysis of these signals reveals some notable facts. Although obviously not corrected for the wavelength response of the phototube, it is the 5308 Å signal that has the largest amplitude. Moreover, the rise time of the collisional luminescence is longest for this signal. As a matter of fact, the 6328 Å amplitude is weaker by at least a factor of 4; the 4000 Å one by a factor of 27.

A simplistic approach, based on energetics alone, would predict that the amplitude should decrease with increasing signal frequency. This result would be expected if only the number of collisions were important in determining which vibronic level was reached. This behavior would have implied emission from one source. Thus, to explain the response of the collisionally induced fluorescence, it is again necessary to assign the emission to more than one specie.

Consistent with the spirit of the present work, we assign the 6328 Å signal as being parental in origin. It is considerably weaker than the 5308 Å emission because this fluorescence cannot only be collisionally quenched via gain or loss of energy but, also, by dissociation. The product (5308 Å) emission, on the other hand, is probably not as efficiently quenched (due to imperfect resonances) by collisions with  $\text{CrO}_2\text{Cl}_2$  molecules. Of course, in addition, the dissociative channel is not open to the thermodynamically stable  $\text{CrO}_2$ . As to the 4000 Å signal, its weak intensity together with its early formation (Figure 20) would seem to indicate that it is due to  $\text{CrO}_2\text{Cl}$  fragments which are formed by collisions of vibrationally (or even electronically) hot  $\text{CrO}_2\text{Cl}_2$  molecules and perhaps even  $\text{CrO}_2\text{Cl}$  radicals that remained excited after laser excitation. The latter is a

possibility since, as already mentioned, the reaction



where the asterisk denotes a vibrationally or electronically excited specie, would be expected to leave the polyatomic radical with most of the excess energy. Additionally, as has been described before, the radical can itself absorb laser photons. Indeed, if it is accepted that the 4000 Å signal is due to  $\overset{\circ}{\text{CrO}}_2\text{Cl}$ , then the paucity of the required excited parent or fragment molecules together with their instability can explain the small amplitude and the relatively early onset of the collisional component.

It is well understood by the present author that the foregoing remarks regarding the collisional component of the emission are purely speculative. Nevertheless, this unproven mechanism is attractive since it coincides with the proposed and empirically verified MPD pathway of  $\text{CrO}_2\text{Cl}_2$ ; the only addition is that collisional energy transfer now plays a role in the formation of excited species. This is but one example of possible future research avenues which the present work has suggested.

References

1. C. Borde, A. Henry and L. Henry, *Compt. Rend. Acad. Sci. (Paris) B* 262, 1389 (1966).
2. V. V. Losev, V. P. Papulovski, V. P. Tischinski and C. A. Fedina, *High Energy Chem.* 8, 331 (1969).
3. N. V. Karlov, Yu. N. Petrov, A. M. Prokhorov and O. M. Stel'makh, *JETP Letters* 11, 135 (1970).
4. N. R. Isenor and M. C. Richardson, *Appl. Phys. Letters* 18, 224 (1971).
5. V. S. Letokhov, E. A. Ryabov and O. A. Tumanov, *Opt. Commun.* 5, 168 (1972).
6. N. R. Isenor, V. Merchant, R. S. Hallsworth and M. C. Richardson, *Can. J. Phys.* 51, 1281 (1973).
7. R. V. Ambartzumian, N. V. Chekalin, V. S. Doljnikov, V. S. Letokhov and E. A. Ryabov, *Chem. Phys. Letters* 25, 515 (1974).
8. R. V. Ambartzumian, N. V. Chekalin, V. S. Doljnikov, V. S. Letokhov and V. N. Kokhman, *J. of Photochem.* 6, 55 (1976).
9. R. V. Ambartzumian, Yu. A. Gorokhov, G. N. Makarov, A. A. Puretski, and N. P. Furzikov, *Chem. Phys. Letters* 45, 231 (1977).
10. M. L. Lesiecki and W. A. Guillory, *J. Chem. Phys.* 66, 4317 (1977).
11. Aa. S. Subdø, P. A. Schulz, Y. T. Lee, and Y. R. Shen, *J. Chem. Phys.* 68, 1306 (1978).
12. Aa. S. Subdø, P. A. Schulz, E. R. Grant, Y. R. Shen, and Y. T. Lee, *J. Chem. Phys.* 70, 912 (1979).
13. M. H. Yu, H. Reisler, M. Mangir, and C. Wittig, *Chem. Phys. Lett.* 62, 439 (1979).
14. Z. Karny, A. Gupta, R. N. Zare, S. T. Lin, J. Nieman, and A. M. Ronn, *Chem. Phys.* 37, 15 (1979).
15. J. Nieman and A. M. Ronn, *Opt. Eng.* 19, 39 (1980).
16. A. Nitzan and J. Jortner, *Chem. Phys. Lett.* 60, 1 (1978).
17. G. D. Flesch, R. M. White and H. F. Svec, *Intern. J. Mass Spectrom. Ion Phys.* 3, 339 (1969).
18. R. Halonbrenner, J. R. Huber, U. Wild and H. H. Gunthard, *J. Phys. Chem.* 72, 3929 (1968).

19. R. DeL. Kronig, A. Schaafsma and P. K. Peerlkamp, *Z. Physik. Chem.* 22, 323 (1933).
20. W. E. Hobbs, *J. Chem. Phys.* 28, 1220 (1958).
21. R. N. Dixon and C. R. Webster, *J. Mol. Spectrosc.* 25, 86 (1968).
22. H. Stammreich, K. Kawai and Y. Tavares, *Spectrochim. Acta* 9, 738 (1959).
23. F. A. Miller, G. L. Carlson and W. B. White, *Spectrochim. Acta* 9, 709 (1959).
24. T. M. Dunn and A. H. Francis, *J. Mol. Spectrosc.* 25, 86 (1968).
25. M. Spolitti, J. H. Thirtle and T. M. Dunn, *J. Mol. Spectrosc.* 52, 146 (1959).
26. J. R. McDonald, *Chem. Phys.* 9, 423 (1975).
27. J. A. Blazy and D. H. Levy, *J. Chem. Phys.* 69, 2901 (1978).
28. L. Helmholtz, H. Brennan and M. Wolfsberg, *J. Chem. Phys.* 23, 853 (1955).
29. J. P. Jasinski, S. L. Holt, J. H. Wood and L. B. Asprey, *J. Chem. Phys.* 63, 757 (1975).
30. T. H. Lee and J. W. Rabalais, *Chem. Phys. Letters* 34, 135 (1975).
31. P. C. Haarhoff, *Mol. Phys.* 7, 101 (1963).
32. A. V. Nowak and J. L. Lyman, *J. Quant. Spectrosc. Radiat. Transfer* 15, 945 (1975).
33. W. Tsay, C. Riley and D. O. Ham, *J. Chem. Phys.* 70, 3558 (1979).
34. V. E. Bondybey, *Chem. Phys.* 18, 293 (1976).
35. Y. Haas and G. Yahav, *Chem. Phys. Letters* 48, 63 (1977).
36. N. V. Chekalin, V. S. Letokhov, V. N. Lokhman, A. N. Shibanov, *Chem. Phys.* 36, 415 (1979).
37. J. C. Stephenson, D. S. King, M. F. Goodman, and J. Stone, *J. Chem. Phys.* 70, 4496 (1979).
38. R. A. Coveleskie and J. T. Yardley, *Chem. Phys.* 9, 275 (1975).

### DISCUSSION

Infrared multiphoton pumping of  $\text{CrO}_2\text{Cl}_2$ , as we have seen, has produced very insightful results. Some of these are consistent with the current theoretical understanding of the excitation and subsequent dissociation of molecules under the influence of infrared-laser radiation. Others have required a new conceptual framework, namely IER, in order to ascertain and understand their origin.

The up-the-ladder absorption of photons in  $\text{CrO}_2\text{Cl}_2$  appears to be a very efficient process as attested by the luminescence that was observed at pressures as low as  $10^{-4}$  torr. Thus, absorption of at least 16 infrared (c.  $1000\text{ cm}^{-1}$ ) photons under collisionless conditions was routinely induced in this molecule at energies as low as 0.10 Joules. Because the unfocused laser radiation did not yield  $\text{CrO}_2\text{Cl}_2$  luminescence nor dissociation, it is quite apparent that a power intensity threshold exists for multiple-photon absorption. At a fluence of  $0.080\text{ J/cm}^2$ , our 200 nsec pulse has a peak power intensity of  $4.0 \times 10^5\text{ watts/cm}^2$ . Although this power intensity is not sufficient to cause emission, soft-focusing this beam to approximately a  $5\text{ mm}^2$  spot and, thereby, increasing the power intensity to megawatts/ $\text{cm}^2$  evidently is. This fact is clearly an indication that at low pressures and low powers, the discrete states, the lower steps in the ladder, do present a barrier to the climbing process. Moreover, accessible  $\text{CO}_2$ -laser radiation of higher energy than the fundamental  $\text{CrO}_2\text{Cl}_2$  band at  $1000\text{ cm}^{-1}$ , namely  $9.6\ \mu$   $\text{CO}_2$ -laser transitions, did not induce luminescence even when focused to power intensities of gigawatts/ $\text{cm}^2$ . This result is as expected, since anharmonic terms in the vibrational Hamiltonian would be expected to redshift the resonance frequency of the excited states of the pumped mode(s). It is, therefore, not surprising

that  $10.6 \mu$  R-branch transitions of the  $\text{CO}_2$  laser are most effective in producing  $\text{CrO}_2\text{Cl}_2$  fluorescence. On the other hand,  $10.6 \mu$  P-branch laser radiation cannot induce multiphoton absorption in  $\text{CrO}_2\text{Cl}_2$  unless very large intensities (several hundreds of megawatts/cm<sup>2</sup>) are used. This result is undoubtedly due to the fact that the closest resonance between P-branch radiation from our laser [P(10) -952.88 cm<sup>-1</sup>] and the fundamental frequency of the Cr-O symmetric stretch at about 990 cm<sup>-1</sup> has an energy defect of 37 cm<sup>-1</sup>. Very intense laser fields are required to overcome this mismatch either through power broadening and/or non-linear absorption.

The fact that intensities of 8.0 megawatts/cm<sup>2</sup> are sufficient to induce absorption of at least 18 photons in  $\text{CrO}_2\text{Cl}_2$  needs further discussion. If we note that  $8.00 \times 10^6$  watts/cm<sup>2</sup> represents a laser field ( $E_0$ ) of  $1.55 \times 10^4$  V/cm and we use equation (2) of the theoretical section

$$\bar{\nu}_R = \frac{\mu E_0}{h} \quad (1)$$

where  $\mu$  is the transition moment and  $h$  is Planck's constant, we obtain a value of 0.10 cm<sup>-1</sup> for  $\bar{\nu}_R$ , the Rabi frequency. Thus, anharmonic compensation by power broadening is no more than 0.1 cm<sup>-1</sup> under the influence of this modest laser field. If it is recalled from the theoretical section that the anharmonic shift is of the order of 5-10 cm<sup>-1</sup> for the second excited ( $v = 2$ ) vibrational level of the pumped transition, then it is obvious that the Rabi frequency is not sufficient to maintain resonance. A laser field almost two orders of magnitude larger is required if this were the only compensating mechanism available. Of course, these calculations are approximate at best, but it is

inconceivable that they are in error by more than one order of magnitude.

Therefore, other factors must be contributing to the highly efficient absorption of laser photons in this molecule. We may look to the "PQR" mechanism as a possible compensatory vehicle for the molecule to overcome the discrete level bottleneck. A condition for this compensation to be effective is that (1)

$$|\Delta\nu_{\text{anh}} - 2BJ_{\text{res}}| \approx \nu_R \quad (2)$$

where  $\nu_R$  is again the Rabi frequency,  $\Delta\nu_{\text{anh}}$  is the anharmonic shift,  $B$  is the rotational constant, and  $J_{\text{res}}$  is the resonant rotational quantum number. Basically, this is a mathematical statement of the conditions under which anharmonic compensation can be realized by a combination of power broadening and rotational compensation. Of course, this formulation neglects higher order effects, such as centrifugal dislocation of the rovibrational Hamiltonian and, therefore, also assumes that the values do not change appreciably among the first three discrete vibrational levels. Nevertheless, it is a reasonable estimate of the compensatory effect. Thus, applying equation (2) to  $\text{CrO}_2\text{Cl}_2$  and using  $0.10 \text{ cm}^{-1}$  for the broadening by the field,  $5.0 \text{ cm}^{-1}$  for  $\Delta\nu$  and  $0.0620 \text{ cm}^{-1}$  for  $B$  (2), the rotational constant, we get a value of  $J$ , the rotational quantum number, of 40. The use of the  $B$  value in the case of  $\text{CrO}_2\text{Cl}_2$  is justifiable if we assume the molecule to be a nearly prolate symmetric top. According to reference (2),  $B = 0.0620 \text{ cm}^{-1}$ ,  $C = 0.0521 \text{ cm}^{-1}$ , and  $A = 0.1073 \text{ cm}^{-1}$ . Since  $B \approx C \neq A$ , the assumption is valid for purposes of this "order of magnitude" calculation. It is advisable at this point to estimate the fraction of molecules in the  $J = 40$  rotational

level. To calculate the energy of the  $J = 40$  level, we use the following sum rule<sup>3</sup>:

$$E_J = \frac{1}{3}(A+B+C)J(J+1). \quad (3)$$

Equation (3) says that the average rotational energy of all levels of a particular  $J$  state is given by  $J(J+1)$  times a rotational constant which is the average of  $A$ ,  $B$ , and  $C$ . Use of this sum rule for  $E_J = 40$  yields a value of  $121.03 \text{ cm}^{-1}$  above the rotational ground state,  $J = 0$ . Then, to obtain the fraction of molecules at  $J = 40$ ,  $f_{j=40}$ , we use (4):

$$f_r = \frac{(2J+1) \exp [(-J_{K-1}K_{+1})/kT]}{[(\pi/ABC)(kT/h^3)]^{3/2}} \quad (4)$$

where all the terms have been defined. Inserting the appropriate values into expression (4) results in  $f_{j=40} = 1.65 \times 10^{-4}$ . Expression (4) for an asymmetric rotor yields the fractional population in the state  $J_{K-1}K_{+1}$ , i.e., in a particular state of the  $J$  manifold of levels where  $K_{-1}$  and  $K_{+1}$  refer to the prolate and oblate  $K$  values respectively. However, our  $E_{J=40} = 121 \text{ cm}^{-1}$  was an average value of the energy range in the  $J = 40$  manifold. If we assume that all the levels are degenerate and of equal probability and, since the multiplicity is  $2J + 1$ , we arrive at the fractional population in the  $J = 40$  rotational manifold

$$f_{J=40} = (25+1)(1.65 \times 10^{-4}) = 1.34 \times 10^{-2}$$

Thus, according to these approximate calculations, 1.34% of the molecules reside in the "proper"  $J$  state for rotational compensation to take place under our TEA-laser conditions. This, unfortunately, is not the

end of the story. The phototube plus filter combination has a viewing window of 1 inch or 2.54 cm parallel to the fluorescence axis. If we estimate that the fluorescence beam has a cross-sectional area of  $5.0 \text{ mm}^2$ --the same as the measured laser spot at the focal point--and that it is constant throughout the viewing window (reasonable approximations for a 10-inch lens), we get an effective volume of interaction between the laser radiation and the  $\text{CrO}_2\text{Cl}_2$  bath of  $0.13 \text{ cm}^3$  assuming a cylindrical shape. These calculations lead to the conclusion that the laser radiation can interact, within the phototube's window, with  $5.1 \times 10^8$   $\text{CrO}_2\text{Cl}_2$  molecules at a pressure of  $1.0 \times 10^{-4}$  torr. Of these, only 1.34% or  $6.8 \times 10^6$  molecules are in the "appropriate"  $J = 40$  state. All that is left at this point is the virtually impossible task of calculating the fraction of molecules that absorb at least the 18 infrared photons required to emit a visible quantum of light. Quantum yield determinations are difficult to perform accurately, particularly using focusing optics, and can at best yield an average number of photons absorbed in multiphoton experiments. Additionally, at low pressures ( $10^{-4}$  torr), they are virtually impossible to perform. To overcome this difficulty and because the present discussion deals with absorption in the discrete (first three, really) levels, we may use the extinction coefficient ( $\alpha$ ) that was measured in the present work using no focusing optics. As such,  $\alpha$  reflects the absorption of one or perhaps two or three photons per molecule. Its use in calculations which depend on observable emission and, therefore, quasicontinuum absorption can be rationalized by noting that experimentally determined absorption cross-sections of molecules in the quasicontinuum do not seem to change very much from those of the discrete states. This fact can be explained by noting that the effect

of a weakened matrix element for quasicontinuum transitions is counterbalanced by an increased density of levels in the upper state and by a virtual "guaranteed resonance" at any frequency. Another justification for the use of the "low intensity  $\alpha$ " is the present understanding that if a bottleneck exists, it is due to interactions in the discrete states and not in the quasicontinuum. This implies that practically any molecule that reaches the quasicontinuum in the presence of sufficient laser energy density (fluence), as in our experiments, will absorb a sufficient number of photons to climb the ladder, i.e., there is a probability of unity for this process. Thus,  $\alpha$  is affected by the transitions in the discrete levels only. It is worth noting that the much reduced dependence of the luminescence signal vs. the exciting  $\text{CO}_2$ -laser 10.6  $\mu$  R-branch transitions (Figure 5) as compared with the dependence of the photoacoustic signal on the exciting frequency (Figure 2) lends credence to the latter argument.

In view of these arguments, it can now be stated that, using the R(30) 10.6  $\mu$  laser line and its measured  $\alpha$  of 0.0074, there are approximately .0074 times  $6.8 \times 10^6$  or  $5.0 \times 10^4$  molecules that are capable of absorbing a sufficient number of photons to effect detectable emission. Although a small fraction of the total molecular population, it is entirely reasonable to assume that this number of molecules is sufficient to yield measurable luminescence. Further calculations that would take into account the emission quantum yield and the phototube's quantum efficiency cannot be performed with any degree of confidence.

Laser induced multiphoton dissociation of several molecules ( $\text{SF}_6$ ,  $\text{CF}_3\text{Cl}$ , and others) has been detected in molecular beams (5,6), however, at pressures three orders of magnitude smaller than those used

in the present work, but under similar laser conditions. Additionally, Levy's (2) fluorescence work on  $\text{CrO}_2\text{Cl}_2$  was done in a supersonic beam. Finally, a few studies of multiphoton induced luminescence at very low pressures ( $10^{-4}$ - $10^{-5}$  torr) have been reported (7,8). Thus, we repeat, our calculations do not rule out that a combination of power broadening and rotational compensation is responsible for the first three absorbed photons in the MPE of  $\text{CrO}_2\text{Cl}_2$  at low pressures and low fluences.

The preceding discussion is not merely an academic exercise. As already mentioned, the low laser power intensity threshold of the  $\text{CrO}_2\text{Cl}_2$  emission pointed to the need for other compensatory mechanisms besides power broadening. The efficiency of the  $10.6 \mu$  R-branch laser lines, which are of lower energy than the fundamental vibrational transition, in inducing luminescence supports the notion that rotational compensation plays a role in multiphoton excitation. Similarly, the increased signal obtained in the presence of rare gases and the existence of only the fast, pulse-limited rise time under these conditions can be explained by rotational hole filling of the non-equilibrium molecular distribution caused by the laser pulse. Thus, it must be concluded that the anharmonicity of the first few levels can be overcome by rotational compensation.

Our experiments, however, are not in complete accord with the PQR mechanism. If it were operative as described by its proponents, we would expect for a given laser power density a very sharp dependence of the multiphoton absorption on laser lines. Only at very high intensities would the Rabi frequency be sufficient so as to relax the rigorous dependence on rotational angular momentum. We, therefore, conclude as others have that, although rotational compensation does play a role in

overcoming the anharmonic bottleneck of the discrete states, the actual mechanism must include a considerable number of J states and, therefore, is not necessarily limited to a "PQR-type" process.

So far, our discussion has been limited to the first few steps of the vibrational ladder-climbing process. Indeed, the PQR mechanism can explain only the first three molecular transitions in the presence of a moderate laser field. For large polyatomics, such as  $S_2F_{10}$  (9) or  $SF_5NF_2$  (10), which are almost in the vibrational quasicontinuum at room temperature, absorption of the first three photons guarantees access to the quasicontinuum and, therefore, to subsequent excitation. Smaller molecules, such as  $CrO_2Cl_2$ , and perhaps even  $SF_6$ , need considerable further excitation in order to reach vibrational levels where incoherent pumping characterizes the absorption process.

At this point, the second energy region, the quasicontinuum, must be considered. Unfortunately, experimental studies of this region are difficult and, particularly, empirical assignment of the onset of this energy domain has not been established. Additionally, it must be remembered that the experimental conditions, such as pressure, laser energy, and pulse width, to name a few, determine to a critical extent where the quasicontinuum begins for a particular molecule. Theoretical analysis of this region is, moreover, complicated by inexact knowledge of the required molecular conditions that must be met to achieve population of this energy domain. It should be mentioned, however, that these difficulties are not the result of researchers' ineptitude but, rather, of the processes that are involved, such as absorption and emission of radiation, intra and intermolecular energy transfer, and the concept of ergodicity (energy randomization) which has occupied many great scientists much before laser chemistry appeared on the scientific

scene. It is important to note that it is not only crucial to ascertain whether molecular behavior is statistical but also the time required for the redistribution of energy among the vibrational modes.

Despite these concerns, it is universally accepted that it is the exponential increase in the density of states with increasing vibrational energy that permits the absorption of the several tens of single-frequency photons required for MPD. This belief is buttressed by very convincing evidence, such as the 2-frequency experiments of Ambartzumian, et al (11) described in the theoretical section and the fact that no diatomic, and very few triatomic, molecules have been dissociated via multiphoton pumping. The latter fact is the direct result of the small density of vibrational states for small molecules even at fairly high levels of vibrational heating; i.e., the quasicontinuum does not begin at sufficiently low energies and, therefore, the resonance condition cannot be maintained except perhaps using extremely large laser power intensities.

With the preceding discussion in mind, we return to the discussion of  $\text{CrO}_2\text{Cl}_2$ . Assuming that we have accounted for the absorption of the first three photons by a combination of power broadening and rotational compensation of the anharmonicity, we now explore the next few up-the-ladder steps.

Table I lists the density of states,  $\rho(E)$  of  $\text{CrO}_2\text{Cl}_2$  at different energies, determined using the semi-classical calculations of Haarhoff (12). Also included in the table are the similarly calculated values for  $\text{SF}_6$  in the range of interest. It is, at first, striking that  $\text{CrO}_2\text{Cl}_2$ , with only  $3N-6$  or 9 vibrational modes has almost as many states/cm<sup>-1</sup> as  $\text{SF}_6$ , with 15 modes, in the lower energy region displayed in the Table. This relatively large density of states, due to the considerable number of low frequency fundamentals in  $\text{CrO}_2\text{Cl}_2$  (see Table I of Results) as

TABLE I

<u>Vib. Energy in (<math>\text{cm}^{-1}</math>)</u>	<u><math>\rho(E)\text{CrO}_2\text{Cl}_2</math> (<math>\frac{\text{states}}{\text{cm}^{-1}}</math>)</u>	<u><math>\rho(E)\text{SF}_6</math> (<math>\frac{\text{states}}{\text{cm}^{-1}}</math>)</u>
3000	$7.6 \times 10^1$	$7.8 \times 10^1$
4000	$3.2 \times 10^2$	$4.3 \times 10^2$
5000	$1.1 \times 10^3$	$2.0 \times 10^3$
6000	$3.1 \times 10^3$	$8.0 \times 10^3$
7000	$7.9 \times 10^3$	$2.8 \times 10^4$
8000	$1.8 \times 10^4$	$8.8 \times 10^4$
9000	$3.9 \times 10^4$	$2.6 \times 10^5$
10000	$7.8 \times 10^4$	$6.9 \times 10^5$

compared with SF<sub>6</sub>, undoubtedly plays a major role in permitting MPA of CrO<sub>2</sub>Cl<sub>2</sub> under the very mild conditions we have been discussing. Of course, at higher levels of excitation, the disparity between CrO<sub>2</sub>Cl<sub>2</sub> and SF<sub>6</sub> increases since the number of vibrational degrees of freedom becomes the dominating factor.

It is widely accepted that, for SF<sub>6</sub>, the quasicontinuum begins between 4000 and 6000 cm<sup>-1</sup>, i.e., between the fourth and sixth absorption of a CO<sub>2</sub>-laser photon. Strictly speaking, what is really meant is that in this domain incoherent absorption, Fermi's Golden Rule and, therefore, a rate-equation treatment of the absorption process (see Theoretical Section) may be applied. The onset of region II may be defined by the condition:

$$\frac{\langle |\bar{\mu}|^2 \rangle \rho}{\Gamma(\omega)} \gg 1 \quad (5)$$

where  $|\bar{\mu}|$  is the radiative coupling term (Rabi frequency for the transition),  $\Gamma(\omega)$  is the width into which the oscillator strength is smeared, and  $\rho$  is as before the vibrational level density. By rearranging (5) to read

$$\frac{|\bar{\mu}|^2}{\Gamma(\omega)} \gg \rho^{-1} \quad (5')$$

we may interpret this inequality as demanding that the diluted (presumably by intramolecular vibrational relaxation) Rabi frequency be considerably larger than the level spacings in the quasicontinuum. This requirement, therefore, insures resonance between the laser photons and the vibrational levels and, at the same time, sufficient oscillator strength for the transition to occur. Typically, for SF<sub>6</sub> MPD experiments,

$\bar{\nu}$  or  $\nu_R$  (in  $\text{cm}^{-1}$ ) is 1-10  $\text{cm}^{-1}$ .  $\Gamma^{(w)}$  can be expected to be between 10-100  $\text{cm}^{-1}$  based on indirect experimental evidence such as the broadened  $\nu_3$  absorption (coincident with the  $\text{CO}_2$  laser) in highly excited  $\text{SF}_6$  (13) and an approximate measurement of the intramolecular relaxation time of  $\text{SF}_6$  in the quasicontinuum (14). Use of these values in inequality (5) shows that the quasicontinuum condition is satisfied with a relatively modest,  $\rho \geq 10^3/\text{cm}^{-1}$ , density of states. Thus,  $\text{SF}_6$  vibrationally excited to 5000  $\text{cm}^{-1}$  is in the quasicontinuum (Table I). Returning to  $\text{CrO}_2\text{Cl}_2$  and using the calculated  $\nu_R = 0.1 \text{ cm}^{-1}$  and using the  $\Gamma^{(w)} \sim 10\text{-}100 \text{ cm}^{-1}$ , we can estimate that  $\rho \sim 10^4 \text{ cm}^{-1}$ , which would require excitation to at least 7000 or 8000  $\text{cm}^{-1}$ . The value of  $\Gamma^{(w)}$  for  $\text{CrO}_2\text{Cl}_2$  is somewhat arbitrary. However, since the density of states of  $\text{CrO}_2\text{Cl}_2$  is similar to that of  $\text{SF}_6$  in the relevant energy region and because of the lesser symmetry of the former and, therefore, a reduced mixing of the vibrational levels (at least in the lower excited states),  $\Gamma^{(w)}$  is probably somewhat smaller in  $\text{CrO}_2\text{Cl}_2$  than in  $\text{SF}_6$ . We can, thus, cautiously assume that, at 7000  $\text{cm}^{-1}$  (or perhaps even at 6000  $\text{cm}^{-1}$ ) or after absorption of about 7  $\text{CO}_2$ -laser photons,  $\text{CrO}_2\text{Cl}_2$  is in the quasicontinuum.

The obvious region that remains unexplored is that between the first three discrete levels and the quasicontinuum. Parenthetically, this is perhaps the most difficult region to analyze theoretically, since there is probably a mixture of discrete and quasicontinuum character to these levels. Furthermore, access to the quasicontinuum is probably a gradual process, or a question of degree, rather than a sharp and distinct event. Besides power broadening and rotational compensation effects, there are two characteristics of  $\text{CrO}_2\text{Cl}_2$  that probably facilitate access from the discrete states, through the "mixed" region into the quasicontinuum. The arithmetic relationship among the

fundamental frequencies and overtones is such that many near degeneracies can occur with the laser-pumped modes even when the density of states is relatively low. Thus, as can be seen in Table I of the Results Section, the  $\nu_8$  vibrational fundamental has a frequency of  $499 \text{ cm}^{-1}$  or just about one-half that required for the resonance condition with the laser photons. Thus,  $\Delta\nu = 2$  transitions in the  $\nu_8$  vibrational manifold, albeit weaker, would provide an alternate ladder for the multiphoton absorption process to occur. A similar statement applies to the  $\nu_1 + \nu_6$  combination band which has been observed by Hobbs (15) in the gas phase at  $1980 \text{ cm}^{-1}$ . Because of its existence, the resonance condition is relaxed for the first few even-numbered transitions. Since it can be expected that the anharmonic shifts of these levels,  $\nu_8$  or  $\nu_1 + \nu_6$ , will differ from those of the  $\nu_1$  and  $\nu_6$  pumped modes, access to the quasicontinuum is facilitated by these accidental near-degeneracies.

The second spectroscopic characteristic, which is directly related to the first, is the possibility of Fermi resonance between vibrational levels. Briefly, this perturbation arises between levels that are nearly degenerate in the harmonic oscillator approximation. Their proximity leads to level mixing theoretically treatable by perturbation theory as a  $2 \times 2$  matrix. The result is an increase in energy in the higher frequency level and a decrease in the lower frequency one. Additionally, this perturbation can affect the intensities of the transitions. Thus, for example, the  $\Delta\nu = 2$  overtone  $\nu_8$  transitions can become stronger or less forbidden, by borrowing oscillator strength from the  $\nu_1$  fundamental. For Fermi resonance to occur between two vibrational levels, they must be of the same symmetry. This requirement, as evidenced by the example just mentioned where both  $\nu_1$  and  $\nu_8$  belong to the totally symmetric  $a_1$  representation, is easily met in  $\text{CrO}_2\text{Cl}_2$ .

Other possibilities for Fermi resonance include the interaction between the even overtones of the  $\nu_6$  ( $b_1$  symmetry) mode, which belong to the  $a_1$  representation and the almost degenerate even overtones of the  $\nu_8(a_1)$  fundamental at  $496 \text{ cm}^{-1}$  and also that between the even overtones of the pumped  $\nu_1$  and  $\nu_6$  modes. It should be mentioned that the anharmonic splitting of the triply degenerate  $\nu_3$  pumped-mode in  $\text{SF}_6$  has been similarly invoked to explain the first few up-the-ladder steps in  $\text{SF}_6$  (16).

It can be concluded, therefore, that the experimentally observed multiphoton excitation of  $\text{CrO}_2\text{Cl}_2$  under collisionless conditions and using very low laser powers can be understood, at least qualitatively, within the theoretically accepted model of MPE. To summarize, it is the combination of strong infrared absorption together with the Rabi frequency broadening and rotational compensation of anharmonic shifts that maintains the resonance condition through the first few levels. Additionally, the spectroscopic characteristics of  $\text{CrO}_2\text{Cl}_2$  may provide additional paths and/or compensation of the anharmonic shifts (Fermi Resonance) that facilitate the up-pumping process. Once the quasi-continuum is reached, i.e., after absorption of six or seven laser photons by  $\text{CrO}_2\text{Cl}_2$ , the high level density insures the maintenance of resonance between the molecule and the laser field. The vibrational heating then continues until the dissociative continuum is reached and unimolecular dissociation occurs.

As already mentioned, the resulting dissociation of  $\text{CrO}_2\text{Cl}_2$  under high-order infrared multiphoton excitation is not unique. Neither is the observation that it is the weakest bond--the Cr-Cl bond (68 kcal/mole or 83 kcal/mole)--that is severed though the exciting radiation coincides with the frequencies of the Cr-O vibrations. These results

are consistent with energy randomization in the quasicontinuum and, therefore, statistical thermodynamic control of the reaction products. This behavior has been generally observed in virtually all MPD experiments to date. Moreover, RRKM calculations of such experiments performed under molecular beam conditions (5,6) have resulted in reasonable agreement between theory and experiment, again implying a statistical unimolecular path of the dissociation. The observation of electronic emission induced by multiphoton excitation, however, is not addressed by the foregoing analysis. Statistical theories, such as RRKM, predict dissociation from the ground state potential energy surface and typically concomitant formation of ground state products. Thus, the visible luminescence obtained under collision-free conditions in the present work and particularly that originating from the parent,  $\text{CrO}_2\text{Cl}_2$ , molecule needs further clarification.

As a result of the present work, it is appropriate to divide the MPE of  $\text{CrO}_2\text{Cl}_2$  into two regions. One is the low fluence and low pressure regime where absorption of approximately 18  $\text{CO}_2$ -laser photons produces predominantly electronically excited parent molecules. In the second region, which is reached under more severe fluence and/or pressure conditions, further excitation of  $\text{CrO}_2\text{Cl}_2$  molecules takes place resulting in dissociation. The origin of the collisionlessly induced electronic emission is, we believe, firmly established as emanating from parent molecules. Briefly, at low fluence and low pressures ( $10^{-4}$  torr), the fluorescence spectrum is the same as that obtained by conventional spectroscopic (one photon) studies of  $\text{CrO}_2\text{Cl}_2$ . Similarly, the pressure and fluence behavior of this signal, monitored at  $6300 \text{ \AA}$ , is consistent with parent emission. Moreover, the Stern-

Volmer data, yields a collisional quenching rate which is the same as that obtained under single-photon electronic excitation. That the V-E relaxation process is intramolecular is also firmly established. At a pressure of  $10^{-4}$  torr, which means approximately  $10^{-1}$  collisions/ $\mu$ sec, the rise time of the fluorescence signal clearly follows that of the laser pulse. Using a  $N_2$ -free laser mixture, our pulse is 200 nsec F.W.H.M. Evidently, the process is collisionless and, therefore, results from the radiation-molecule interaction and from subsequent intramolecular relaxation processes in the absence of perturbing collisions. As a matter of fact, when a collisional component is present, it can easily be experimentally distinguished from the collision-free fluorescence.

Originally we interpreted the V-E energy transfer in  $CrO_2Cl_2$  as arising via cross over from the high vibrational levels of the  $CrO_2Cl_2$  ground state to the low vibrational levels of the  $7a_1^*$  electronically excited state. However, we were convinced, somewhat against our will, by a persistent referee that density of states considerations mitigated the appeal of this explanation. Thus, the density of ground state vibrational levels is  $3 \times 10^6/cm^{-1}$  at the origin of the first excited state. With this overwhelming statistical weight against what may be called "reverse internal conversion," we temporarily abandoned this hypothesis in favor of direct infrared transitions to the electronically excited state. The latter explanation was apparently more palatable, although it is also not favored by the ratio of density of states, because presumably the strong laser field would provide the driving force. Thus the reviewer was satisfied or, perhaps, appeased, the paper was published, and in it our change of heart was duly noted.

During this time, we were beginning to obtain results on the lifetime of the fluorescence signal. It was obvious that the mono-

molecular lifetime was considerably longer than that obtained by McDonald with single-photon excitation. Additionally, the very large fluorescence-quenching collision cross-section, the low laser energy required to induce emission, and the linear dependence of the luminescence on fluence, among others, supported the notion of population of very high ground state vibrational levels together with crossover to low lying vibronic levels of the excited state. This process can be also represented in terms of mixed (ground and electronic vibronic levels) states as has been proved useful in the theory of radiationless transitions. This latter formulation obviates the need of differentiating between intra and interstate transitions and, additionally, is a truer representation of the eigenstates of the molecular Hamiltonian.

Concurrently with these developments, Professor Joshua Jortner visited our laboratory and his interest in the origin of the fluorescence led him and Nitzan to publish (17,18), within a short time, a theoretical treatment of the V-E energy transfer induced by multiphoton pumping. Thus, the theory of inverse electronic relaxation (IER) was born.

Under the Born-Oppenheimer approximation, the ground and excited electronic states of a polyatomic molecule, such as  $\text{CrO}_2\text{Cl}_2$ , may be represented by  $\{|G\alpha\rangle$  and  $\{|S\beta\rangle$ , respectively, with vibrational level densities,  $\rho_G$  and  $\rho_S$ , corresponding to these electronic states. The indices,  $\alpha$  and  $\beta$ , describe the levels within the vibrational manifold of each electronic state. Jortner's theory of IER, which will be briefly outlined, allows for multiphoton excitation within the ground vibrational manifold resulting in excitation of mixed or scrambled molecular eigenstates of the form  $(\{|G\alpha\rangle + \{|S\beta\rangle$ ). These mixed states, designated as  $\{|j\rangle$ , consist of quasidegenerate ground and excited vibronic levels coupled via nonadiabatic perturbations,  $V_{G\alpha S\beta}$ , such as

nuclear kinetic energy or, in the case of different spin multiplicities, spin-orbit interactions. The molecular eigenstates, thus formed, have radiative widths due to the  $\{|S\beta\rangle\}$  character. As a matter of fact, as emphasized by Jortner, it is the coupling to a radiative continuum to low-lying ground state vibronic levels that renders the IER process practically irreversible.

In a polyatomic molecule, we can distinguish between two energy regions, A and B. The former is characterized by groups of  $\{|j\rangle\}$  states, each composed of a single  $|S\beta\rangle$  level. The molecular eigenstates are separated by pure uncontaminated  $|G\alpha\rangle$  states. This lower energy regime also includes the pure ground state vibrational manifold below  $|S_0\rangle$ , the excited state's origin.

Range A is characterized by the condition

$$\rho_S \Delta_{S\beta,G} < 1 \quad (5)$$

where  $\rho_S$  is the average excited-state vibronic level density and  $\Delta_{S\beta,G}$  is the dephasing width or the radiationless decay rate of each  $|S\beta\rangle$  state, and it is given by

$$\Delta_{S\beta,G} = 2\pi V_{S\beta,G\alpha}^2 \rho_G \quad (6)$$

where  $V_{S\beta,G\alpha}^2$  is the average ground-excited state interaction energy and  $\rho_G$  is the mean density of ground vibrational levels in the energy region of  $|S\beta\rangle$ . Thus, above the excited state electronic origin, range A consists of a set of  $\{|j|\}$  states, originating from level mixing between  $\{|G\alpha\rangle\}$  and  $\{|S\beta\rangle\}$ , whose width is  $\Delta_{S\beta,G\alpha}$ , and whose members are separated

by uncontaminated "black holes," as Jortner describes them, of pure  $|G_\alpha\rangle$  states. Obviously, this description corresponds to energy regions where the excited state vibronic level density is relatively sparse.

The total width of each  $|j\rangle$  state,  $\gamma_j(E_j)$ , is approximately given by

$$\gamma_j(E_j) \approx \gamma_{G_\alpha}(E_j) + \sum_B \theta(E_j - E_{S_B}) \frac{\gamma_S}{N_A(E_{S_B})} \quad (7)$$

and  $N_A(E_{S_B})$ , which is the number of ground state vibronic levels that interact with  $|j\rangle$ , is:

$$N_A = \rho_G(E_{S_B}) \Delta_{S_B, G} \quad (8)$$

In (7),  $\gamma_{G_\alpha}$  is the total width of the  $\{|G_\alpha\rangle$  levels. It arises from spontaneous infrared emission or from collisional deactivation. Under collisionless conditions of MPE and since infrared radiative decay times are of the order of mseconds,  $\gamma_{G_\alpha}$  is vanishingly small and can thus be neglected in expression (7).  $\theta(E_j - E_{S_B})$  is a step function that satisfies:

$$\theta(x) = \begin{cases} 1, & -\frac{1}{2}\Delta_{S_B, G} \leq x \leq \frac{1}{2}\Delta_{S_B, G}, \\ 0 & \text{otherwise} \end{cases} \quad (9)$$

Finally, then the expression for the width of each  $|j\rangle$  state in range A can be written as:

$$\gamma_j^A(E_j) \approx \sum_B \theta(E_j - E_{S_B}) \frac{\gamma_S}{N_A(E_{S_B})} \quad (10)$$

Before continuing with a description of range B, it should be noted that  $\gamma_j^A$  which may be equated with the IER rate in region A, is basically given by the radiative rate of the excited-state vibronic level diluted by a factor of  $N_A(E_{SB})$ , which is the number of ground state levels coupled to  $|SB\rangle$ . Thus, the IER rate, which is derived in terms of the molecular eigenstates  $\{|j\rangle\}$ , can presumably be obtained from measurable,  $\gamma_S$ , and calculable,  $N_A$ , quantities described in the Born-Oppenheimer basis sets,  $\{|G\alpha\rangle\}$  and  $\{|SB\rangle\}$ .

The higher energy region, B, is characterized by a moderately high density of  $|SB\rangle$  states, so that

$$\rho_S \Delta_{SB,G} \geq 1 \quad (11)$$

holds. Because of level congestion, the black holes are absent and instead two coupled quasicontinua exist. The dilution factor is, thus, given by

$$N_B(E_j) = \rho_G(E_j) / \rho_S(E_j), \quad (12)$$

the ratio of the state densities. The total decay width is again given by an expression similar to (7)

$$\gamma_j^B = \gamma_{G\alpha}(E_j) + \frac{\gamma_S}{N_B} \quad (13)$$

but, of course, without the step function since, in B, the width of each  $|SB\rangle$  state exceeds the level spacing,  $\rho_S^{-1}$ . Again neglecting  $\gamma_{G\alpha}$  as small, we arrive at the desired expression for  $\gamma_j$  in range B

$$\gamma_j^B(E_j) = \frac{\gamma_S}{N_B} = \gamma_S \frac{\rho_S(E_j)}{\rho_G(E_j)} \quad (14)$$

Thus, the IER rate in this region is again characterized by the radiative decay rate divided by the dilution factor,  $N_B$ , which is the ratio of ground to excited state level density. Alternatively and consistent with the right-most expression in (14), the IER rate, which we will denote by  $\Gamma_{IER}$ , in range B is given by the radiative decay rate of the  $\{|S_B\rangle\}$  manifold multiplied by the ratio of level densities of emitting ( $\rho_S$ ) to non-emitting ( $\rho_G$ ) or ground state.

We have, therefore, arrived at the expressions (10) and (14) that describe the inverse electronic relaxation process in medium-sized polyatomic molecules. As is often the case, we have facilitated the treatment and the understanding of the IER process by dividing, somewhat arbitrarily, the energy manifold into two regions that are characterized by low and high density of states in the excited electronic or "doorway" state. It must be added, however, that as with the ladder-climbing process in MPD, the transition from region A to B is undoubtedly a continuous, smooth process and our subdivision is a simplified model of the process. Bearing this admonition in mind, we may nevertheless examine the outstanding features of the process.

Because in both energy domains the  $\Gamma_{IER}$  is given by the radiative lifetime of the excited state, divided by a dilution factor,  $N_A$  or  $N_B$ , and since  $N_A, N_B \gg 1$  for most accessible energy ranges, we expect that the IER rate will be slower than the purely radiative one. This, in turn, means that the experimentally measured lifetime of the MPE-prepared state will be longer than that calculated on the basis of

oscillator-strength measurements obtained from absorption experiments, for example. This fact again underlines the similarities between the IER and the radiationless transitions processes, the latter having been described in the early literature (19) as resulting in "anomalously" long radiative lifetimes.

In range A, only a part of the  $\{|G\alpha\rangle\}$  manifold is coupled to the  $|S\beta\rangle$  level. As was mentioned, the mixed  $\langle j|$  states are separated by black holes or uncontaminated  $\{|G\alpha\rangle\}$  states. As pointed out by Jortner, this decreases the effective value of  $\rho_G$  and, in turn, enhances the IER rate. This also implies that an exceedingly large value of  $\rho_G$ , in range A, as is the case for a large polyatomic molecule, may dilute the radiative rate sufficiently so as to prevent IER (emission, really) detection. Additionally, the inverse dependence on  $\rho_G$ , also sets an upper limit on the observation of IER within range A. As we ascend in energy in this range,  $\rho_G$  is increasing exponentially, the lifetime of the emission is increasing, and eventually IR emission and collisions, even at low pressures can damp the electronic fluorescence.

However, in range B, the situation is different. The dilution factor is really the ratio of level densities,  $N_B = \frac{\rho_G}{\rho_S}$ , which means that the radiative lifetime multiplied by  $\frac{\rho_S}{\rho_G}$  is the  $\Gamma_{IER}$ . Increasing the vibrational excitation in this range, therefore, would be expected to help the IER rate. If we assume a constant  $\Gamma_S^{(R)}$  for the moment and we focus on the ratio  $\frac{\rho_S}{\rho_G}$ , we see that it increases with increasing energy, resulting in a faster IER rate. In practice, this effect may not be easily observed since, at these high levels of excitation, dissociation is usually the preferred process. Nevertheless, it is interesting to note the opposite trends expected in the two energy ranges as a function of vibrational excitation.

To focus on the vibrational to electronic (V-E) energy transfer process in  $\text{CrO}_2\text{Cl}_2$ , we will briefly review the relevant spectroscopic parameters of this molecule. Under the  $C_{2v}$  symmetry group, the two lowest electronically excited states correspond to  $A_2$  ( $16970 \text{ cm}^{-1}$ ) and  $B_1$  ( $17248 \text{ cm}^{-1}$ ); thus, their origins are only  $278 \text{ cm}^{-1}$  apart. Additionally, there is a  $B_2$  state of somewhat higher energy which is completely dissociative. If one includes the triplet states of the same symmetry, there are at least three single-singlet and three singlet-triplet (spin forbidden) transitions from the  $A_1$  ground state in this general energy region. Additionally, it is worthwhile to reiterate that the lowest dissociative channel ( $\text{CrO}_2\text{Cl}-\text{Cl}$  bond rupture) exceeds the origin of the first excited state by 19-34 kcal/mole.

The density of ground state vibrational levels is  $3 \times 10^6/\text{cm}^{-1}$  at the origin of the  $A_2$  state and  $6.5 \times 10^6/\text{cm}^{-1}$  at the  $B_1$  state's origin. McDonald's fluorescence study (20) and subsequently Levy's supersonic-beam emission experiments (2) established the  $B_1$  state as that responsible for the  $\text{CrO}_2\text{Cl}_2$  luminescence in the gas phase. However, the  $A_2$  state, non-emissive in  $\text{CrO}_2\text{Cl}_2$  vapor, or perhaps an unidentified triplet state, is responsible for the emission in low temperature solids regardless of the excitation wavelength used (21). Bondybey (21) attributes this result to fast vibrational relaxation and radiationless transitions from the  $B_1$  to the emissive ( $A_2$  or triplet) state, when the former is resonantly excited. This "physical state" dependent fluorescence appears to reflect the fact that, in the gas phase, the density of rovibronic states is the key parameter involved in the required radiationless transition, whereas, in low temperatures matrices, the multitude of phonon states insures the existence of the required level density. Therefore, other molecular parameters, such as the Franck-Condon factors connecting the two vibronic manifolds and the energy defect or excess energy that must be dissipated

into the lattice, basically determine the rate and extent of fluorescence.

Returning to the multiphoton-induced IER process in  $\text{CrO}_2\text{Cl}_2$  vapor, we'll assume that it is the  $B_1 \rightarrow A_1$  transition that leads to the visible fluorescence. Furthermore, we assert that only energy region A, where  $\rho_S \Delta_{SB,G} < 1$ , is involved in the emission. To verify this, we need to know  $\Delta_{SB,G}$ , the non-radiative width of each  $|SB\rangle$  vibronic level. McDonald's experiments (20) yield a decay time,  $\tau$ , of 1.34  $\mu\text{sec}$  for the vibrationally cold electronically excited state. Additionally, because this value is in reasonable agreement with that obtained from absorption oscillator strength calculations, he asserts that it is purely radiative. This observation implies that the internal conversion rate, which is basically the non-radiative width,  $\Delta_{SB,G}$ , is slower than the radiative rate. Therefore, a lower limit of 1.34  $\mu\text{sec}$  can be set for the former; i.e., internal conversion into high-lying ground state levels from the vibrationally cold  $B_1$  level must be slower than 1.34  $\mu\text{sec}$ . Using the speed of light, we get an upper limit for  $\Delta_{SB,G} = 2.50 \times 10^{-5} \text{ cm}^{-1}$ . Using this value in  $\rho_S \Delta_{SB,G} > 1$ , expression (11), we get  $\rho_S = 4.02 \times 10^4 \text{ states/cm}^{-1}$  for  $\Delta_{SB,G} > 2.50 \times 10^{-5} \text{ cm}^{-1}$ . This is the value of  $\rho_S$  required to meet the region B strong coupling condition. Obviously, this high density of states is absent at the  $B_1$  origin. Moreover, although the frequencies of the  $B_1$  state vibrational fundamentals are not known, a level density of more than  $10^4 \text{ states/cm}^{-1}$  is surely not reached until an energy region where the levels are not fluorescent, but on the contrary probably dissociative. Therefore, the electronically excited vibrationless level is well within region A, where  $\rho_S \Delta_{SB,G} < 1$ . The non-radiative rates of vibrationally hot  $B_1$  levels cannot be derived from McDonald's data, since no collisionless lifetimes could be obtained under his experimental conditions. Moreover, the low pressure lifetimes seemed to vary, by an order to magnitude in some cases, for very

closely lying levels. His data clearly show that the radiationless transition is, surprisingly, strongly dependent on the vibrational mode that was laser-excited. Because of these interesting, but conflicting, problems, we merely assert that all the fluorescing states had radiationless rates comparable to or probably considerably smaller than his 50 nsec dye laser pulse. We note that this is consistent with the fact that these levels are active in emission, whereas those to the blue of  $5650 \text{ \AA}$  ( $5550 \text{ \AA}$  in Levy's supersonic jet) are not. In this higher energy region, the internal conversion rate is so fast that, instead of only dominating the emission decay, molecules undergo a radiationless transition to the ground state before they have had a chance to emit. Moreover, this process is irreversible since no emission is observed. In this connection, it should be mentioned that McDonald suggests the possibility that the onset of photodissociation may occur at considerably longer wavelengths than those observed by Halonbrenner, et. al. (22) This would account for the sudden drop in fluorescence yield. We briefly investigated this possibility by irradiating  $\text{CrO}_2\text{Cl}_2$  samples ranging in pressure from 0.5 - 10 torr with a Q-switched frequency-doubled Neodymium-Yttrium Aluminum Garnet (Nd-Yag) laser\*, capable of producing a 10 nsec pulse containing 7.0 J at  $5320 \text{ \AA}$ . As expected from previous reports cited, including McDonald's, no visible luminescence was observed even when the laser radiation was tightly focused. Similarly, however, no particles were detected by scattering with a He-Ne continuous wave (cw) laser and no  $\text{CrO}_2$  could be detected in the cell or windows after the  $\text{CrO}_2\text{Cl}_2$  was evacuated.

---

\*The author wishes to thank Prof. G. Skorinko of the Brooklyn College Physics Department for graciously allowing the use of his laser.

Although by no means exhaustive, these experiments together with that of others (22), indicate that photodissociation of  $\text{CrO}_2\text{Cl}_2$  requires light to the blue of  $5320 \text{ \AA}$ . Based on this evidence, the negligible or zero fluorescence quantum yield blue of  $5650 \text{ \AA}$  must be attributed to a fast internal conversion that is rendered irreversible by the high ground-state vibrational level density. The fluorescent levels on the other hand undergo radiationless transitions at a rate which is either slow or at most comparable to McDonald's 50 nsec pulse. Returning to the identification of the IER energy region in  $\text{CrO}_2\text{Cl}_2$ , we proceed as before using  $\tau_{nr} = 50 \text{ nsec}$  and we get a value of  $6.7 \times 10^{-4} \text{ cm}^{-1}$  for  $\Gamma_{S\beta, G}$ . Again, use of expression (11) yields a level density,  $\rho_S$ , of  $1.5 \times 10^3 \text{ states/cm}^{-1}$  in order to be in region B of the IER theory. Again, it is doubtful that this density can be reached in the  $B_1$  electronic state before dissociation; it is certainly orders of magnitude above that found in the region of interest of the present work. Therefore, we again assert that IER in  $\text{CrO}_2\text{Cl}_2$  belongs to the weak coupling case ( $\rho_S \Delta_{S\beta, G} < 1$ ) or to region A of the IER formalism.

High order infrared multiphoton pumping prepares the  $\text{CrO}_2\text{Cl}_2$  molecule in highly excited vibrational levels of the ground electronic state. The high level congestion in this energy region, the quasi-continuum, results in fast intramolecular vibrational relaxation (IVR). This essentially leaves all normal modes of vibration of  $\text{CrO}_2\text{Cl}_2$ , and not just those resonant with the laser field, vibrationally excited. This loss of coherence is manifested, for example, in the fact that pumping the Cr-O stretch of  $\text{CrO}_2\text{Cl}_2$  results in Cr-Cl bond fission. Additionally, IVR together with power broadening broaden these levels to what is almost a true continuum. Thus, the nature of the MPE process itself insures efficient overlap between the dense ground vibrational

manifold and the comparatively sparse excited vibronic levels. Undoubtedly, this efficient coupling assists the V-E energy transfer process and, thus, increases the IER rate. We note that this mode of excitation is consistent with the broad, devoid of fine structure, emission that we observed in the MPE of  $\text{CrO}_2\text{Cl}_2$  as well as that detected in other systems that reportedly undergo IER (23,24,25). Parenthetically, this featureless broad luminescence would also be expected if the fragments, rather than the parent, produced via MPD are the origin of the luminescence. This is consistent with production of vibrationally hot daughter species, such as  $\text{CrO}_2\text{Cl}$ , via MPD, which are pumped further by the laser field to excited vibrational levels from which they can undergo IER and, therefore, luminesce. Indeed, broad featureless spectra seem to be the rule in almost all the MPE-induced luminescing systems studied to date.

Although the behavior of the MPA-induced luminescence in  $\text{CrO}_2\text{Cl}_2$  with regard to pressure, fluence and, particularly, spectral range supports the IER notion, the lifetime data, on the surface, do not. In the single-photon excitation of  $\text{CrO}_2\text{Cl}_2$ , the emission of the vibrationally cold level had a lifetime of 1.34  $\mu\text{secs}$ , in reasonable agreement with oscillator strength calculations.(20) Additionally, the vibrationally hot electronically excited levels generally exhibited even shorter lifetimes. In our experiments, particularly those in the presence of Ar, the collision-free lifetime was in excess of 50.0  $\mu\text{secs}$ . This 40-fold lifetime increase is paradoxical, when we are claiming that the  $B_1$  state, the one with a significant radiative width, is responsible for the emission observed in both single and multiphoton experiments. We will show that this seeming contradiction is really strong evidence in favor of V-E energy transfer in  $\text{CrO}_2\text{Cl}_2$  as depicted by the IER theory.

We should, at the outset, raise the possibility that it is the nearby ( $278 \text{ cm}^{-1}$ ) lower energy state that is emitting. The most compelling evidence against it is that its emission was not observed in the gas-phase fluorescence experiments of both McDonald (20) and of Blazy and Levy (2). Only emission from the  $B_1$  state, an allowed transition, was detected. As already mentioned, phosphorescence from the lower state, whether from a triplet or perhaps a symmetry forbidden  $A_2$  state, has been reported only in low temperature matrices (21,26). Additionally, the lifetime of this emission has been reported (21) to be in the msec domain; its exact value being dependent upon the nature and history of the rare gas matrix. To assume that this is the emissive state in our MPA experiments would require postulating a lifetime shortening mechanism which is highly improbable given our ground-state pumping method of excitation. Mixing of this triplet with the  $B_1$  state, a possible lifetime shortening process, does not occur according to Bondybey's polarization studies (21). Therefore, we emphasize that the evidence weighs heavily against emission from the lower-lying state.

High order infrared multiphoton excitation of  $\text{CrO}_2\text{Cl}_2$  prepares the molecule in mixed molecular eigenstates,  $\{|j\rangle\}$ , whose parentage is an admixture of a single vibronic  $B_1$  level ( $|S_\beta\rangle$  of the IER formalism) with a set of quasi-degenerate ground state levels,  $\{|G_\alpha\rangle\}$ . Since we have shown that, in  $\text{CrO}_2\text{Cl}_2$ , IER-region A is the only one of interest, the emission rate  $\gamma_j^A$  is given by (10),

$$\gamma_j^A(E_j) = \sum_{\beta} \theta(E_j - E_{S\beta}) \frac{\gamma_S}{N_A(E_{S\beta})}$$

$\theta$  is a step function, defined by (9), and since we are interested in an emissive level where crossover from the ground state into the  $B_1$  vibronic

level must have occurred, we set it equal to 1. Therefore, (10) becomes,

$$\gamma_j^A = \frac{\gamma_S}{N_A(E_{SB})} \quad (10')$$

or since  $N_A = \rho_G(E_{SB})\Delta_{SB,G}$ ,

$$\gamma_j^A = \rho_G^{-1}(E_{SB}) \frac{\gamma_S}{\Delta_{SB,G}} \quad (10'')$$

In this form, we see that the IER rate is proportional to the level spacing in the ground vibrational manifold and to the ratio of radiative to dephasing widths of the vibronic  $B_1$  level of interest. According to McDonald (20), the decay of the vibrationally cold  $B_1$  level is basically purely radiative, i.e.,  $\Delta_{SB,G} \lesssim \gamma_S$ . He bases this assumption of no, or little, interstate mixing on the similarity between the calculated and the empirically determined lifetime, as well as on the experimental fact that the  $B_1$  state is emissive in low temperature matrices (26). The latter observation would not be expected, as previously implied in this discussion, for strongly mixed electronic states. Subsequently, as already mentioned, Bondybey established that, indeed, the  $B_1$  state does not fluoresce in rare-gas matrices (21). Thus, it is very possible that the dephasing rate is at least comparable to the radiative width even for the low-lying vibronic  $B_1$  levels. Thus, prudently, letting  $\Delta_{SB,G} \sim \gamma_S = 2.50 \times 10^{-5} \text{ cm}^{-1}$  and using the vibrational level population at the  $B_1$  origin,  $\rho_G = 3.0 \times 10^6 \text{ states/cm}^{-1}$  in (10'').

$$\gamma_j^A = \left( \frac{3.0 \times 10^6}{\text{cm}^{-1}} \right)^{-1} \frac{2.50 \times 10^{-5} \text{cm}^{-1}}{2.50 \times 10^{-5} \text{cm}^{-1}}$$

$$\gamma_j^A = 0.333 \times 10^{-6} \text{cm}^{-1}$$

Using the speed of light,  $3.0 \times 10^{10}$  cm/sec, we can calculate the lifetime of this emission and, since  $(\gamma_j^A)^{-1} \equiv \tau_{\text{IER}}$ , we obtain:

$$\tau_{\text{IER}} = (\gamma_j^A)^{-1} / 3 \times 10^{10} \text{ cm/sec} = 90 \text{ } \mu\text{sec}$$

Thus, IER theory predicts a 67-fold ( $90 \text{ } \mu\text{sec}/1.34 \text{ } \mu\text{sec}$ ) increase in lifetime if the coupling is between the  $B_1$  cold vibronic level and the complete manifold of the quasidegenerate  $\{|G\alpha\rangle$  set. Experimentally, in the presence of Ar, we demonstrated that the collision-free MPA-induced emission lifetime is at least  $50 \text{ } \mu\text{sec}$ . Thus, even with the approximations used, agreement between theory and experiment is not unreasonable. Moreover, in range A, where the  $B_1$  level-density is very sparse, the "effective" density of  $\{|G\alpha\rangle$  vibrational levels coupled to the excited vibronic state may very well be reduced.

This reduced density of states will increase  $(\rho_G)^{-1}$ , the level spacing, yielding a shorter lifetime or faster IER rate. At higher excitations, as already stated,  $(\rho_G)^{-1}$  would decrease and a longer  $\tau$  is expected. Additionally,  $\Delta_{S\beta,G}$ , which is itself proportional to  $\rho_G$ , would also increase, thereby decreasing the IER rate. In range A, where the  $B_1$  level density remains low, even for considerable vibrational excitation, the only counteracting effect would be a faster radiative

rate,  $\gamma_S$ , due to, for example, favorable Franck-Condon factors. The general pattern observed by McDonald (20) is that the fluorescence quantum yield decreases for higher members of a vibrational progression; thus the increased radiationless rate,  $\Delta_{S\dot{B}G}$ , predominates. The culmination of this trend occurs at about 5600 Å, where the ratio of the radiative to radiationless rates is so small, i.e.,

$$\frac{\gamma_S}{\Delta_{S\dot{B}G}} \ll 1,$$

that the emission disappears.

According to this picture, collisional deactivation, as was experimentally shown, should be very efficient in quenching the fluorescence. The larger than gas kinetic cross-section obtained indicates that long-range forces are sufficient to deactivate the MPA-produced electronically excited state. The laser pulse produces an ensemble of  $\text{CrO}_2\text{Cl}_2$  molecules in mixed states,  $\{|j\rangle\}$ , that carry oscillator strength due to their partial  $|B_1\rangle$  character. Superimposed on these is the dense background of dark levels that have, practically, no radiative widths. Because of the high level density of the latter, collisions can be expected to quench the luminescence effectively. Within this framework, therefore, our experimentally observed  $\text{CrO}_2\text{Cl}_2$  collisional self-quenching rate constant of  $10^7 \text{ sec}^{-1} \text{ torr}^{-1}$ , is not unexpected. Very efficient collisional deactivation of electronic fluorescence, even with larger than gas kinetic cross-sections, is not unusual when the quenching proceeds via internal conversion or intersystem crossing (27,28,29 for example). Since the same interstate vibrational relaxation would be expected to operate regardless of the excitation conditions, our agreement with McDonald's rate is comforting. Hard-sphere collisions, with rare gases

for example, would not be expected to be very efficient. Actually, that the fluorescence is quenched at all by the He and Ar is further support for the IER concept. Rare gases do not normally quench electronic fluorescence. However, when such emission stems from mixed levels, as in the  $\text{CrO}_2\text{Cl}_2$  case, inert gases have been found to deactivate the excited molecules but with very low efficiency (30,31,32). This is the behavior observed when the MPE of  $\text{CrO}_2\text{Cl}_2$  was carried out in rare-gas baths. Thus, the quenching of the  $\text{CrO}_2\text{Cl}_2$  fluorescence by He is displayed in Figure 16 of the Results. Moreover, the deactivation of the emission induced in an Ar: $\text{CrO}_2\text{Cl}_2$  (200:1) mixture also supports the mixed-states hypothesis. The Stern-Volmer plot of these experiments yields a slope of  $4.6 \times 10^7 \text{ sec}^{-1} \text{ torr}^{-1}$  or a bimolecular quenching constant ( $k^{-1}$ ) of  $2.2 \times 10^{-8} \text{ sec} \cdot \text{torr}$ , in units that facilitate the following discussion. This rate constant is similar to that obtained in neat  $\text{CrO}_2\text{Cl}_2$ ,  $5.9 \times 10^{-8} \text{ sec} \cdot \text{torr}$ . The slower rate obtained in the mixture, if significantly different, may be due to collisions among the Ar bath and the cold  $\text{CrO}_2\text{Cl}_2$  molecules. The latter are much more numerous than excited  $\text{CrO}_2\text{Cl}_2$  species, since the laser only excites a small population of even those molecules residing within the interaction volume. These "intra-bath" collisions would tend to reduce the frequency of  $\text{CrO}_2\text{Cl}_2$ - $\text{CrO}_2\text{Cl}_2^*$  deactivating collisions. At lower pressures, however, a slower rate is obtained with a very approximate constant of about  $7.3 \times 10^{-10} \text{ sec} \cdot \text{torr}$ . A possible explanation for this observation is that, as the pressure is reduced, the deactivation process is dominated by Ar- $\text{CrO}_2\text{Cl}_2^*$  collisions. At these pressures, remembering that the Ar: $\text{CrO}_2\text{Cl}_2$  ratio remains constant, the time between  $\text{CrO}_2\text{Cl}_2$  collisions becomes very long and the quenching rate is primarily determined by the specie in large excess, namely Ar. Expressing the rate constant for this process in terms of Ar pressure yields a value of  $3.6 \times 10^{-12}$

sec-torr--more than four orders of magnitude smaller than the  $\text{CrO}_2\text{Cl}_2$  self-quenching rate constant. Such an inefficient rate is, as already discussed, expected. That He and Ar quench the MPE-induced emission is consistent with our understanding of the excitation process. Rare-gas deactivation reflects the high density of levels belonging to the "black holes" as compared to those belonging to the emissive group of  $\{|j\rangle\}$  states. Therefore, vibrational relaxation via inelastic hard sphere collisions can take place, since quenching can be realized with a minimal amount of energy transfer between collision partners. Thus, we see that weakly inelastic collisions are, paradoxically, responsible for the enhancement of the  $\text{CrO}_2\text{Cl}_2$  emission, by rotational hole filling as already mentioned, and for its collisional deactivation by rare gases. Indeed, whether any energy conversion (V-T or R-T) has to occur or if dephasing collisions that populate isoenergetic, but basically pure  $\{|G\rangle\}$ , levels are sufficient to quench the fluorescence remains an open question. The latter route, which amounts to  $T_2$ -type processes familiar from NMR experiments, might be operative in the low temperature matrix emission studies done on  $\text{CrO}_2\text{Cl}_2$  (21,26). In the present work, however, where population of emissive  $\text{CrO}_2\text{Cl}_2$   $|j\rangle$  states is achieved via incoherent excitation, the nature of the quenching process cannot be ascertained. On the other hand, the collisional dependence of the decay rate in  $\text{CrO}_2\text{Cl}_2$  offers strong supporting evidence for the IER model.

In this regard, the lifetime and collisional deactivation experiments also serve to elucidate the pumping mechanism in the energy region of the  $B_1$  state origin. If radiative coupling of high vibrational levels of the  $A_1$  ground state with low lying  $B_1$  levels were responsible for populating the latter, it would be difficult to understand why the fluorescence decay behavior does not mimic that observed by McDonald. Both experiments would involve the same initially prepared level, and,

therefore, its decay should be the same regardless of the photon used. That MPE yields a longer lifetime is a reflection of the "mixed" ( $\{|G\rangle$  and  $\{|S\rangle\}$ ) nature of the resulting state. In a less accurate, but perhaps more easily visualized, kinetic description, we would say that after the  $\{|G\rangle$  levels are populated via MPE, a slow, rate-determining crossover step takes place into the  $|B_1\rangle$  state followed by a fast radiative step. The latter is rendered virtually irreversible, in the isolated molecule, by the coupling of  $|B_1\rangle$  to the radiative continuum into low lying  $|A_1\rangle$  levels. As in all kinetic schemes, the slow step, nonradiative conversion from quasidegenerate  $\{|A_1\rangle\}$  to  $\{|B_1\rangle\}$  in the present work, determines the rate of the overall process--in this case, the emission lifetime. That the fluorescence amplitude scales up with fluence or energy (Figure 9 of Results) without any "anomalous" power intensity effects is further evidence that multiphoton excitation to fluorescent levels occurs via the ground state ladder or, preferably, via the mixed  $\{|j\rangle\}$  manifold. If population of low-lying  $B_1$  vibronic levels resulted from infrared transitions into and within its sparse vibrational manifold, additional power intensity effects, similar to those operative within the discrete region of  $A_1$ , should have been observed. Their absence, therefore, lends credence to the IER description of the V+E energy transfer process in  $\text{CrO}_2\text{Cl}_2$ .

The broadened emission observed under more intense conditions of fluence and/or pressure were assigned to  $\text{CrO}_2\text{Cl}$  and  $\text{CrO}_2$ . The rationale behind these assignments was presented in the previous chapter. Although the luminescence to the blue of  $5600 \text{ \AA}$  must be due to species other than  $\text{CrO}_2\text{Cl}_2$ , direct, unequivocal assignment of this emission is not really possible. The experimental evidence presented, however, is overwhelmingly in favor of at least one, or probably, both daughter species producing the emission.

Although much more common than parent luminescence, the observation of MPE-induced fragment luminescence is not predicted, a priori, by the currently accepted models of infrared-multiphoton chemistry. This statement follows from the general rule that the ground state of a molecule correlates adiabatically with ground state products. Thus, vibrational heating within the ground-state manifold of the parent molecule is not generally expected to yield electronically excited fragments. Nevertheless, electronic luminescence of fragments, even under collisionless conditions, has been observed in our as well as in other systems. This experimental observation, we believe, can be explained within the IER formalism. Before briefly discussing the probable mechanism, an alternative explanation should be raised--namely, electronically excited parent molecules yielding excited products. As appealing as this hypothesis may seem, the evidence is strongly against it. First of all, as has been stated, laser chemistry has been found to generally follow the thermal route to dissociation. Product yields are usually very similar to those obtained under thermal decomposition. When different products are formed, the evidence strongly favors thermal decomposition followed by one or more additional steps. Furthermore, Dannen and co-workers (33) have shown that molecules that obey Woodward-Hoffman rules of electrocyclic reactions don't dissociate via the photoexcited path. In the systems studied, where the thermal and photolytic routes yield quite distinct products, the former is the preferred path. Moreover, when ground-state dissociation is not favored, these molecules forego the concerted mechanism in favor of free radical decomposition. Lastly, and bearing directly on the MPD of  $\text{CrO}_2\text{Cl}_2$ , electronic excitation of sufficient energy to dissociate this molecule in the gas phase does not result in luminescence (2,30). We have confirmed this fact by dissociating  $\text{CrO}_2\text{Cl}_2$  with an ultraviolet (Hg)

lamp. The evidence, therefore, is overwhelming that, as a rule, multiphoton excitation and dissociation do not occur via excited electronic states.

We postulate that the production of  $\text{CrO}_2\text{Cl}_2$ -derived excited fragments occurs as follows. Under collisionless conditions, a stronger laser field is required to bypass the IER channel in  $\text{CrO}_2\text{Cl}_2$ . This is reflected by the larger fluence threshold of the 4000 Å and 5300 Å signals as compared with the parent's at 6300 Å (Figure 9 of Results). Additionally, the daughter signals exhibit much stronger fluence dependence. This can be interpreted as a competition between the IER rate and the up-pumping rate in the energy neighborhood of the  $B_1$  state. For a given laser pulse width, the vibrational excitation will increase as the energy of the pulse increases. Only at very low laser energies, where the available number of photons is relatively small, can the IER rate effectively compete with the multiphoton absorption rate. When this competition is no longer fluence limited the dissociative channel, at an energy of 19-34 kcal/mole above the  $B_1$  origin, becomes available to the molecule. Since the larger value is, as previously shown, undoubtedly more accurate, unimolecular dissociation can take place after absorption of some 24 infrared-laser photons. However, at the dissociation limit, competition between the up-pumping and dissociation rates occurs. In this energy region, absorption of a few more laser photons can continue until levels with very large dissociative widths are reached. As predicted by RRKM theory, the dissociation lifetimes of these levels increases exponentially with excess energy. Thus, dissociation soon becomes the preferred channel. Experimentally, as mentioned in the Results, this MPD mechanism is strongly supported by the crossed laser and molecular beams experiments of Lee and co-workers (5,6). These authors have found that, typically, polyatomics similar

in size to  $\text{CrO}_2\text{Cl}_2$ , dissociate with an average excess energy of 4-6 laser photons. As a result, dissociation lifetimes of these levels are in the nanoseconds to hundreds of picoseconds regime. Laser pulses of several to hundreds of nanoseconds, such as ours, lose the battle in this energy region. The additional energy, typically, appears as vibrational energy of the larger fragment. In  $\text{CrO}_2\text{Cl}_2$ , practically all of it will remain in the  $\text{CrO}_2\text{Cl}$  fragment, since atomic chlorine can only accept excess energy to its translational degrees of freedom. Thus, a vibrationally hot  $\text{CrO}_2\text{Cl}$  fragment is formed in a matter of nanoseconds, well within the envelope of our shortest pulse-- 200 nanoseconds. Laser radiation of sufficient fluence can further excite the vibrationally hot  $\text{CrO}_2\text{Cl}$  fragments until an excited electronic state is reached, effecting emission, or the dissociative continuum is attained and dissociation occurs. Absorption of additional photons by the vibrationally excited fragment can occur if dissociation of the parent  $\text{CrO}_2\text{Cl}_2$  leaves the  $\text{CrO}_2\text{Cl}$  in its quasicontinuum, where frequency matching is not a requirement for absorption of laser photons. Indeed, this mechanism seems to explain the dissociative route of many polyatomics under  $\text{CO}_2$ -laser excitation, such as the proposed  $\text{SF}_6 \xrightarrow{-F} \text{SF}_5 \xrightarrow{-F} \text{SF}_4$  (5). Actually, even  $\text{CrO}_2\text{Cl}$  fragments that are not sufficiently hot to attain their vibrational quasicontinuum may absorb additional laser photons. The asymmetric Cr-O stretch, present in  $\text{CrO}_2\text{Cl}$ , retains its frequency of about  $1000 \text{ cm}^{-1}$  in such diverse species as  $\text{CrO}_2$  (34) and  $\text{CrO}_2\text{F}_2$  (15). It is reasonable to assume that this is also the approximate value in  $\text{CrO}_2\text{Cl}$ , and that, therefore, the resonance condition between the fragments and the laser field can exist even for transitions within the "discrete" region of the vibrational ladder. This resonant secondary pumping is particularly attractive to explain the luminescence assigned to  $\text{CrO}_2$ . This triatomic specie is not likely to reach its quasicontinuum

even when produced with considerable vibrational temperature by the laser-induced dissociation of  $\text{CrO}_2\text{Cl}$ . However, frequency matching between the driving field and the  $\text{CrO}_2$  molecule can explain the further excitation and luminescence of this specie. Exactly, the same considerations apply if this specie were formed, as previously discussed, from the direct, though higher energy, fragmentation channel  $\text{CrO}_2\text{Cl}_2 \rightarrow \text{CrO}_2 + \text{Cl}_2$ . Implicit in this discussion is the assumption that infrared-laser pumping of these fragments eventually drives them to fluorescent levels, i.e., an energy region where an IER-type process can occur.

A novel process, involving collisionless V-E energy transfer following  $\text{CO}_2$ -laser excitation, has been described in the present work. It has been shown that the parent fluorescence induced in  $\text{CrO}_2\text{Cl}_2$  can be described within the current theoretical framework of MPA with the additional interpretation of IER. Moreover, though this molecule was particularly suited for these experiments, it is believed that  $\text{CrO}_2\text{Cl}_2$  is only one of a family of molecules where V-E energy conversion can be detected as parent emission. Indeed, any polyatomic molecule possessing a reasonable absorption cross-section to a  $\text{CO}_2$  TEA laser, a relatively low-lying excited electronic state and a ground state level density of  $10^4$  to  $10^8/\text{cm}^{-1}$  in the neighborhood of the excited state may be a candidate for MPA-induced parent fluorescence. Work in progress at several laboratories, including ours, is directed towards confirming this prediction.

Because all the experimental work and most of the writing presented up to this point were completed three years ago, it seems appropriate to briefly mention new research relevant to the present study. Parent fluorescence, as already mentioned, has also been ascribed to other molecular systems undergoing multiphoton-induced

emission (23,24,25). Additionally, the heightened interest in this process has resulted in some controversy. Regarding  $\text{CrO}_2\text{Cl}_2$  in particular, one study (35) performed with two-color excitation, electronic with a frequency-doubled Nd:Yag laser at 532 nm followed by  $\text{CO}_2$ -laser radiation, indicated that, following optical excitation, the molecule undergoes a radiationless decay into high-lying vibrational levels of the ground state. From these levels, non-resonant absorption of  $\text{CO}_2$ -laser photons can take place leading to emission. The authors do not address the question of the origin of the luminescence and, given the relatively high pressures ( $\geq 20$  mtorr) and the long delays ( $> 1$   $\mu\text{sec}$ ) between the two lasers, collisions probably played an important role. Additionally, it is likely that, at the  $\text{CO}_2$  fluences used, considerable dissociation took place and most, if not all, the luminescence originated from daughter species.

The controversy over parent fluorescence and the IER formalism has generally surfaced at meetings or via private communications. One study, however, by Watson, et al (36) seemed to show convincingly that the emission of  $\text{CO}_2$ -laser excited  $\text{CrO}_2\text{Cl}_2$  in a molecular beam was overwhelmingly due to fragments. This conclusion was derived from the resolved angular distribution of the emitting species. Actually, that product luminescence predominated was not unexpected since, at the high fluence ( $100 \text{ J/cm}^2$ ) used by Watson, et al (36), our study also predicts, or at least implies, this result.

In a recent report by Ruhman and Haas (37), the  $\text{CrO}_2\text{Cl}_2$   $\text{CO}_2$ -laser induced emission was examined with emphasis on the effect of inert gases on the yield and branching ratio of "blue" and "red" signals. The interesting possibility of a rotational bottleneck in the quasi-continuum is raised by their findings. Although these authors do not identify the emitting species, they do conclude that the blue

luminescence arises from a different and more endoergic specie than that emitting in the red. Addition of foreign gases and an increase in pulse energy enhance the blue signal more than the longer-wavelength one. Other results obtained comparing different pulse shapes are similarly consistent with those of the present work.

Bloembergen and co-workers (38), using a relatively novel time-of-flight technique, have systematically analyzed the multiphoton-induced luminescence of  $\text{CrO}_2\text{Cl}_2$ . Additionally, by comparing this emission with that induced by a frequency-doubled ruby laser (347 nm) preceding low fluence  $\text{CO}_2$ -radiation, they were able to ascertain under what conditions the emission was due to photofragments. Since, at high  $\text{CO}_2$ -laser fluences, the wavelength-resolved luminescence mimicked that using two-color excitation, they concluded, in agreement with our and Watson's results, that the emission originates from daughter species. This blue-peaked emission must originate from fragments since 347-nm radiation is expected to dissociate  $\text{CrO}_2\text{Cl}_2$  with unit quantum efficiency (22). With, exclusively, low fluence  $\text{CO}_2$  irradiation of  $\text{CrO}_2\text{Cl}_2$ , the emission spectrum, as expected, resembles the published single-photon fluorescence spectrum (2,20). Additionally, this very red infrared-laser induced emission could not be reproduced with the two-color excitation.

Further support for the fluence-dependent dual source of the emission,  $\text{CrO}_2\text{Cl}_2$  and  $\text{CrO}_2\text{Cl}$ , was obtained by these workers using time-of-flight measurements. Their results show that the red luminescence decay matches that of room temperature  $\text{CrO}_2\text{Cl}_2$ , whereas the blue luminescence is only consistent with either  $\text{CrO}_2\text{Cl}_2$  at a much higher temperature, about the 430 K range, or, more likely, to a fragment such

as  $\text{CrO}_2\text{Cl}$ . Additionally, they found evidence that, at high fluence ( $\geq 20 \text{ J/cm}^2$ ), a third specie, probably  $\text{CrO}_2$ , begins to luminesce in the red portion of the spectrum.

During the period of time under discussion, the present author was employed by L.I.C. Industries, Inc. Since my work involved laser-related technology, I was fortunate to have access to a  $\text{CO}_2$  laser and to an understanding boss; this combination gave me an opportunity to perform a few experiments. The commercial Lumonics-103 TEA  $\text{CO}_2$  laser used was capable of producing pulses with as much as 15 Joules of energy. More importantly, by excluding  $\text{N}_2$  from the lasing mixture, pulses delivering 1 Joule in approximately 60 nsec were routinely obtained using the high members of the R-branch  $10.6 \mu$  transition. Such a laser, coupled with a cell and vacuum system that could be evacuated to  $10^{-5}$  torr yielded reasonable  $\text{CrO}_2\text{Cl}_2$  emission signals at low pressures. The rest of the experimental set-up was basically the same as that described before with the following modifications. The cell used was 39 in. long and 2 in. in diameter. A transverse flow of  $\text{CrO}_2\text{Cl}_2$ , perpendicular to the laser axis, was set up at approximately 16 in. from the entrance window. Under these conditions, fresh  $\text{CrO}_2\text{Cl}_2$  sample was insured, the NaCl windows were very far from the sample and from the excitation region--thereby eliminating the possibility of window fluorescence--and luminescence quenching at the cell walls was minimized. A 22-inch focal length mirror was used to soft-focus the laser-radiation. The mirror was placed immediately in front of the cell, thereby producing a beam of fairly uniform fluence within the relatively large, compared to previous experiments, radiation- $\text{CrO}_2\text{Cl}_2$  interaction volume. The luminescence was observed perpendicular to both the  $\text{CrO}_2\text{Cl}_2$  flow and the laser axis. A focusing lens was used to direct the emission into

the entrance slit of a monochromator and, as usual, detection was accomplished with a phototube, and the signals were displayed on a Tektronix 7704 oscilloscope. When appropriate, the monochromator was replaced by laser filters, as before.

Firstly, it was reestablished that, at low pressures (below a few mtorrs and as low as  $10^{-4}$  torr) and low fluences, the signal is very red. As either of these parameters was increased, broadening to the blue, as expected, was observed. However, perhaps the most surprising results that had been presented were the long lifetimes observed. The experiments at L.I.C. confirmed and extended these data. Studies of fluorescence decay rates, at  $6328 \text{ \AA}$ , as a function of  $\text{CrO}_2\text{Cl}_2$  pressure confirmed the previously obtained Stern-Volmer slope in the range of  $10^7 \text{ sec}^{-1}\text{torr}^{-1}$ . Similarly, at  $5300 \text{ \AA}$  and  $4000 \text{ \AA}$ , the quenching rate constants obtained were of the same order of magnitude as that of the parent's emission. As already mentioned in the Discussion, this result is consistent with luminescence deactivation effected by the cold bath of  $\text{CrO}_2\text{Cl}_2$  molecules present in large excess. Similar findings have been obtained by other workers (38,40). Interestingly, these experiments yielded an extrapolated monomolecular lifetime of the  $6328 \text{ \AA}$  signal in the neighborhood of  $250 \text{ \mu sec}$ . The  $5320 \text{ \AA}$  signal displayed an even larger decay time--perhaps as long as  $350 \text{ \mu sec}$ --whereas, most hesitantly, the  $4000 \text{ \AA}$  collisionless decay time should be on the order of  $100 \text{ \mu sec}$ . These values are in general agreement with the  $250 \text{ \mu sec}$  and  $160 \text{ \mu sec}$  lifetimes, respectively, obtained for the red emission by Burak and Tsao (40), and by these authors and Bloembergen in a subsequent report (38). The latter group also obtained a value of  $35 \text{ \mu sec}$  for the lifetime of the blue luminescence. Similarly, Watson, et al found that  $\tau$  was

> 75  $\mu\text{sec}$  (36) and 250  $\mu\text{sec}$  (41), although it is not clear if the lifetimes are for the total or the resolved emission. It is important to note that the decay rates are not only cell dependent because of wall collisions, but, as we found experimentally, vary with the length of the exciting laser pulse. Interestingly, details about the IER mechanism may be ascertained by studying the wavelength and time dependence of the emission as a function of pulse length or perhaps with a variable delay between two short laser pulses.

This subsection has highlighted the ongoing research on the  $\text{CO}_2$ -laser MPE-induced emission of  $\text{CrO}_2\text{Cl}_2$  since the work was first reported. The phenomenon of collisionlessly promoted emission and particularly parent fluorescence has been verified in this and in other systems. The long lifetimes observed, we believe, are a general result that is explainable and, at least, qualitatively predicted by the ground state mode of excitation together with the V-E energy coupling necessary to effect emission. The exact details of the process, whether explained by the IER or other theories, must await further experimentation. With the advent of faster laser pulses, better fluorescence detection equipment, and new infrared laser sources, the fine points of both the multiphoton absorption and the induced luminescence processes may very well be ascertained. Additionally, one suspects, some unexpected results will also be forthcoming.

## References

1. R. V. Ambartzumian and V. S. Letokhov, *Acc. Chem. Res.* 10, 61 (1977).
2. J. A. Blazy and D. H. Levy, *J. Chem. Phys.* 69, 2901 (1978).
3. C. H. Townes and A. L. Schawlow, "Microwave Spectroscopy," McGraw Hill Book Co., Inc., 1955.
4. M. D. Harmony, "Introduction to Molecular Energies & Spectra," Holt, Rinehart & Winston, Inc., 1972.
5. (a) M. J. Coggiola, P. A. Schulz, Y. T. Lee and Y. R. Shen, *Phys. Rev. Lett.* 38, 17 (1977); (b) P. A. Schulz, Aa. S. Sudbø, E. R. Grant, Y. R. Shen and Y. T. Lee, *J. Chem. Phys.* 72, 4985 (1980).
6. (a) Aa. S. Sudbø, P. A. Schulz, Y. T. Lee and Y. R. Shen, *J. Chem. Phys.* 68, 1306 (1978); (b) 69, 2312 (1978); (c) Aa. S. Sudbø, P. A. Schulz, E. R. Grant, Y. R. Shen and Y. T. Lee, *J. Chem. Phys.* 70, 912 (1979).
7. M. H. Yu, H. Reisler, M. Margit and C. Wilty, *Chem. Phys. Lett.* 62, 439 (1979).
8. A. A. Makarov, G. N. Makarov, A. A. Puzetsky and V. V. Tyakti, *Appl. Phys.* 23, 391 (1980).
9. J. L. Lyman and K. M. Leary, *J. Chem. Phys.* 69 1858 (1978).
10. J. L. Lyman, W. C. Danen, A. C. Nilsson and A. V. Nowak, *J. Chem. Phys.* 71, 1206 (1979).
11. R. V. Ambartzumian, Yu. A. Gorokhov, V. S. Letokhov, G. N. Makarov, A. A. Puzetski and N. P. Furzikov, *Pis'ma Zh. Eksp. Teor. Fiz.*, 23, 217 (1976).
12. P. C. Haarhoff, *Mol. Phys.* 7, 101 (1963).
13. N. Bloembergen and Y. Lablonovitch, *Phys. Today*, 31, 23 (1978).
14. H. S. Kwok and Y. Lablonovitch, *Phys. Rev. Lett.*, 41, 745 (1978).
15. W. E. Hobbs, *J. Chem. Phys.* 28, 1220 (1958).
16. C. D. Cantrell and H. W. Galbraith, *Optics Commun.* 21, 374 (1977).
17. A. Nitzan and J. Jortner, *Chem. Phys. Lett.* 60, 1 (1979).
18. A. Nitzan and J. Jortner, *J. Chem. Phys.*, 71, 3524 (1979).
19. A. E. Douglas, *J. Chem. Phys.* 45, 1007 (1966).
20. J. R. McDonald, *Chem. Phys.* 9, 423 (1975).

21. V. E. Bondybey, Chem. Phys. 18, 293 (1976).
22. R. Halonbrenner, J. R. Huber, U. Wild and H. H. Gunthard, J. Phys. Chem. 72, 3929 (1968).
23. R. V. Ambartzumian, G. N. Makarov and A. A. Puretski, JETP Lett. 28, 647 (1978).
24. J. W. Hudgens, J. L. Durant, D. J. Bogan and R. A. Coveleskie, J. Chem. Phys. 70, 5906 (1979).
25. G. L. Wolk, R. E. Weston and G. W. Flynn, J. Chem. Phys. 73, 1649 (1980).
26. M. Spoliti, J. H. Thirtle and T. M. Dunn, J. Molec. Spectrosc. 52, 146 (1974).
27. P. B. Sackett and J. T. Yardley, J. Chem. Phys. 57, 152 (1972).
28. J. R. McDonald and L. E. Brus, J. Chem. Phys. 61, 3895 (1974).
29. L. E. Brus and J. R. McDonald, J. Chem. Phys. 61, 97 (1974).
30. E. S. Young and C. B. Moore, J. Chem. Phys. 58, 3988 (1973).
31. L. E. Brus and J. R. McDonald, J. Chem. Phys. 58 4223 (1973).
32. R. A. Coveleskie and J. T. Yardley, Chem. Phys. 9, 275 (1975).
33. W. C. Danen, D. F. Koster, R. N. Zitter, J. Amer. Chem. Soc. 101, 4281 (1979).
34. G. Nagarajan, Aust. J. Chem. 16, 908 (1963).
35. D. F. Heller and G. A. West, Chem. Phys. Lett. 69, 419 (1980).
36. T. A. Watson, M. Mangir, C. Wittig and M. R. Levy, J. Phys. Chem. 85, 754 (1981).
37. S. Ruhman and L. Haas, J. Chem Phys. 76, 1317 (1982).
38. J. Y. Tsao, N. Bloembergen and I. Burak, J. Chem. Phys. 75, 1 (1981).
39. S. Ruhman and Y. Haas, J. Chem. Phys. 76, 1317 (1982).
40. I. Burak and J. Y. Tsao, Chem. Phys. Lett. 77, 536 (1981).
41. T. A. Watson, M. Mangir, C. Wittig and M. R. Levy, J. Chem. Phys. 75, 5311 (1981).